A COMPUTER-CONTROLLED TRACKING SYSTEM

A thesis submitted for the degree of Master of Science
at Rhodes University, Grahamstown.

by

GRAHAM EDMUND OBEREM

Supervisor: Prof. E.E. Baart

January 1979

ACKNOWLEDGEMENTS

There are many people to whom my sincere thanks is due.

I am most grateful to my supervisor, Prof. E.E.Baart, for his guidance and criticism during the course of my work.

I should also like to thank Clive Way-Jones whose help with the electronics was invaluable, Pete Mountfort for his numerous suggestions about the use of the computer, and the technical staff of the Physics Department for their advice and skilful assistance with many aspects of the constructional work.

I am very grateful to all my friends and colleagues for their criticism, help and encouragement.

I am also indebted to the CSIR, the late Mr. F.R.Furter and Rhodes University for their financial assistance in 1975, and to the Physics Department for the use of the Microcomputer in the production of this thesis.

Finally, my thanks go to my parents for their unfailing interest and encouragement and to my wife for her patient understanding and many hours of typing.

Graham Oberem

CONTENTS

CHAPTER THREE

THE ARITHMETIC LOGIC UNIT

CHAPTER FOUR

THE COMPUTER JUNCTION, THE DIGITAL JUNCTION AND THE MOTOR DRIVE UNIT

CHAPTER FIVE

PERFORMANCE AND CALIBRATION

CHAPTER SIX

TRACKING PROGRAMS

CHAPTER SEVEN

TRACKING THE SUN

CHAPTER EIGHT

APPENDICES

ABSTRACT

A computer-controlled tracking system has been designed and constructed for the two metre antenna of the 22 GHz radio telescope at Rhodes University. The control system has been tested and its step response has been analysed with a view to response time optimization. Computer programs for tracking the sun and the moon have been written. Initial results of tracking the sun have revealed linearity and temperature stability problems. These problems have been investigated and suggestions have been made as to how they might be removed.

PREFACE

A 22 GHz Radio Telescope has been under construction at Rhodes University for some years. Nunn (1974) reported on the design of the Cassegrain feed system for the two metre parabolic antenna, Mutch (1975) presented the design of the spectral line and continuum receivers and Gaylard (1976) reported the satisfactory operation of the microwave section of the telescope and presented the results of some observations made with the telescope.

Until now, however, no means have been available for the automatic positioning of the antenna or for tracking a radio source across the sky. This thesis reports on the computer-controlled tracking system which has been built to provide these facilities.

CHAPTER ONE

ANALYSIS OF THE REQUIREMENTS

The beamwidth of the two meter Radio Telescope Antenna has been measured (Mutch 1975) and was found to be 27 minutes of arc. As can be seen from the telescope beam pattern (Figure 1.1), a possible error of one percent in the observed source temperature can occur if there is an uncertainty of three minutes of arc, one tenth of a beamwidth, in the point in the sky to which the telescope is directed. If an uncertainty of one percent in the observed source temperature due to the positioning of the antenna can be tolerated, the co-ordinates of the antenna at any time must be known to within 2,7 minutes of arc.

Furthermore, if long integration times are to be used in the receiver, a computer-controlled system for tracking a source is required. Such a system would have to be able to direct the telescope to within 2,7 minutes of arc of a desired point in the sky and to up-date the co-ordinates of that point in real time in order to track the source across the sky.

The two meter parabolic antenna is attached to an alt-azimuth mount (Figure 1.2). In the alt-azimuth (or horizon) system of co-ordinates (Figure 1.3), a point in the

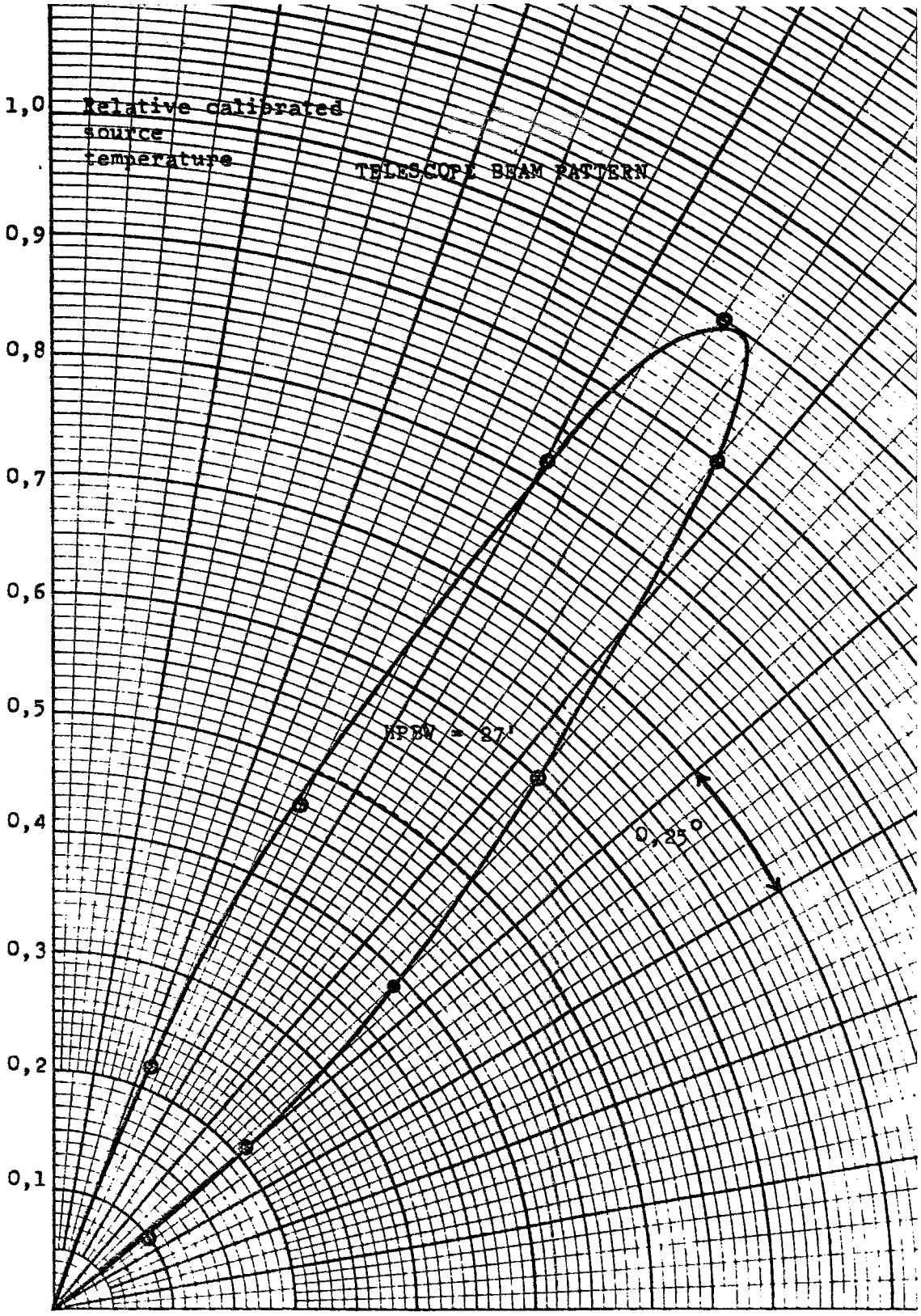

Figure 1.1 The telescope beam pattern (Mutch 1975)

Figure 1.2 The antenna mount

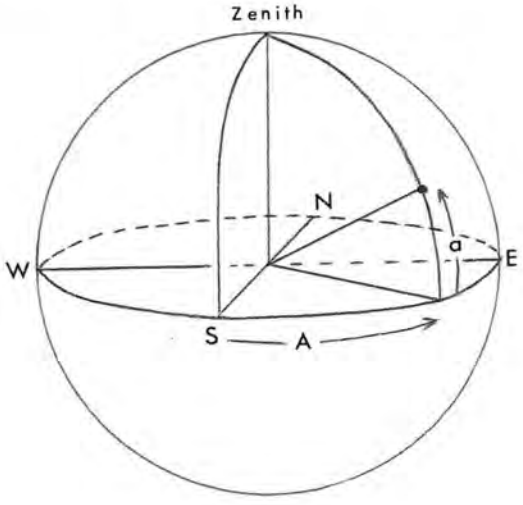

Figure 1.3 The alt-azimuth co-ordinate system

sky is specified by its azimuth and its altitude . The azimuth, A, of such a point is the angle between the vertical circle through the south point on the horizon and the vertical circle through the point of interest, measured eastwards along the horizon. (This definition of azimuth is used by observers in the Southern Hemisphere.) The altitude, a, of the point is the angle along the vertical circle through the point, measured from the horizon to the point of interest.

A pair of synchros (Figure 1.4) is geared to each axis of

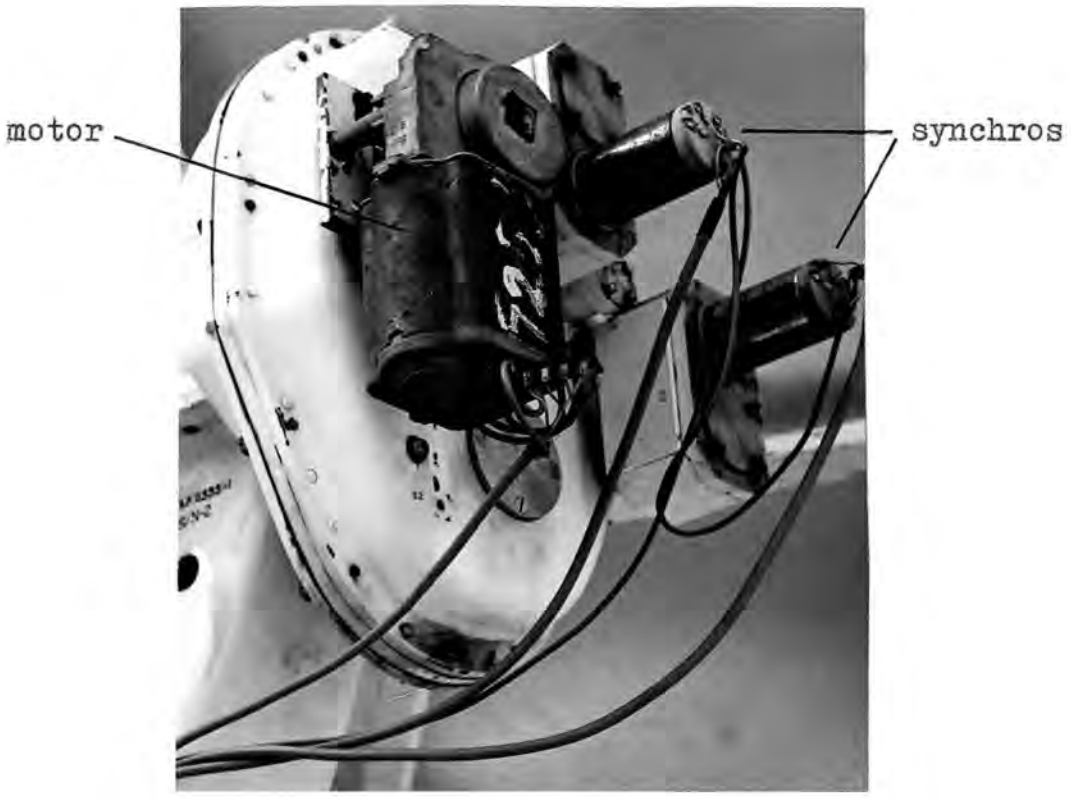

Figure 1.4 The altitude motor and synchros

movement of the telescope. A synchro (section 2.1) is a

device which is used to transmit angular information electrically from one place to another when a high degree of accuracy is required. To achieve greater accuracy a two-speed coarse/fine synchro system has been employed on this antenna mount with a gear-ratio of 36:1 between the coarse and fine synchros in each pair.

The accuracy of synchros is best portrayed by their electrical error which is defined (Upson and Batchelor 1966, page 148) as the angular amount by which the mechanical angle deviates from the electrical angle. For the synchros supplied with the antenna mount, the electrical error is specified (Bendix Aviation Corporation 1962) as a maximum of 7 minutes. In the case of the fine synchros, this is reduced by a factor of 36 because of the gear ratio, to a maximum of 12 seconds. This is well within the requirements of the present system.

In order to interpret the synchro signals, it is convenient to convert them to digital form. It is possible to buy synchro-to-digital converters which operate with the required accuracy but they were extremely expensive at the time that this project was begun. The possibility of using stepper motors was also considered. This would have simplified the tracking system considerably but the cost of suitable motors was found to be too great. It was therefore decided to make use of the synchros on the antenna mount and to design and build a computer-controlled tracking system

compatible with these synchros.

Figure 1.5 is a block diagram of the tracking system which has been built. The analogue signals from the two pairs of synchros are converted to digital form by the synchro-to-digital converter which is discussed in detail in Chapter 2. From the four numbers thus obtained, the two co-ordinates of the telescope are calculated in the arithmetic logic unit and displayed on the front panel. These calculations are done by "hardwired" logic and a description of this is given in Chapter 3. The co-ordinates of the telescope are compared with the computed co-ordinates in the digital junction and an error signal is derived which is then converted back to analogue form and used to drive the motors until the telescope is pointing to the required co-ordinates. The computer junction receives information directly from a Nova II mini-computer and also allows for manual position encoding. The details of these two sections appear in Chapter 4 together with a discussion of problems encountered in connection with the motor drive system. Appendix 1.1, a photograph of part of the tracking system shows the modular construction which has been used throughout.

The performance of the tracking system is analysed in Chapter 5 whilst Chapter 6 and Chapter 7, respectively, present the tracking programs which have been written and the first results of tracking the sun.

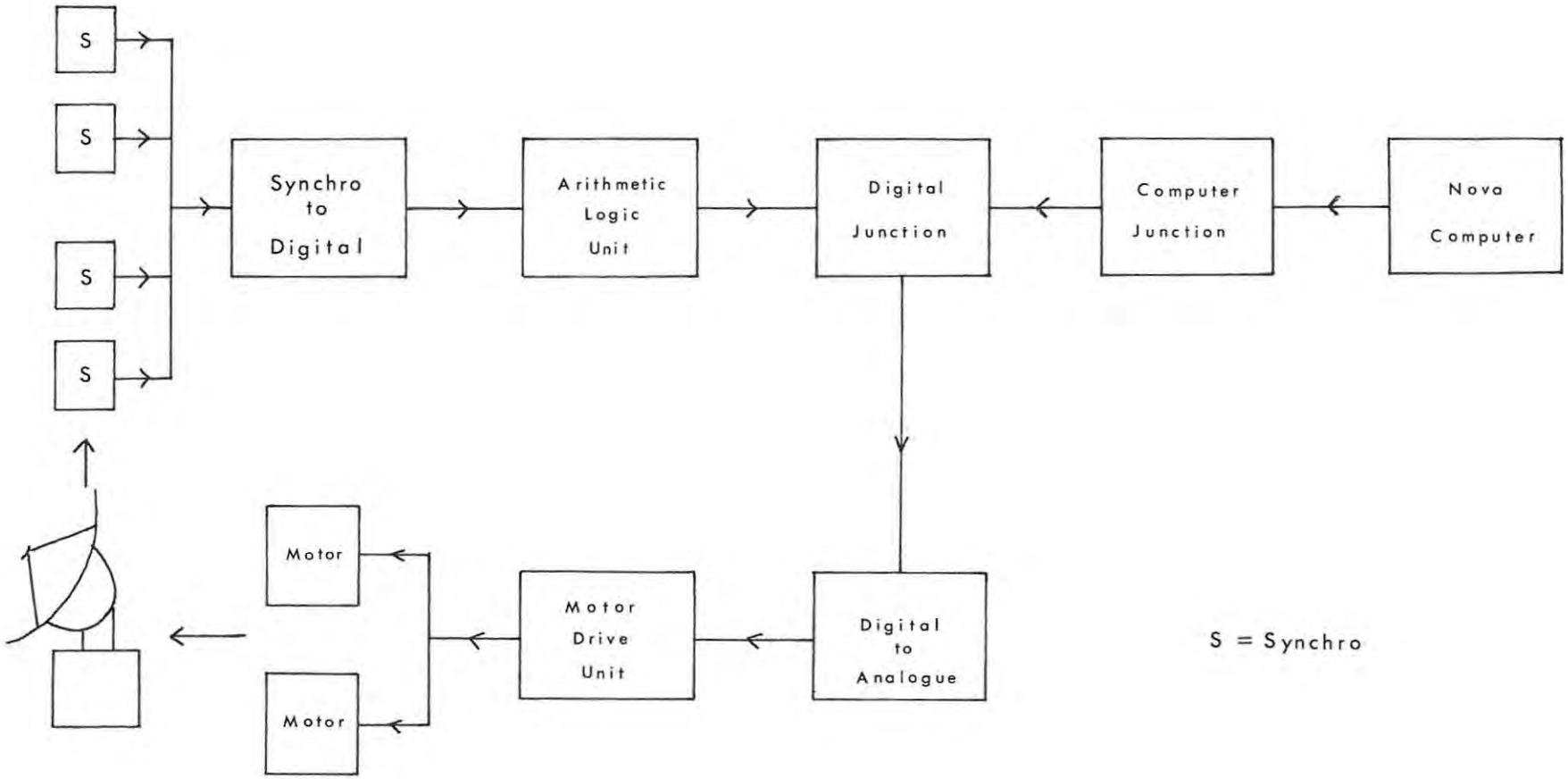

Figure 1.5 Block diagram of the tracking system

CHAPTER TWO

SYNCHRO-TO-DIGITAL CONVERTER

2.1 THE SYNCHROS

2.1.1 CONSTRUCTION

The construction and use of synchros is discussed widely in the literature (Upson and Batchelor 1976; Thaler and Brown 1960, Appendix B; Miller 1977, Chapter 5) but a brief description of the type of synchro supplied with the antenna mount is given in this section.

A synchro is a transformer in which the coupling between windings may be varied by rotating one winding with respect to the others. Figure 2.1 is a cutaway drawing of one of the synchros. The fixed (stator) windings are three star connected coils spatially displaced 120 degrees from each other, wound in the slots of a laminated iron stack. The rotor consists of a movable coil wound in 'H' form on a laminated iron stack mounted on a shaft, the one end of which protrudes from the housing and bears a square post which locks into the gearbox. The movable winding is the primary and the reference voltage is applied to this winding via sliprings and brushes. The brushes are designed to make contact on both sides of each slipring in order to lessen the possibility of bad contact due to dirt or vibration.

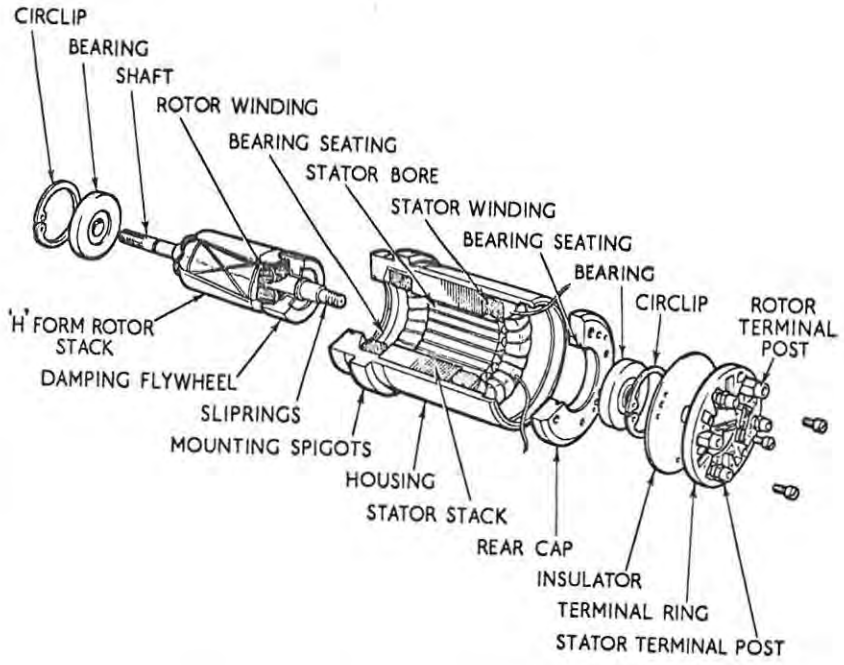

Figure 2.1 Cutaway drawing of a synchro
(Upson and Batchelor 1966)

2.1.2 THE INDUCED VOLTAGES

If the reference applied to the rotor is an alternating voltage, the stator windings will have voltages induced in them, the amplitudes of which will be proportional to the sine of the angle, θ_R, between the rotor and stator axes. Figure 2.2 shows the equivalent circuit of a synchro.

Expressions (Upson and Batchelor 1966, page 46) for the three voltages induced in the stator windings are as follows:

$$E(R_2R_1) = E_R \text{ Sin } \omega t \qquad 2.1$$

$$E(S_1S_3) = KE_R \text{ Sin } \theta_R \text{ Sin } (\omega t + \phi_1)$$
$$= E_1 \text{ Sin } (\omega t + \phi_1) \qquad 2.2$$

$$E(S_3S_2) = KE_R \text{ Sin } (\theta_R + 120^\circ) \text{ Sin } (\omega t + \phi_1)$$
$$= E_2 \text{ Sin } (\omega t + \phi_1) \qquad 2.3$$

$$E(S_2S_1) = KE_R \text{ Sin } (\theta_R + 240^\circ) \text{ Sin } (\omega t + \phi_1)$$
$$= E_3 \text{ Sin } (\omega t + \phi_1) \qquad 2.4$$

where K is the transformer ratio. (K = 0,783 for the

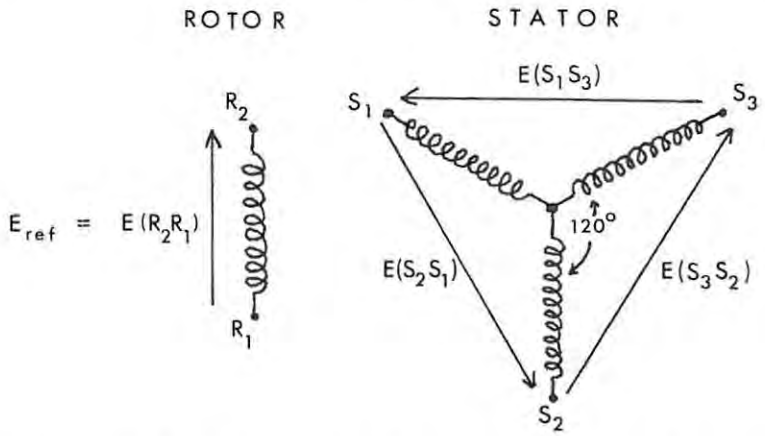

Figure 2.2 The equivalent circuit of a synchro

synchros described in this section.) Figure 2.3 is a graphical representation of the way in which the amplitudes of the induced stator voltages vary as the rotor is turned through 360 degrees. Although the stator voltages may lead the reference voltage by an angle of a few degrees (ϕ_1 in the equations above), the relative phase difference between the three stator voltages is always either 0° or 180°, as can be seen from the example in Figure 2.4.

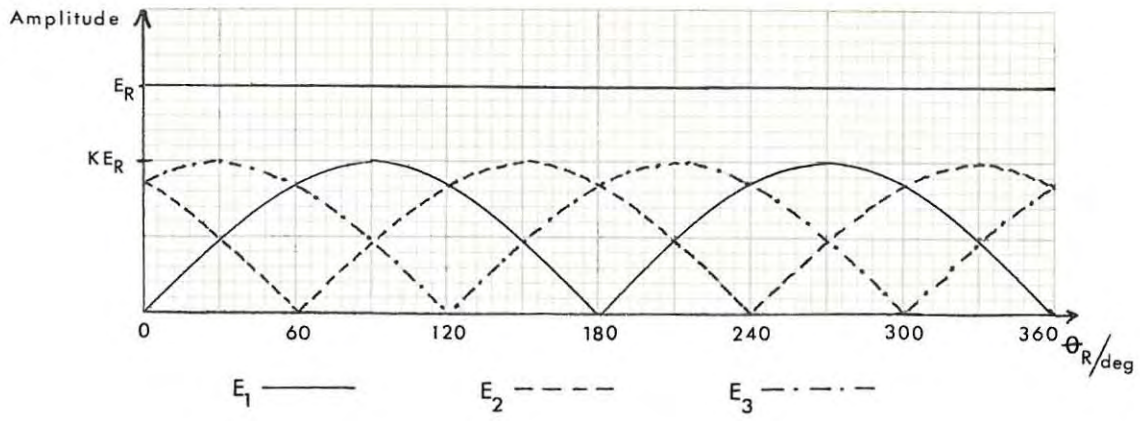

Figure 2.3 The variation of stator voltage with θ_R

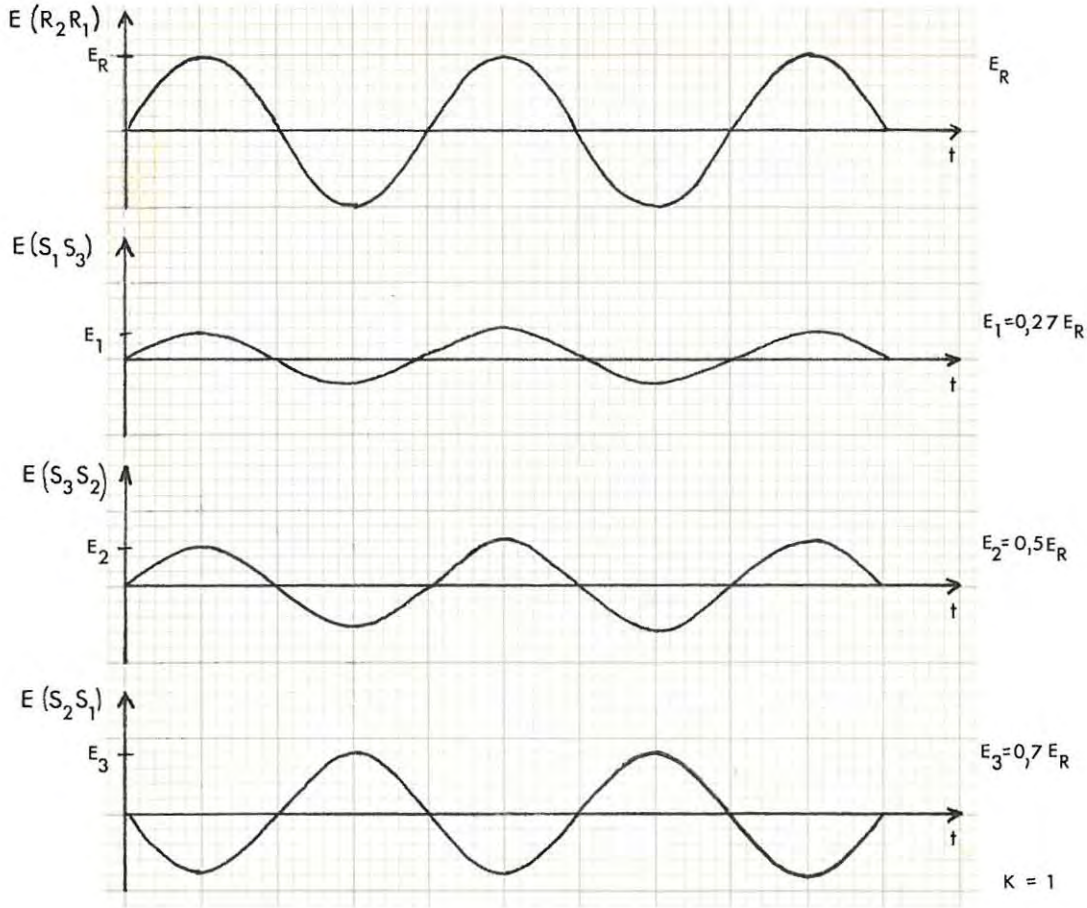

Figure 2.4 The stator voltage versus time for $\theta_R = 20^o$ ($\emptyset_1$ has been neglected.)

2.1.3 INTERPRETATION OF THE INDUCED VOLTAGES

In the interpretation of the stator voltages, both the amplitude and the phase of each of the voltages is

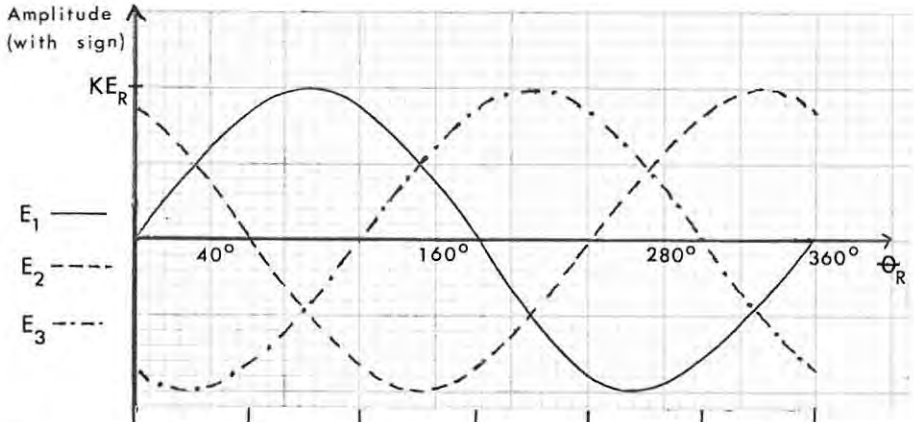

Binary	1	1	1	0	0	0
Segment	1	0	0	0	1	1
Number	0	0	1	1	1	0
Segment Number	6	4	5	1	3	2
Measure	E_1	E_2	E_3	E_1	E_2	E_3

Figure 2.5 Stator voltage amplitude with sign versus θ_R

important. These two quantities are combined (Figure 2.5) by making the amplitude positive if the voltage is in phase with the reference (ignoring ϕ_1) and negative if it is in antiphase with the reference.

Further inspection of Figure 2.5 reveals that one of the stator voltages changes phase relative to the reference after every 60° of movement of the rotor. It is therefore possible to split the 360° through which the rotor can move

into six segments of 60° each. In each of these segments the stator voltages maintain a constant phase relative to the reference voltage.

Suppose that in a particular segment the phase of each voltage with respect to the reference is represented by a "1" for in phase and a "0" for 180° out of phase. A unique three-bit binary number, derived from the phases of the three stator voltages relative to the reference voltage, can then be used to represent each segment. These numbers are indicated in Figure 2.5. With appropriate circuitry they may be converted to an angle of the form:

$n \times 60^{\circ}$ where $n = 0, 1, 2, \ldots 5$

in the correct sequence. This angle represents the start of the segment in which the rotor lies.

From Figure 2.3 it can be seen that in each 60° segment the amplitude of one of the three stator voltages increases from KE Sin 0° to KE Sin 60° as the rotor moves through that segment.

The angle that the rotor makes with the stator can therefore be represented by the sum of two angles, the segment starting angle, $n \times 60^{\circ}$, which can be obtained by examining the phases of the three stator voltages relative to the reference voltage, and an angle θ_1 ($0^{\circ} \leqslant \theta_1 < 60^{\circ}$) which is obtained by measuring the amplitude of the appropriate stator voltage, E_S (S = 1,2,3), and allowing for the fact

that the amplitude is proportional to the sine of the angle θ_1. The angle indicated by the stator voltages is then given by the equation:

$$\theta_R = n \times 60^o + \text{Sin}^{-1} \frac{E_S}{KE_R} \qquad 2.5$$

The stator voltage to be measured in each segment is also indicated in Figure 2.5.

2.1.4 THE COARSE - FINE SYSTEM

As was mentioned in Chapter One, there are two synchros geared to each axis of the telescope. The coarse synchro is geared to the telescope in such a way that 360^o of telescope movement corresponds to 360^o of rotor movement. This means that the angle θ_R given by equation 2.5 is equal to the angle through which the telescope has moved from some aribitrary zero corresponding to θ_R equals zero.

To achieve greater accuracy in the determination of the angle through which the telescope has moved, a two-speed synchro system is used. A second synchro is geared to the same shaft as the first but with a gear ratio of 36:1. This means that the rotor of this synchro, called the fine synchro, moves through 360^o while the telescope moves through only 10^o. The angle indicated by the stator voltages of a fine synchro must therefore be reduced by a factor of 36 to give the amount of telescope movement.

The following is the method used to combine the angular information from the coarse synchro and the fine synchro in order to get a more accurate value for the position of the telescope than would be obtained from the coarse synchro alone:

The coarse synchro angle, θ_C, from equation 2.5, is used only to determine the 10^o interval in which the telescope lies. The 10^o interval is then specified by its starting angle, θ_C'. The fine synchro is used to determine the position within the 10^o interval in the same way as described in section 2.1.3. The fine synchro angle, θ_F, which is given by the equation

$$\theta_F = \frac{1}{36} \cdot n \times 60^o + \frac{1}{36} \cdot \mathrm{Sin}^{-1} \frac{E_S}{KE_R} \qquad 2.6$$

is then combined with θ_C' to give the position of the telescope.

This method is illustrated in Figure 2.6. Miller points out that the use of a coarse/fine system in position determination is analogous to the hourhand/minutehand system of a watch.

The synchro-to-digital converter discussed in the next section performs the necessary measurements and produces, in digital form, the four angles θ_C, θ_F (altitude) and θ_C, θ_F (azimuth) as defined by equations 2.5 and 2.6. The arithmetic logic unit (ALU) then determines θ_C' and combines the coarse and fine angles in each case to give the altitude

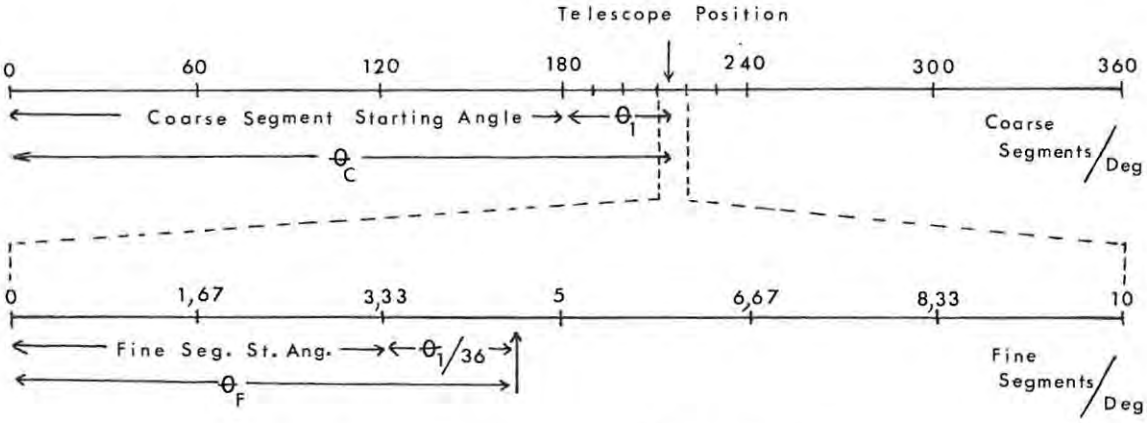

$$\theta_C = 180^\circ + \theta_1 \qquad \theta_C' = 210^\circ$$

$$\theta_F = 3{,}33^\circ + \theta_1/36$$

$$\text{Telescope position} = \theta_C' + \theta_F = 210^\circ + \theta_F$$

Figure 2.6 Use of the coarse-fine system

and azimuth co-ordinates to which the telescope is pointing.

2.2 THE CONVERTER

The synchro-to-digital converter consists of two parts. The first part (Figure 2.7) for reasons given below, is situated in the base of the telescope mount as close to the synchros as possible. The rest of the converter (Figure 2.9) is mounted, together with the other parts of the tracking system, in a rack in the telescope control room.

2.2.1 CHOICE OF REFERENCE VOLTAGE

The synchros are designed to operate with a reference

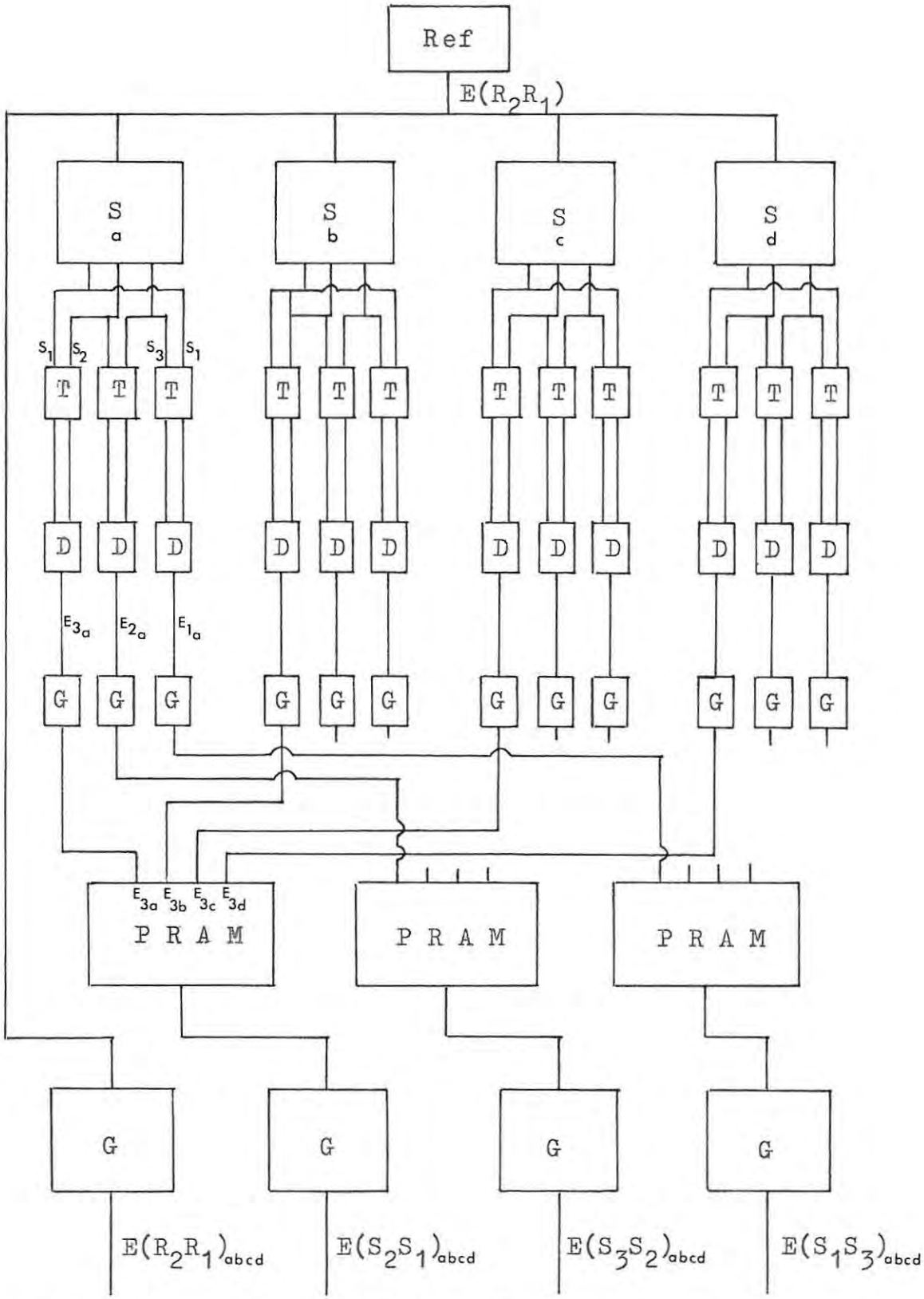

T = Transformer; D = Difference Amp; S = Synchro

G = Gain adjustment amplifier

Figure 2.7 The synchro-to-digital converter (Part 1)

voltage of 115 volts (r.m.s.) at 60 Hz (Bendix Aviation Corporation 1962), the American standard mains supply. It was therefore decided to use a reference voltage derived directly from the mains supply but with a much smaller amplitude to maintain compatibility with the low voltage levels in the rest of the converter without the use of bulky step-down transformers. A reference of 8 volts (r.m.s.) at 50 Hz is being used. Three problems are associated with the use of a reference voltage derived from the mains supply.

i) Interference due to spike voltages on the mains can produce large errors in the calculations.

ii) The mains voltage may vary and with it the amplitudes of the induced stator voltages.

iii) Pick up of stray voltages could cause the amplitudes of the induced voltages to change in an arbitrary way and the effect could differ from one voltage to the next.

The first of the three is not troublesome as long as the spikes are not repetitive and their duration is less than the response time (section 5.3) of the tracking system. In practice spike voltages have not been found to cause problems.

Variations in the reference voltage are removed by the synchro-to-digital converter in the divider section (section 2.2.5).

The pick up of stray voltages is potentially the most

serious of the three effects, and is most likely to influence the measurements when the amplitude of a particular stator voltage is close to zero. In order to minimise the possibility of errors caused in this way, the first few stages of the synchro-to-digital converter have been placed as close to the synchros as posible. Cable with a well-earthed shield has been used throughout.

This effect was examined during the initial testing and alignment of the converter and was found to be neglibible.

2.2.2 DIFFERENCE AMPLIFIERS AND GAIN SETTING

The induced voltages in the stator windings cannot be measured relative to earth potential since they appear as potential differences between the stator terminals, S_1, S_2, and S_3 (Figure 2.2). A set of difference amplifiers is therefore used to convert the potential differences between the stator terminals to voltages referenced to earth potential. The circuit used (National Semiconductors 1972a) is given in Appendix 2.1, together with the theory of operation. To avoid the connection of each stator terminal to more than one difference amplifier a set of twelve d.c. isolation (1:1) transformers has been placed between the synchros and the difference amplifiers (Figure 2.7). The pickup of stray signals and intertransformer coupling has been minimised by placing the transformers, which are physically small, in the compartments of a well-earthed

brass box which was constructed for this purpose. Since there might be small variations in transformer ratio from one transformer to the next and also to allow for the fact that the gains of the difference amplifiers, which were designed for unity gain, may not be identical, each difference amplifier is followed by an operational amplifier with adjustable gain. The maximum amplitude of each of the induced voltages can thus be set independently. (The need for this adjustment will become apparent in section 5.1).

2.2.3 FOUR-TO-ONE-MULTIPLEXING

Rather than duplicate electronic circuitry it was decided that the four angles should be measured one at a time in the synchro-to-digital converter. Each of the four angles is measured once every 80 milliseconds. This figure was chosen because it is conveniently related to the reference frequency (50 Hz) and thus enables the reference voltage to be used to control the timing of the measurements. Figure 2.8A shows when each measurement is performed in relation to the reference voltage. Because the four angles are measured sequentially only three signal lines are required, one for each of the stator voltages, with the signals from the four synchros time division multiplexed into four channels on these three lines as illustrated in Figure 2.8B. (The term "channel" will be used to denote the 20 millisecond period for which each stator voltage is present on the line.) As can be seen from Figure 2.7, the

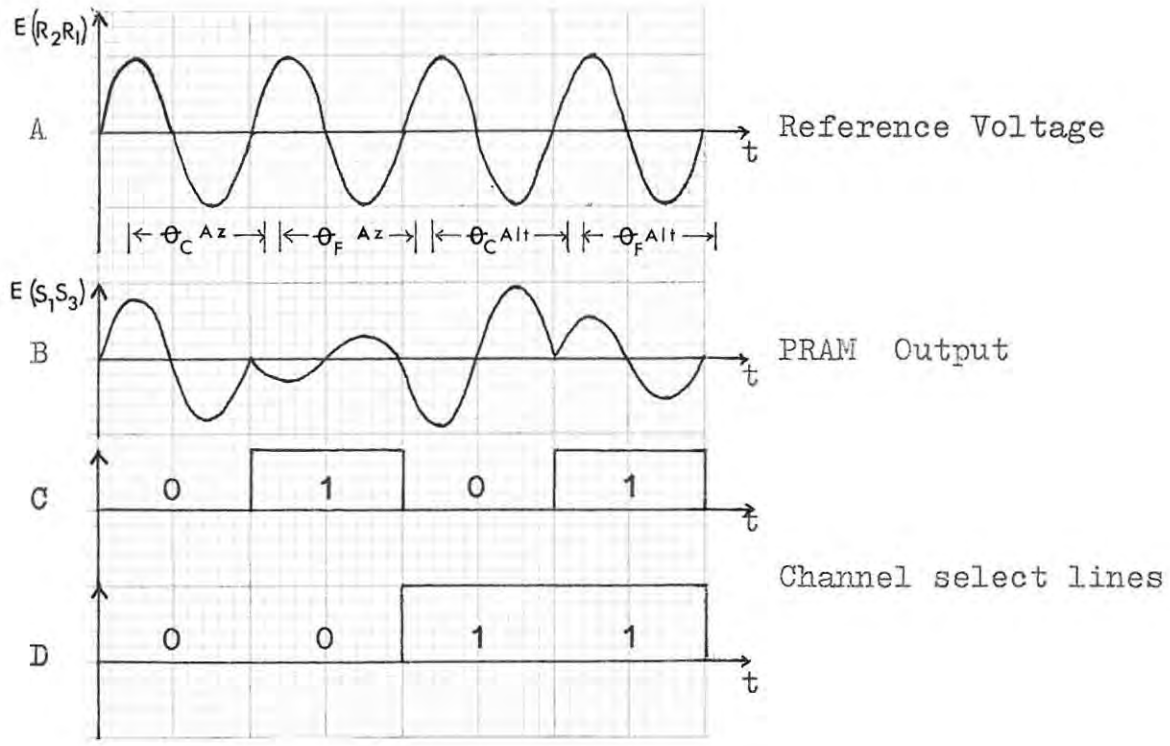

Figure 2.8 Reference derived multiplexing

multiplexing is done in such a way that all the voltages corresponding to E (S_1S_3) are put onto the same line and similarily for E (S_3S_2) and E (S_2S_1).

The multiplexing is done by means of three programmable amplifiers (PRAMS) (Harris Semiconductor 1973). A PRAM consists of four operational amplifiers in a single integrated circuit with one output common to all four. Any one of the four amplifiers may be selected by applying a two-bit binary number between 00 and 11 to the channel

select inputs of the PRAM. (Throughout the digital part of the tracking system binary numbers are represented by positive logic signals i.e. logic "0" is represented by 0 volts and logic "1" by +5 volts.) Figures 2.8 C & D indicate how these numbers are derived from the reference voltage.

The PRAMS are operated at unity gain and provision is made for further signal level adjustment by the operational amplifiers in the next stage. A fourth operational amplifier is also provided to allow adjustment of the reference voltage level if necessary.

2.2.4 PEAK DETECTORS AND ZERO-CROSSING DETECTORS

The four signals are then brought along shielded cable to the second part of the synchro-to-digital converter (Figure 2.9) where they go in parallel to the postive peak detectors and the zero-crossing detectors. The peak detectors provide a means of measuring the amplitudes of the stator voltages and the zero-crossing detectors are used to determine their relative phases.

A positive peak detector produces a positive dc voltage level at its output equal to the amplitude of voltage applied to its input (National Semiconductors 1972a). (The circuit may be found in Appendix 2.2). The outputs of three of the peak detectors, equal to the amplitudes E_1, E_2 and E_3

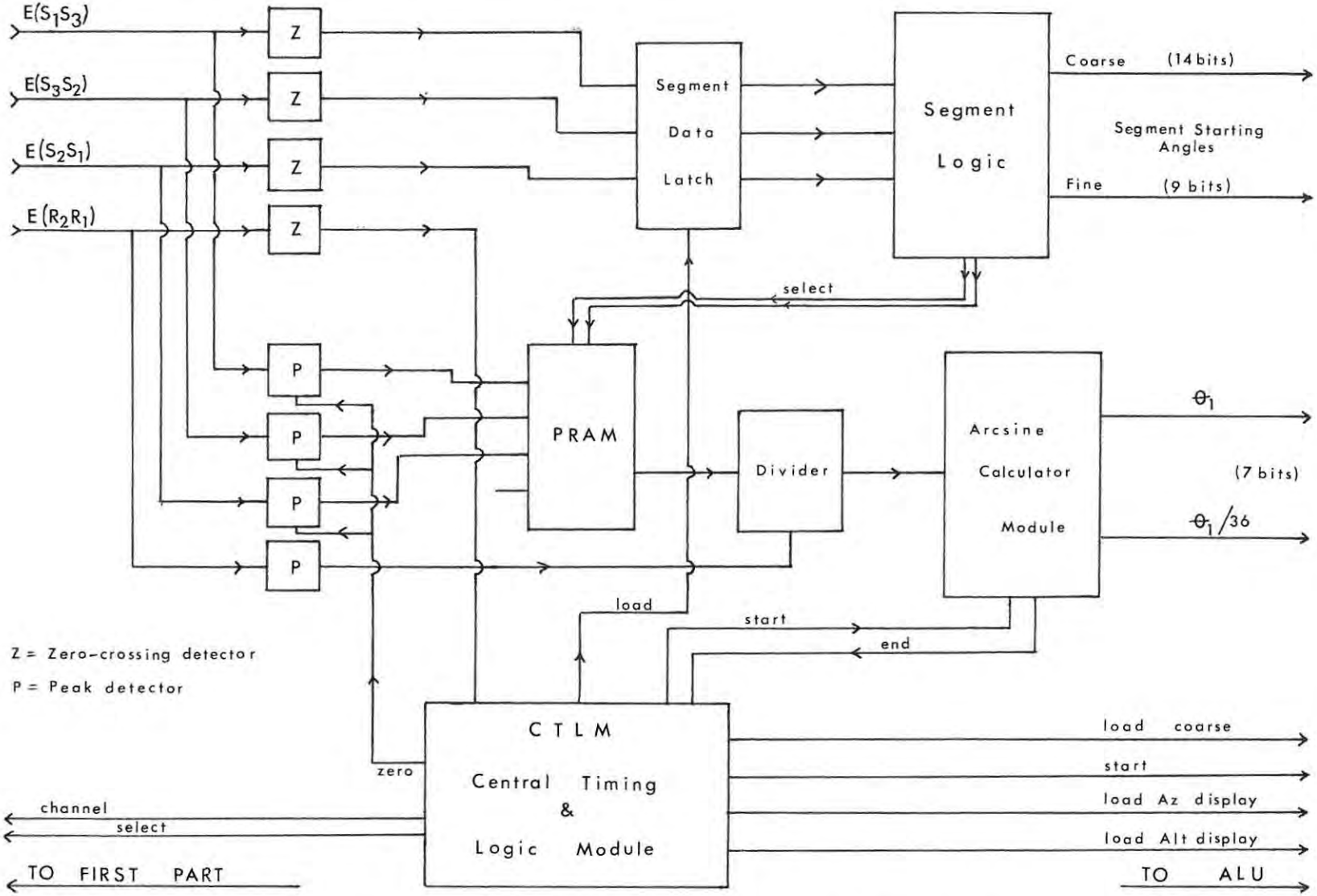

Figure 2.9 Synchro-to-digital converter (Part 2)

of the voltages $E(S_1S_3)$, $E(S_3S_2)$ and $E(S_2S_1)$, respectively, are applied to the inputs of another PRAM and, depending upon which segment the rotor is in, one of these three voltages is selected (see below) for measurement.

After the measurement is complete, but not later than 2,5 ms (section 2.2.7) into the next channel the peak detectors are zeroed so that new levels can be established for the voltages in that channel. The peak detectors are zeroed by triggering a f.e.t. switch (Appendix 2.2) at the correct time (Figure 2.11E) with a pulse from the central timing and logic module (CTLM) (section 2.2.7).

The output of a zero-crossing detector, an operational amplifier with one of the inputs held at zero volts, will be high (logic "1") if the level of the signal on the input is greater than zero volts and low (logic "0") if the level of the signal is less than zero volts. The output of the reference zero-crossing detector is therefore a squarewave voltage. This voltage is applied to the central timing and logic module to produce the channel select data and the other control signals. The outputs of the other three zero-crossing detectors are applied to the inputs of a latch which is loaded by a pulse from the CTLM 5 ms after the channel to be measured has been selected (Figure 2.11C). This timing was chosen to correspond to the centre of the first half cycle of the channel in order to give the zero-crossng detectors maximum sensitivity. The output of

the latch represents the numbers characteristic of the segments as indicated in Figure 2.5.

These numbers are decoded in three ways by suitable logic circuitry.

i) A two-bit binary number is produced to select the appropriate peak detector output for measurement.

ii) A fourteen-bit binary number, the coarse segment starting angle ($n \times 60^{o}$), is produced (section 2.2.6).

iii) A nine-bit (section 2.2.6) binary number, the fine segment starting angle ($1/36 \times n \times 60^{o}$), is also produced.

The two-bit number is applied directly to the PRAM which has the outputs of the positive peak detectors connected to it (Appendix 2.3). The PRAM then functions as a three-to-one multiplexer, the voltage which is to be measured appearing at its output. The two segment starting angles are applied directly to the arithmetic logic unit (ALU) where the appropriate one is selected for use in the calculation (Chapter 3) by a control signal from the CTLM.

2.2.5 THE DIVIDER

The next stage in the converter is the division of the voltage to be measured, by the reference voltage level, obtained from the fourth peak detector. The division is performed by an analogue multiplier (Motorola 1973) and the circuit diagram may be found in Appendix 2.3. The output of

the divider is given by the expression

$$V_{out} = \frac{+5V_{in}}{V_{ref}} \qquad 2.7$$

In this case

$$V_{out} = \frac{+5E_S}{E_R} \qquad \text{where } E_S = E_1,\ E_2 \text{ or } E_3 \qquad 2.8$$

This is done in order to make allowance for variations in the reference voltage, since E_S is always a constant fraction of the amplitude of the reference voltage, when the telescope is stationary. The output of the divider will always be a dc voltage between 0 and +5 volts. This voltage is applied to the input of an analogue-to-digital converter.

2.2.6 ANALOGUE-TO-DIGITAL CONVERSION AND ARCSINE CALCULATION

The analogue-to-digital conversion is started by a pulse from the CTLM (Figure 2.11D) one millisecond after the center of the second cycle half of the channel, to ensure that the voltage on the ouput of the peak detector has reached the value corresponding to the amplitude of the stator voltage in that channel. The analogue-to-digital converter takes a maximum of one millisecond (Datel 1973) to convert the dc voltage on its input to an 10-bit binary number. The converter used (ADC-E10B, Datel 1973) is of the dual-slope integrating type. A dual-slope integrating converter is much slower than a successive approximations converter having the same clock rate, but costs less for any given accuracy (Hnatek 1976). In the synchro-to-digital

converter, speed is not as important as accuracy and the choice was made on those grounds. The 10-bit binary number thus obtained is proportional to the sine of the angle θ_1 (section 2.1.3).

Figure 2.10 is a block diagram of the arcsine calculator

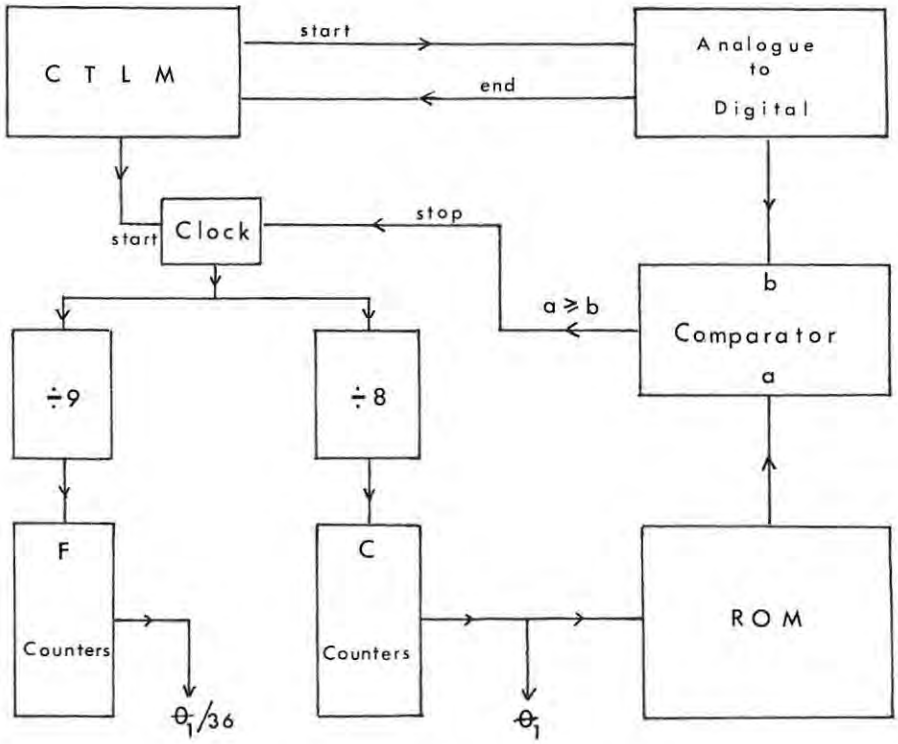

Figure 2.10 The arcsine calculator module

module. When the analogue-to-digital conversion is complete, the analogue-to-digital converter sends a pulse to the CTLM. The CTLM in turn starts a clock which increments the input to a sine look-up table read-only memory (ROM). The output of the ROM (National Semiconductors 1972b) is an eight-bit binary number equal to the sine of the angle (0° to 90°) on its input. The 8-bit number from the ROM and the eight most

significant bits of the output of the analogue-to-digital converter are compared bit for bit by a digital comparator. When the output of the ROM is greater than or equal to the output of the analogue-to-digital converter, the comparator stops the clock. The output of the C-counters (Figure 2.10) is then equal to the angle θ_1.

In order to avoid the use of fractional numbers in the synchro-to-digital converter, a unit of angular measurement, the Rhodes Unit (R.U.), was introduced. The Rhodes Unit is defined in such a way that

$$360^{\circ} = 2^{14} \text{ R.U.} = 16384 \text{ R.U.}$$

thus

$$1 \text{ R.U.} = 0{,}2196^{\circ} = 1{,}32'$$

Only the seven most significant bits of the input to the ROM are used. This means that 128 steps correspond to 90°(4096 R.U.) in the case of the coarse angle and therefore each step corresponds to $0{,}7^{\circ}$ which is 32 R.U. Thus in the case of the coarse angle, the least significant bit of the C-counters corresponds to exactly 2^5 R.U.

In the case of the fine angle, 128 steps correspond to $2{,}5^{\circ}$ so that each step is equal to $0{,}01953^{\circ}$ = 8/9 R.U. Because the use of steps equal to 8/9 R.U. each is undesirable, a scaling factor is required to convert these steps to steps of one Rhodes Unit each. For this reason, the signal which increments the C-counters is 1/8 of the frequency of the clock and the signal which increments the F-counters is 1/9

of the clock frequency. The number on the output of the F-counters is thus 8/9 of that on the output of the C-counters, and since this is required scaling factor, the output of the F-counters gives the desired angle, $\theta_1/36$, between 0 and 2,5° steps of 1 R.U. The outputs of both sets of counters are applied to the arithmetic logic unit where the number from the F-counters is treated as the fine angle, $\theta_1/36$, (section 2.1.3) and the one from the C-counters as the coarse angle, θ_1. The CTLM produces the necessary control pulses to indicate which of these two angles is to be used after the measurement of a particular channel (synchro).

The resolution of the synchro-to-digital converter is thus 1 R.U. which is equal to 1,32', less than one half of one tenth of a beamwidth. This meets the specifications indicated in Chapter 1.

Table 2.1 shows the coarse and fine segment starting angles and the range of the coarse and fine angles.

2.2.7 THE CENTRAL TIMING AND LOGIC MODULE (CTLM)

A good over view of the operation of the synchro-to-digital converter may be gained by considering the operations performed by the CTLM (Figure 2.9 and Figure 2.11). The reference output from the zero-crossing detectors (Figure 2.11A) enters the CTLM which produces one signal of

	Degrees	R.U.	Binary (MSB … LSB)
Coarse segment starting angle	0	0	0 0 0 0 0 0 0 0 0 0 0 0
	60	2731	0 0 1 0 1 0 1 0 1 0 1 1
	120	5461	0 1 0 1 0 1 0 1 0 1 0 1
	180	8192	1 0 0 0 0 0 0 0 0 0 0 0
	240	10923	1 0 1 0 1 0 1 0 1 0 1 1
	300	13653	1 1 0 1 0 1 0 1 0 1 0 1
Coarse angle θ_1	0	0	0 0 0 0 0 0 0 0
	0,7	32	0 0 0 0 0 0 0 1
	1,4	64	0 0 0 0 0 0 1 0
	.	.	.
	59,8	2730	1 0 1 0 1 0 1
Fine segment starting angle	0	0	0 0 0 0 0 0 0 0 0
	1,67	76	0 0 1 0 0 1 1 0 0
	3,33	152	0 1 0 0 1 1 0 0 0
	5	228	0 1 1 1 0 0 1 0 0
	6,67	303	1 0 0 1 0 1 1 1 1
	8,33	379	1 0 1 1 1 1 0 1 1
Fine angle $\theta_1/36$	0	0	0 0 0 0 0 0 0 0 0
	0,022	1	0 0 0 0 0 0 0 1
	0,044	2	0 0 0 0 0 1 0
	.	.	.
	1,648	75	1 0 0 1 0 1 1
	359,978	16383	1 1 1 1 1 1 1 1 1 1 1 1 1 1 1 1 1 1

Table 2.1 The coarse and fine segment starting angles and the ranges of the C- and F-counters.

half the reference frequency and another of one quarter of the reference frequency (Figure 2.11B). These two signals are fed to the set of PRAMS which multiplexes the signals from the synchros into four channels on three lines (Figure 2.8).

Five milliseconds after a channel has been selected the outputs of the zero-crossing detectors are loaded into a latch to produce the segment starting angles and to select the appropriate peak detector output for measurement (Figure 2.11C). Eleven milliseconds later, 16 ms after the start of the channel, the analogue-to-digital conversion is started (Figure 2.11D). The end of conversion signal from the analogue-to-digital converter is used to produce pulses which zero the peak detectors (Figure 2.11E) and start the arcsine calculation (Figure 2.11F). The peak detectors are held at zero until approximately 1 ms into the next channel to avoid interference between channels. When the arcsine calculation is complete, approximately 1 ms before the next channel is selected, a pulse is sent to the ALU which either loads the coarse angle into a latch (Figure 2.11G) or starts the calculation (Figure 2.11H), depending on whether the present channel contains information for a coarse or a fine synchro. After every second channel, i.e. the completion of a coarse-fine pair, a pulse is produced which loads the appropriate ALU front panel display. This pulse occurs approximately 2 ms into the next channel, and is also used to load the result of the calculation performed by the

ALU (Figure 2.11 I & J) into the digital junction.

Thus the CTLM controls the entire determination and display of the telescope co-ordinates.

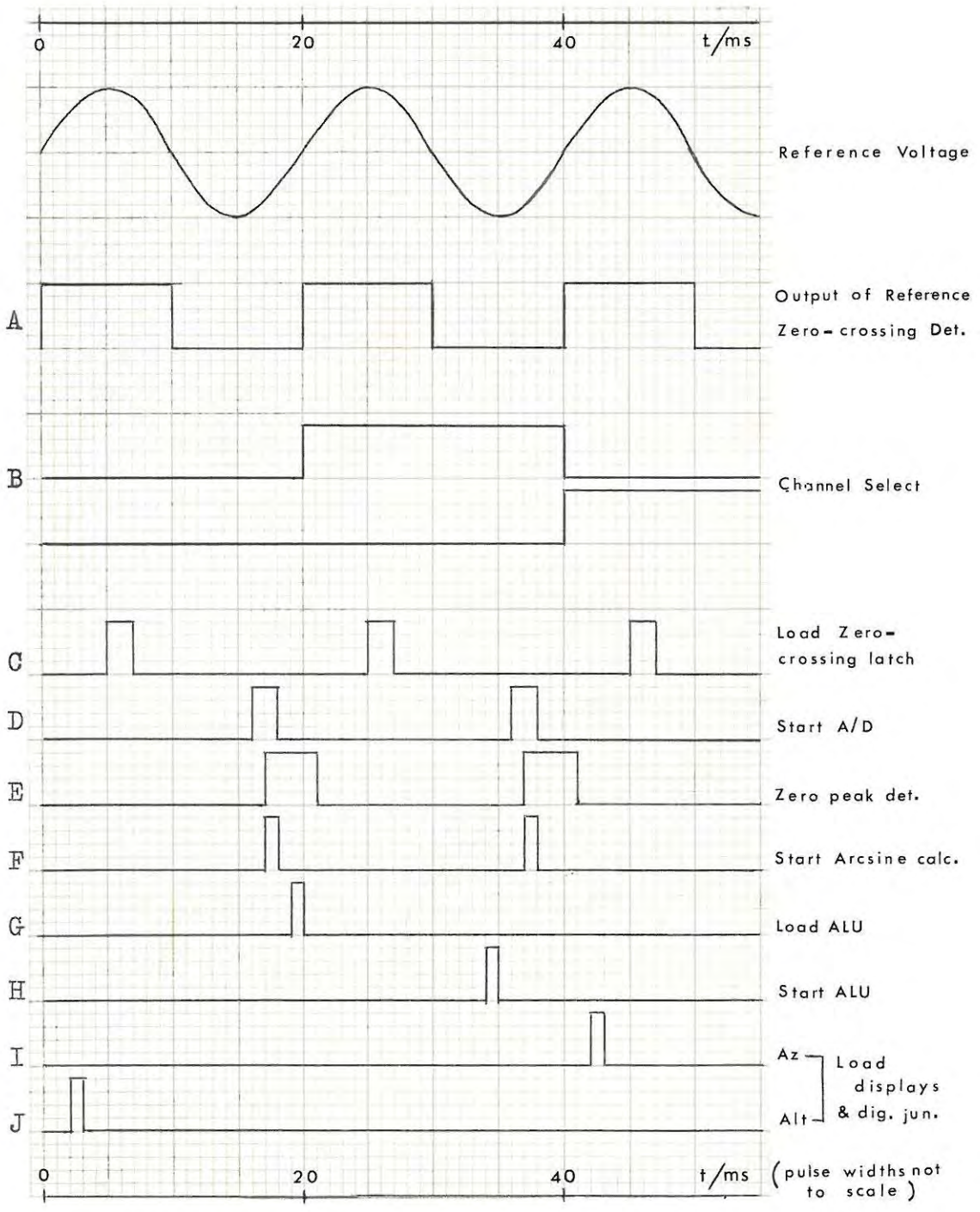

Figure 2.11 The timing and control pulses produced by the CTLM shown for two channels

CHAPTER THREE

THE ARITHMETIC LOGIC UNIT

3.1 INTRODUCTION

It is the task of the arithmetic logic unit (ALU) to perform the following three operations:

i) Combine the coarse segment starting angle (14 bits) with the coarse angle θ_1 (7 bits) to give the coarse angle θ_C (14 bits).

ii) Combine the fine segment starting angle (9 bits) with the fine angle $\theta_1/36$ (7 bits) to give the fine angle θ_F (9 bits).

iii) Combine the coarse angle, θ_C, with the fine angle, θ_F, to give the altitude or the azimuth as might be the case.

In the first two cases the operation is one of simple binary addition, the only unusual feature being the fact that the least significant bit of the coarse angle, θ_1, represents 32 R.U. (section 2.2.6).

The combination of θ_C and θ_F requires more care. As was pointed out in section 2.1.4, the coarse and fine synchros operate in much the same way as the hands of a watch. The desired angle can therefore be found by taking θ_C to the nearest 10°, θ_C', such that θ_C' is less than θ_C and adding θ_F

to θ_C'.

There are two possible conditions which will lead to error in this calculation due to irregularities in the mechanical alignment of the synchro windings. Suppose that θ_F is less than 10 degrees by a very small amount (say $\theta_F = 9{,}9^\circ$). One would then expect θ_C to be less than n x 10° (where n is an integer) by a very small amount. If, however, θ_C is greater than instead of less than n x 10° by a very small amount due to misalignment, the calculated angle, θ, will be n x 10° + $9{,}9^\circ$ instead of (n - 1) x 10° + $9{,}9^\circ$ (Error 1). Alternatively, if θ_F is greater than 0 degrees by a small amount (say $\theta_F = 0{,}1^\circ$) and θ_C is less than n x 10° by a small amount, then θ will be (n - 1) x 10° + $0{,}1^\circ$ instead of n x 10° + $0{,}1^\circ$ (Error 2). This is best illustrated by the two examples in Figure 3.1 in which a coarse synchro reading from 0 to 80° has been used for the sake of clarity.

In practice synchros are aligned at θ_C and θ_F equal to zero i.e. electrical zero (Miller 1977, section 5.13) and therefore there is no error at that point. There are a further thirty-five positions at which the two errors can occur and a very small nonlinearity at one of these positions can produce either of the errors described above.

This error can be removed by comparing the combined angle θ with θ_C. If $\theta - \theta_C$ is greater than or equal to $+5^\circ$, 10° must be subtracted from θ. If $\theta - \theta_C$ is less than or equal

Error I

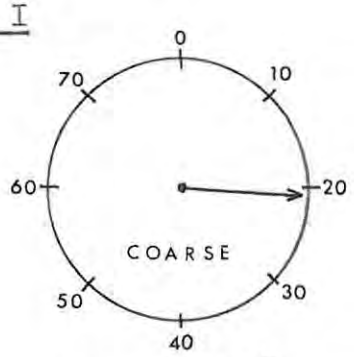

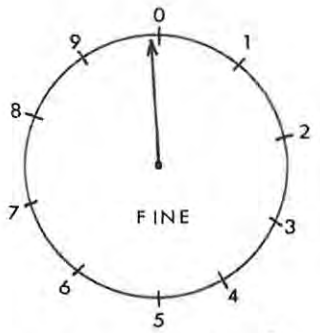

$\theta_C = 20{,}01^\circ$ $\qquad$ $\theta_F = 9{,}999^\circ$

$\theta'_C = 20^\circ$ $\qquad$ $\therefore \theta = 29{,}999^\circ$

It can be seen that θ should be $19{,}999^\circ$

Correction: $\theta - \theta_C > +5^\circ$ $\quad$ let $\theta = \theta - 10^\circ = 19{,}999^\circ$

Error II

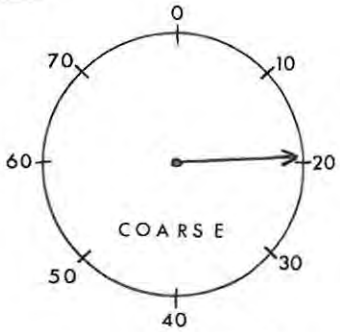

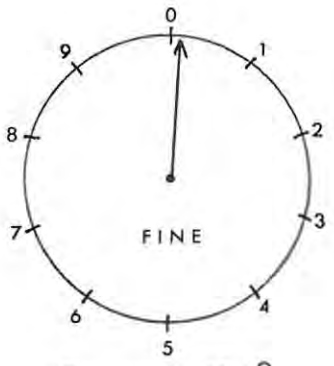

$\theta_C = 19{,}99^\circ$ $\qquad$ $\theta_F = 0{,}001^\circ$

$\theta'_C = 10^\circ$ $\qquad$ $\therefore \theta = 10{,}001^\circ$

It can be seen that θ should be $20{,}001^\circ$

Correction: $\theta - \theta_C < -5^\circ$ $\quad$ let $\theta = \theta + 10^\circ = 20{,}001^\circ$

Figure 3.1 The errors which can occur when combining θ_C and θ_F

to -5°, 10° must be added to θ. This allows for the nonlinearities which might occur and eliminates the possible errors arising from them. (The correction is also illustrated in Figure 3.1).

Mathematically, the calculations performed by the ALU are represented by the following set of equations:

$$\theta_C = \text{coarse segment starting angle} + \theta_1 \qquad 3.1$$

$$\theta_F = \text{fine segment starting angle} + \theta_1/36 \qquad 3.2$$

$$\begin{aligned}\theta &= n \times 10^\circ + m \times 10^\circ + \theta_F \\ &= \theta_C' + m \times 10^\circ + \theta_F \end{aligned} \qquad 3.3$$

where $n = 0,1,2,3, \ldots, 35$

such that $\theta_C - 10^\circ < n \times 10^\circ \leqslant \theta_C$

$$\text{and } m = \begin{cases} +1 & \text{if } \theta_C - \theta_C' - \theta_F \geqslant +5^\circ \\ 0 & \text{if } -5^\circ < \theta_C - \theta_C' - \theta_F < +5^\circ \\ -1 & \text{if } \theta_C - \theta_C' - \theta_F \leqslant -5^\circ \end{cases}$$

3.2 THE CALCULATION OF θ_C AND θ_F

Figure 3.2 is a block diagram of the ALU. The outputs of the C-counters and the coarse segment logic in the synchro-to-digital converter are applied to the fourteen-bit binary adder, A1. A fourteen-bit binary adder consists of 4 four-bit adders cascaded together as shown in Figure 3.3. Also illustrated in Figure 3.3 is the way in which θ_1 and the coarse segment starting angle are applied to A1. The inputs a_0 to a_4 of A1 are held at "0" since the coarse angle θ_1, increases in steps of 2^5 R.U. corresponding to the bit a_5 of the angle θ_C. At the end of a coarse channel in the synchro-to-digital converter the output of A1 is equal to the angle, θ_C, which is the angle the rotor of the coarse

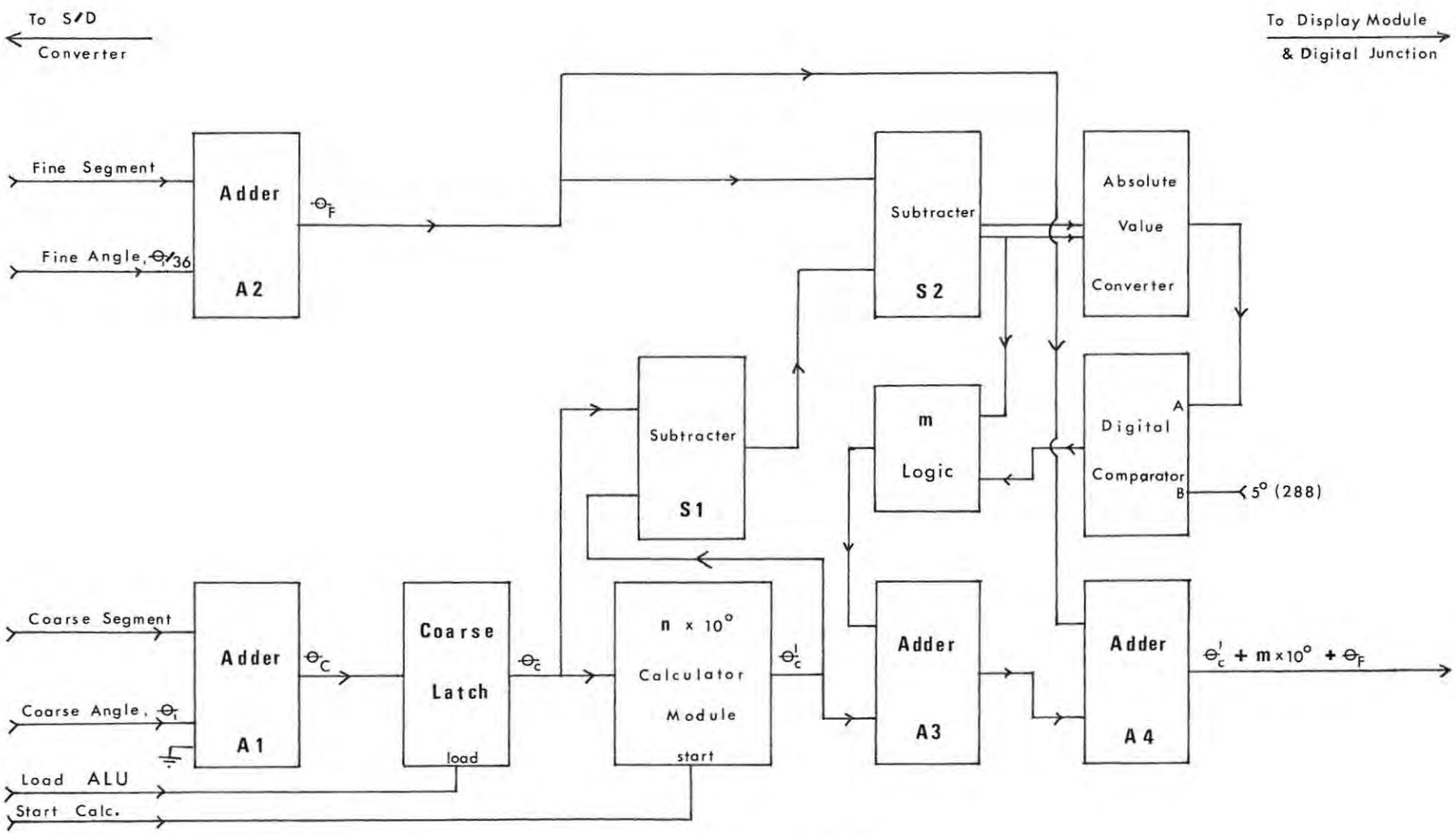

Figure 3.2 The ALU

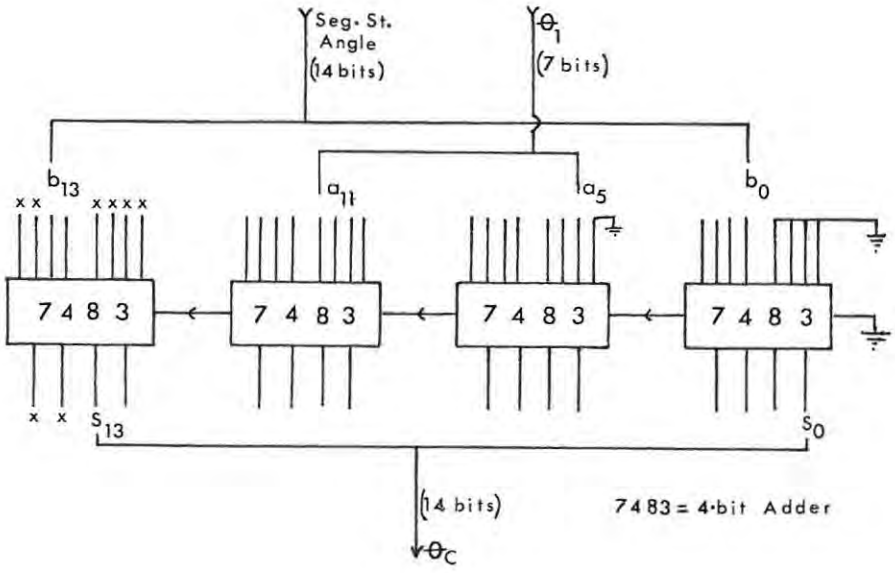

Figure 3.3 A typical 14-bit binary adder

synchro makes with its stator axis. This angle, θ_C, is loaded into the coarse latch (Figure 3.2) at the completion of a coarse channel by a pulse from the CTLM in the synchro-to-digital converter (Figure 2.11G). Twenty milliseconds later, on the completion of the fine channel, the output of the nine-bit binary adder, A2, which has on its inputs the fine segment starting angle, and the fine angle $\theta_1/36$ from the F-counters, is equal to the fine angle θ_F. A pulse from the CTLM (Figure 2.11H) then starts the "n x 10^o" calculator module in order to produce the angle θ'_C.

3.3 THE "n x 10^o" CALCULATOR MODULE

The "n x 10^o" calculator module (Figure 3.4) consists of a 14-bit binary adder with 10^o (455 R.U.) permanently wired to

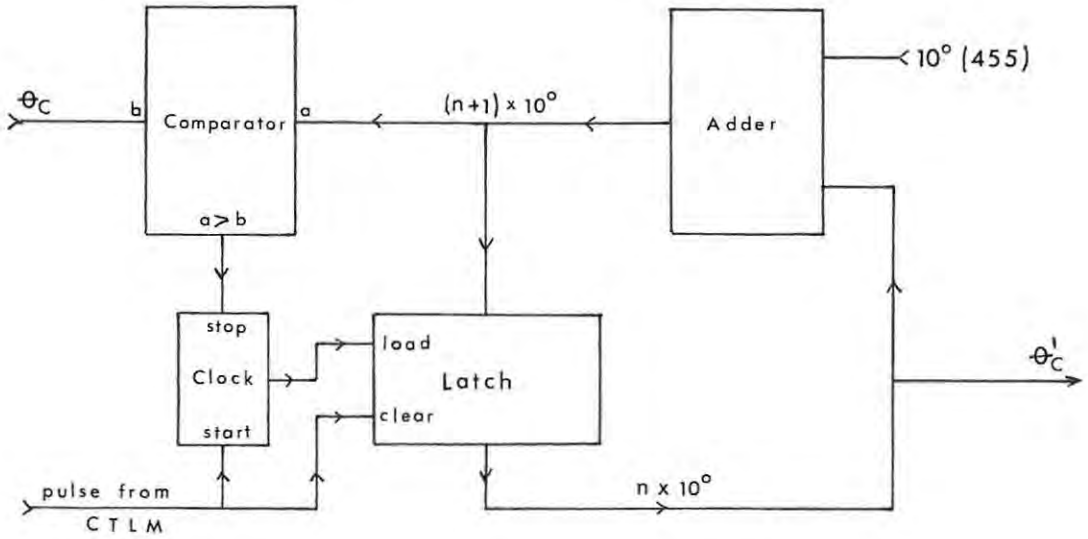

Figure 3.4 The "n x 10^{o}" calculator module

one of the inputs. The output of the adder is compared bit for bit with the angle θ_C in a digital comparator, and is also applied to the input of a latch. The output of the latch is connected to the second input of the adder. The start pulse from the CTLM simultaneously clears the latch and starts the clock which loads the latch with the number on the output of the adder. When the number on the output of the adder is greater than θ_C the clock will immediately be stopped by the output of the digital comparator. At this stage the output of the latch will be equal to n x 10^{o} (θ'_C) as defined by equations 3.3. The output of the latch will not change until the next start pulse from the CTLM.

3.4 DETERMINATION OF "m"

From equation 3.3 it can be seen that the value of "m" is

determined by the magnitude and the sign of the expression $\theta_C - \theta_C' - \theta_F$. The subtracter, S1 (Figure 3,2). adds the 2's complement of θ_C' to θ_C. The output of S1 is therefore equal to $\theta_C - \theta_C'$. The 2's complement of θ_C' is obtained by inverting all the bits of θ_C' and adding "1" via the carry bit of the adder as illustrated in Figure 3.5. The subtracter S2 adds the 2's complement of θ_F to $\theta_C - \theta_C'$

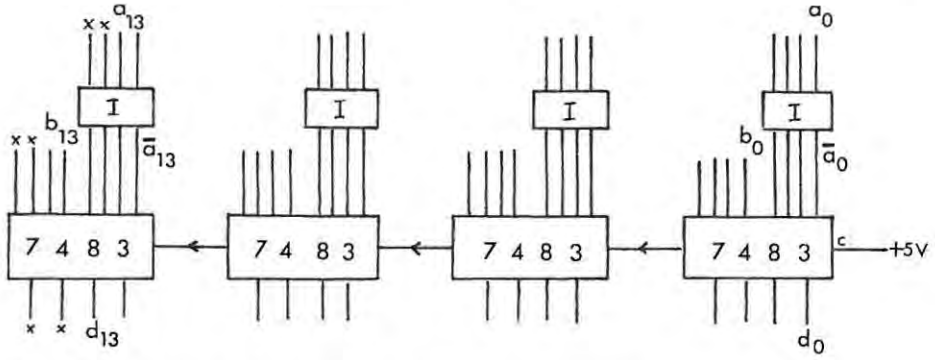

7483 = 4-bit adder I = Inverter C = Carry

Figure 3.5 A typical 14-bit binary subtracter

thereby producing $\theta_C - \theta_C' - \theta_F$ at its output.

Since $-10^\circ < \theta_C - \theta_C' < +10^\circ$

and $-10^\circ < \theta_C - \theta_C' - \theta_F < +10^\circ$

where $+10^\circ = +455$ R.U. $= +707_8 = 00\ 000\ 111\ 000\ 111_2$

and $-10^\circ = -455$ R.U. $= -707_8 = 11\ 111\ 000\ 111\ 001_2$,

only twelve bits are used for $\theta_C - \theta_C'$ and $\theta_C - \theta_C' - \theta_F$. The most significant bit (MSB) from the output of S2 gives the sign of $\theta_C - \theta_C' - \theta_F$, "0" for positive and "1" for negative. This bit is used in the "m"-logic, since "m" will be 0 or +1 if it is a "0" and 0 or -1 if it is a "1".

This sign bit from S2 is also used in the next stage of the ALU to produce the absolute value of $\theta_C - \theta'_C - \theta_F$.

The absolute value converter (Figure 3.6) consists of a

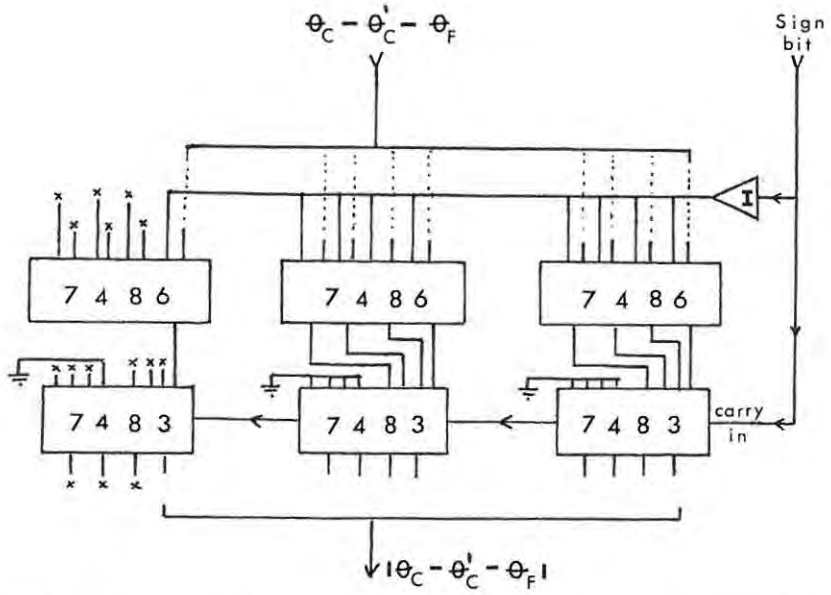

7483 = Adder 7486 = Exclusive-or I = Inverter

Figure 3.6 The Absolute value converter

9-bit binary adder with all the bits of one input set equal to zero. The output of S2 is wired to the other input of the adder via a set of exclusive-or gates. The sign bit is connected to the second input of each exclusive-or gate and also to the carry-in bit of the adder. If the sign bit is a zero, the output of the adder will not be different from the output of S2. If the sign bit is a one, however, all the bits of $\theta_C - \theta'_C - \theta_F$ will be inverted by the exclusive-or gates and 1 will be added via the carry-in bit of the adder. The output of the adder in this case is the 2's complement

of the output of S2, i.e. the absolute value of $\theta_C - \theta_C' - \theta_F$.

The value of "m" is only zero if the absolute value of $\theta_C - \theta_C' - \theta_F$ is less than $+5^o$. The output of the absolute value converter is therefore compared bit for bit with $+5^o$ (288 R.U.) in a 9-bit digital comparator. The output of the comparator will be a "1" if $\theta_C - \theta_C' - \theta_F \geqslant +5^o$. The "m"-logic thus receives two bits, the output of the comparator and the sign of $\theta_C - \theta_C' - \theta_F$. It produces a 14-bit binary number equal to m x 10^o as defined by

Sign bit of $\theta_C - \theta_C' - \theta_F$	Comparator output	m	number produced m-logic
0	0	0	00 000 000 000 000
0	1	+1	00 000 111 000 111
1	0	0	00 000 000 000 000
1	1	-1	11 111 000 111 001

Table 3.1 The numbers produced by the m-logic

equation 3.3 according to the scheme in Table 3.1.

3.5 CALCULATION OF THE ANGLE θ

The number produced by the "m" logic is m x 10^o, as required by equations 3.3 to avoid errors due to small nonlinearities in the stator windings, and this is added to θ_C' by the adder A3 (Figure 3.2). The adder A4 adds θ_F to the output of A3

thereby producing the desired angle

$$\theta = \theta_C' + m \times 10^\circ + \theta_F$$

In this system, there is no need for a modulo 360° (2^{14} R.U.) converter. (This is illustrated by the two examples in Figure 3.7.) The angle θ, a 14-bit binary number, is then fed to the digital junction and to the display module.

Example 1

$$\begin{aligned} \text{If } \theta_C' &= 15929 \text{ R.U.} = 11\ 111\ 000\ 111\ 001_2 \\ \text{and } m \times 10^\circ &= 455 \text{ R.U.} = 00\ 000\ 111\ 000\ 111_2 \\ \text{then } \theta_C' + m \times 10^\circ &= 16384\ (0) \text{ R.U.} = 00\ 000\ 000\ 000\ 000_2 \end{aligned}$$

which is correct.

Example 2

$$\begin{aligned} \text{If } \theta_C' &= 0 \text{ R.U.} = 00\ 000\ 000\ 000\ 000_2 \\ \text{and } \theta_F &= 319 \text{ R.U.} = 00\ 000\ 100\ 111\ 111_2 \\ \theta_C' + \theta_F &= 319 \text{ R.U.} = 00\ 000\ 100\ 111\ 111_2 \\ \text{If } m \times 10^\circ &= -455 \text{ R.U.} = 11\ 111\ 000\ 111\ 001_2 \\ \text{then } \theta_C' + \theta_F + m \times 10^\circ &= 11\ 111\ 101\ 111\ 000_2 \\ &= 16248 \text{ R.U.} \end{aligned}$$

which is correct.

Figure 3.7 Illustration that modulo 2^{14} is not required

3.6 THE DISPLAY MODULE

The display module (Figure 3.8) is mounted in the ALU rack. An array of binary to binary-coded decimal (BCD) decoders is used to convert the 14-bit binary number to a 17-bit (four

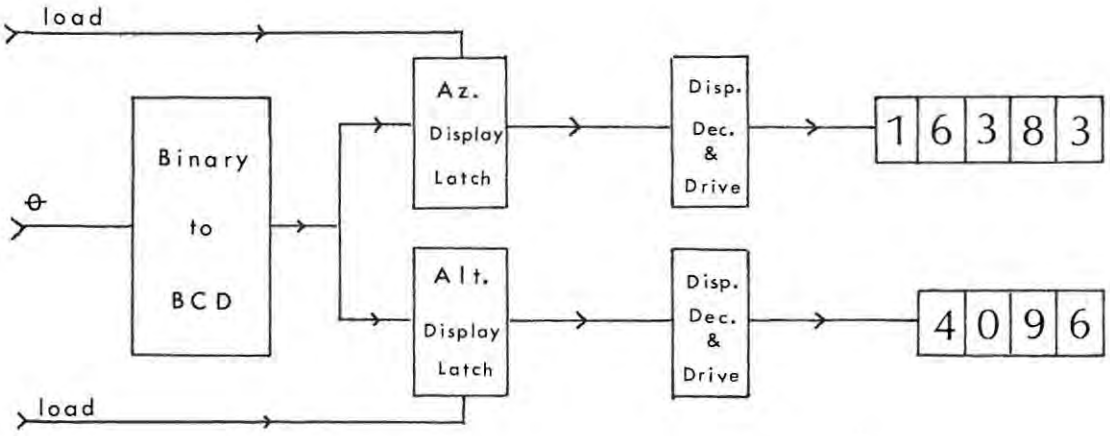

Figure 3.8 The display module

and a half digit) binary coded decimal number. This number is loaded into either the altitude display latch or the azimuth display latch by the appropriate pulse from the CTLM (section 2.2.7, Figure 2.11 I & J). The latches are followed by seven segment decoders and display driver circuitry.

The front panel display shows the altitude and the azimuth in Rhodes Units. Four and a half digits have been used for the azimuth display but only four digits are necessary for altitude because the altitude is never more than 90^{o}

(4096 R.U.). Figure 3.9 is a photograph of the ALU front panel. The off-position l.e.d.s will be discussed in section 4.2.5.

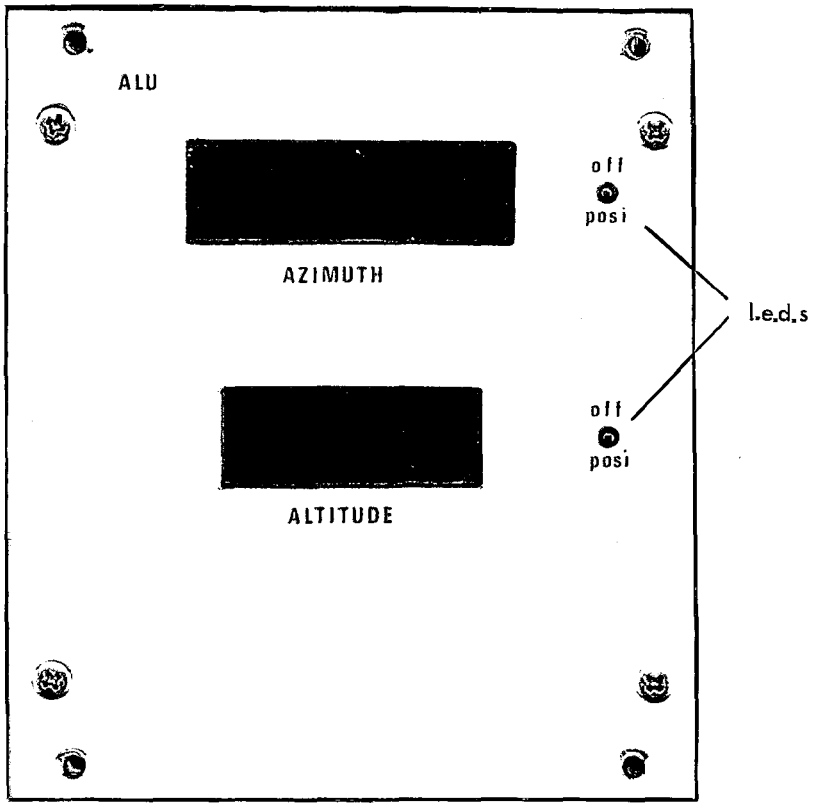

Figure 3.9 The ALU front panel

CHAPTER FOUR

THE COMPUTER JUNCTION, THE DIGITAL JUNCTION AND THE MOTOR DRIVE UNIT

4.1 THE COMPUTER JUNCTION

4.1.1 DESIGN CONSIDERATIONS

The following points were taken into consideration in designing an interface with the computer for the tracking system:

i) A dedicated computer was not available. However, a multi-user version of the language BASIC, MULTEXBASIC, was available for the Nova computer in the Physics Department and the tracking programs, which are demanding neither in terms of time nor storage space, could run in the background with such a system leaving the rest of the computer free for other users. In this case, the interface with the computer can be an asynchronous terminal, which has the advantage that the computer can be replaced by a visual display unit (VDU) or a teletypewriter (TTY) for testing purposes. It obviates the necessity for a direct interface with the computer data lines and therefore ensures compatibility with many other mini- and micro-computers.

ii) Provision was also made for manual position encoding from the front panel. This means that in cases where a single pair of co-ordinates is required e.g. for a drift scan, it is not necessary to use the computer, or to drive the telescope manually.

iii) It was considered desirable to transmit command signals as well as co-ordinates from the computer so that the control of other telescope operations, e.g. firing the noise tube, parking the telescope, etc., could be built into the computer programs. All of these operations can also be performed by the operator by means of front panel switches.

4.1.2 OPERATION

Figure 4.1 is a block diagram of the computer junction. At the time of design, an asynchronous data interface, the Universal Asynchronous Receiver/Transmitter (UART) (Texas Instruments 1973) was readily available. The receiver section of this device accepts serial data of programmable word length from a transmission line and converts it to parallel data making the appropriate checks for stop, start and parity bits. The baud rate is externally selected by the clock frequency. In the computer junction a crystal oscillator has been provided in conjunction with a programmable divider chain to give baud rates ranging from 110 to 1200 baud. The system is normally operated at 1200

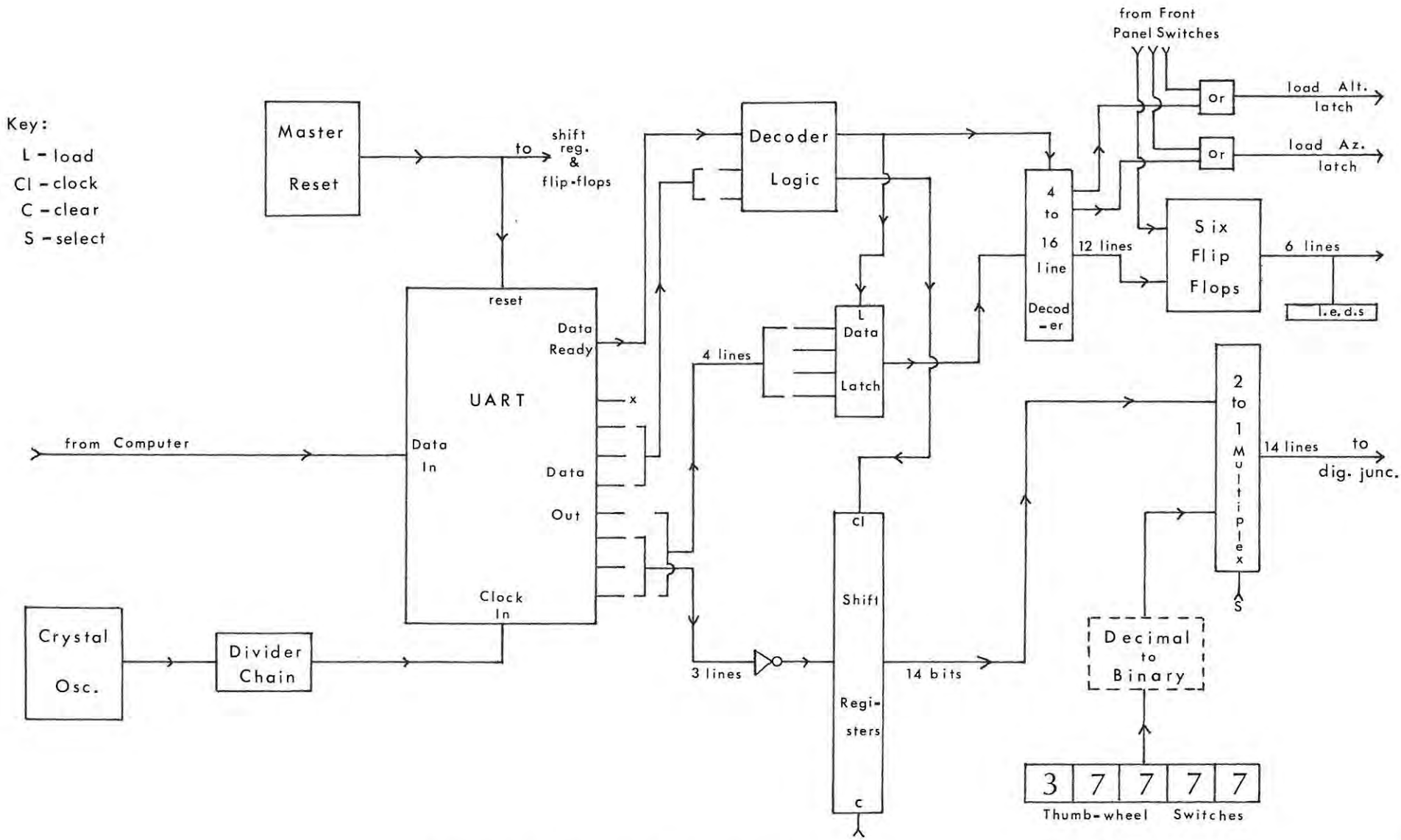

Figure 4.1 The computer junction

baud and at present the baud rate is not switchable, a small change in the wiring on the appropriate printed circuit board being necessary when a different baud rate is required.

The data received from the computer is in the form of extended ASCII code (Kline 1977, page 38; Hilburn and Junlich 1976, section 3.8) including start stop and parity bits. The ASCII code (Appendix 4.1) is a seven-bit code consisting of four bits of character information, and a three-bit zone. From Table 4.1 it can be seen that all numbers have their zone equal to three and that all the letters of the alphabet from "A" to "O" have their zone

Character		ASCII Code	
		Zone	Character
Numbers	0	011	0000
	1	011	0001
	9	011	1001
Letters	A	100	0001
	O	100	1111

Table 4.1 Examples of the ASCII Code

equal to four.

When the data received from the computer has been assembled on the seven data outputs of the UART, which has been programmed to receive a seven-bit word, the "data ready" output of the UART (Figure 4.1) goes high. This output and

the three zone bits go to suitable decoder logic circuitry which determines whether a number or a letter has been received.

Since the character code for a number is the number itself in binary, the desired telescope co-ordinates are converted to octal in the computer and transmitted to the computer junction one octal digit at a time. Each telescope co-ordinate transmitted consists of five octal digits in the range 00000_8 to 37777_8 (16383 R.U.). Every number received is completely specified by the three least significant character bits since numbers greater than 7 are not transmitted.

When a number is received, the decoder logic (Figure 4.1) produces a pulse which clocks the inverted (see Figure 4.1) three least significant character bits in parallel into the first bit of 3 five-bit shift registers. After all five digits corresponding to the octal value of a desired co-ordinate have been clocked into the three five-bit shift registers, the shift registers will have on their outputs the complement of the desired 14-bit binary number corresponding to either the altitude or the azimuth (Figure 4.2). (The reason for the use here of the complementary form of the numbers will become apparent in section 4.2.2.) This 14-bit number and the 14-bit number from the thumbwheel switches on the front panel of the computer junction (see below) are applied to the inputs of a

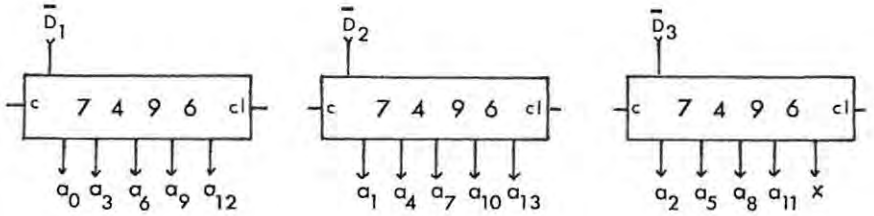

7496 = 5-bit shift register c = clear cl= clock

Figure 4.2 The shift register output

two-to-one multiplexer (Figure 4.1). Unless the pushbutton switch on the front panel of the computer junction ("load", see below) is depressed, the number from the shift registers will appear on the output of the multiplexer. The output of the multiplexer goes in parallel to 2 fourteen-bit latches, the altitude latch and the azimuth latch, in the digital junction (Figure 4.4).

Each five-digit octal number transmitted by the computer is followed by either the letter "A" or the letter "B" to indicate whether the number corresponds to the altitude or the azimuth. When a letter of the alphabet is indicated by the zone bits, a pulse is produced by the decoder logic which loads all four character bits into a latch and enables the four-to-sixteen line decoder for the duration of the pulse. The latch is redundant in the present circuit but was included to facilitate the addition of more versatile decoder circuitry if that should become necessary. The outputs of the latch are applied to the inputs of the four-to-sixteen line decoder. A pulse therefore appears on the decoder output line corresponding to the letter of the alphabet received.

The pulse produced when the letter "A" is received is used to load the altitude latch in the digital junction with the number on the output of the two-to-one multiplexer. The azimuth latch is loaded in a similar fashion when the letter "B" is received. A set of six flip-flops, F_1 to F_6, each of which may be used to control one of the telescope functions, e.g. firing the noise tube, has also been provided. The flip-flops F_1 to F_6 are set by pulses from the output of the four-to-sixteen line decoder when the letters "C", "E", "G", "I", "K" and "M" respectively are received and cleared similarly by the reception of the letters "D", "F", "H", "J", "L" and "N" respectively. At present the only telescope functions wired to these flip-flops are "lock", "hold" and "automatic return inhibit" all of which are described in the next section. A light emmitting diode on the front panel of the computer junction (Figure 4.3) has been wired to the output of each flip-flop to provide the operator with visual information concerning the status of each function. If necessary many more control functions can be provided by making use of the letters "P" to "Z" (zone 5) and the other characters of the ASCII code. The circuitry required for such additions is minimal.

A desired set of co-ordinates may also be loaded into the tracking system via the thumbwheel switches on the front panel of the computer junction (Figure 4.3). Unfortunately, because the decimal-to-binary converter (Figure 4.1) has not yet been built, the co-ordinates on the thumbwheel switches

Figure 4.3 The computer junction front panel

must be in octal. When the "load" button on the front panel is depressed, the 14-bit number from the thumbwheel switches, which is the complement of the number dialled in, appears at the output of the two-to-one multiplexer and a pulse is produced which loads the appropriate latch in the digital junction depending on the setting of the altitude/ azimuth selector switch on the front panel.

The six flip-flops which are used to control some of the telescope functions may also be set or cleared from the front panel of the computer junction, by means of the selector and on/off switches provided (Figure 4.3).

A master reset unit which initialises the UART, and clears the flip-flops and the shift registers, to ensure a predetermined set of conditions at switch-on, or after a power failure, has been included in the computer junction (Figure 4.1).

At present the transmitter section of the UART is not being used. In the system as it was originally envisaged, the data capture would have been on paper tape (Nunn 1974). With a few minor changes to the present circuit, the UART, which can operate either in full duplex (simultaneous transmission and reception) or in half duplex (alternate transmission and reception) mode, could be used to transmit the data obtained with the telescope directly to the computer.

4.2 THE DIGITAL JUNCTION

4.2.1 DESIGN SPECIFICATIONS

The digital junction was originally designed to be compatible with the motor drive unit built for the motors supplied with the antenna mount. Owing to difficulties experienced with the driver/amplifier circuit built for these motors, they were later replaced with motors of a different kind and a new motor drive unit was designed and built (section 4.3). In the present section the original design of the digital junction is presented together with the changes which were made to achieve compatibility with

the new motor drive unit.

The digital junction receives the desired altitude and azimuth co-ordinates from the computer junction and the actual telescope altitude and azimuth from the ALU. It produces an error signal in the correct form for the motor drive unit which drives the motors until the telescope altitude and azimuth are equal to the desired altitude and azimuth.

A number of special functions have been included in the digital junction and they are as follows:

i) "RUN/HOLD"- If this function is on, the telescope will drive automatically to its "parked" position (0^{o} azimuth; 90^{o} altitude).

ii) "LOCK"- The telescope will remain in its present position until this function is off.

iii) "AUTOMATIC RETURN"- If the telescope moves through a full 360^{o} in azimuth, this function causes the azimuth to rewind by 360^{o} and pick up the program where it left off. This is done to prevent the cables leading up to the yolk of the telescope from becoming twisted up. This function is overidden if the "AUTOMATIC RETURN INHIBIT" function is on.

iv) "LIMITS"- Limit switches on the altitude drive axis will stop the telescope if it moves to very low altitudes which could result in the dish being damaged against the antenna mount.

The option of superimposing a pair of offsets on the desired set of co-ordinates to allow for pointing corrections, has also been provided.

4.2.2 CALCULATION OF THE ERROR

The error in the telescope position is defined as follows:

ERROR = ACTUAL TELESCOPE CO-ORDINATE - DESIRED TELESCOPE CO-ORDINATE

The first few stages in the digital junction (Figure 4.4) calculate the error as defined above and add to it the offsets which may be required for pointing corrections.

The offset in altitude and the offset in azimuth, 8 bits each to allow a maximum offset of ± 127 R.U. ($\pm 2{,}8^{o}$) in each co-ordinate, may be applied to the inputs of the 8-bit two-to-one multiplexer, M1 (Figure 4.4) by means of thumbwheel switches on the front panel of the digital junction. The output of the multiplexer, M1 and the fourteen data lines from the ALU go to the inputs of the adder A1.

A pulse from the CTLM in the synchro-to-digital converter (Figure 2.11 I & J) is used to switch either the altitude offset or the azimuth offset to the output of M1, depending upon which of the two co-ordinates is present on the data lines from the ALU. The output of the adder A1 will

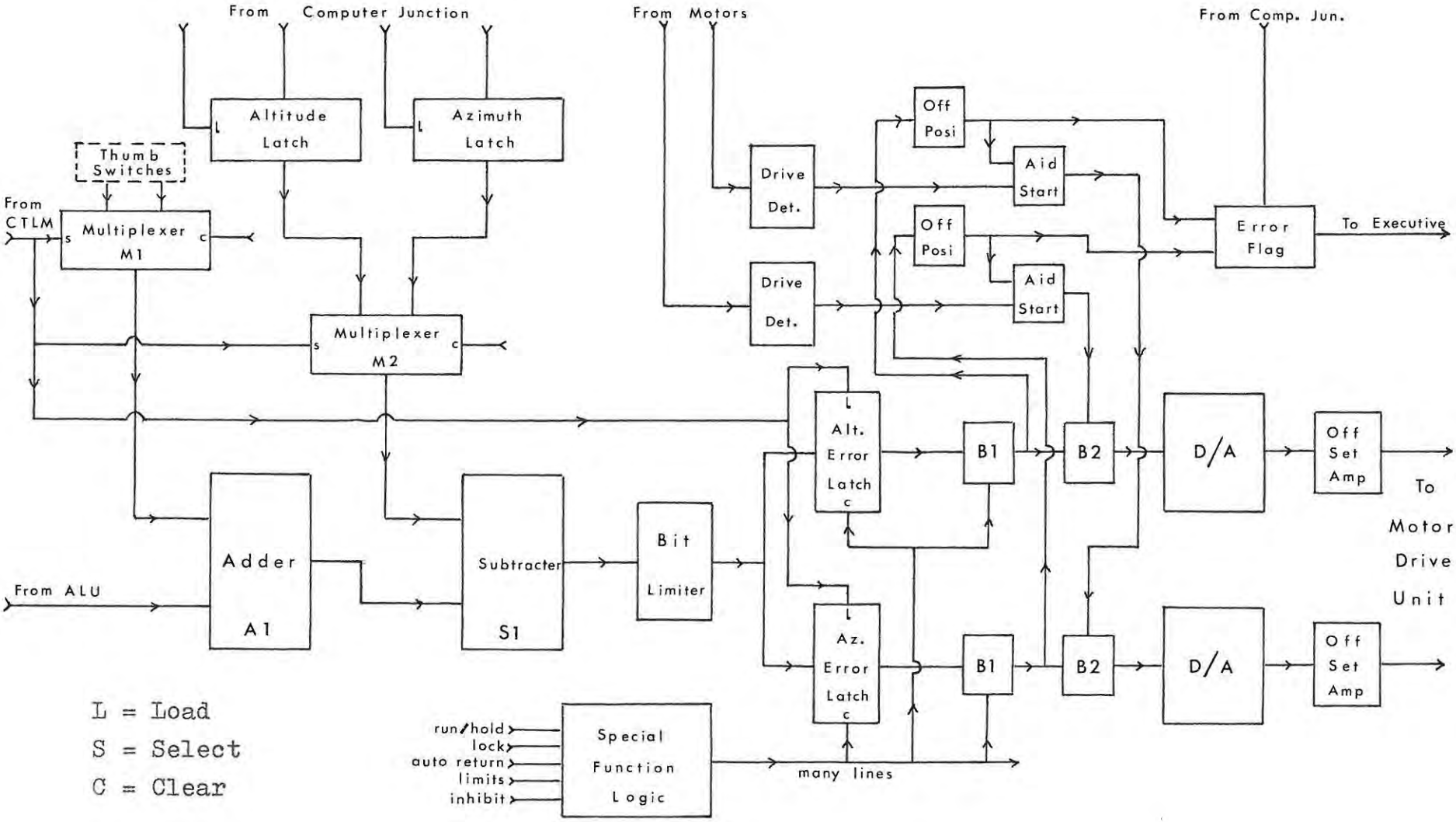

Figure 4.4 The digital junction

therefore be equal to the telescope altitude or azimuth plus or minus the offset required in that co-ordinate.

This method of entering the offsets has not been used because offsets can be entered via the computer while the tracking program is running (section 6.2). It has therefore not been necessary to install the thumbwheel switches referred to above.

The complements of the desired altitude and the desired azimuth are loaded into the altitude latch and the azimuth latch respectively by pulses from the computer junction as described above. The outputs of these two latches are applied to the inputs of a 14-bit two-to-one multiplexer, M2 (Figure 4.4). The same pulse from the CTLM which selects the required offset is used to switch the output of the appropriate latch to the output of M2 when data is present on the fourteen lines from the ALU and hence from A1. The output of M2 is subtracted from the output of A1 by the subtracter S1 (Figure 4.4). In this case the subtraction is done by adding the output of the multiplexer, M2, (already complemented) to the output of A1 and adding +1 via the carry-in bit of the adder. The output of the subtracter S2 is a 14-bit binary number equal to the ERROR in the telescope position.

The error signal which appears on the output of S2 (Table 4.2) may be regarded as a signed 14-bit binary

Error in R.U.	Output of S2
-8192	10 000 000 000 000
-8191	10 000 000 000 001
.	.
+2	11 111 111 111 110
-1	11 111 111 111 111
0	00 000 000 000 000
+1	00 000 000 000 001
+2	00 000 000 000 010
.	.
+8190	01 111 111 111 110
+8191	01 111 111 111 111

Table 4.2 The ERROR produced by S2

number. Anticlockwise errors are negative and clockwise errors are positive. (The "sense" of the error signal is such that both altitude and azimuth increase with anticlockwise rotation.) The magnitude of an anticlockwise error is equal to the two's complement of the output of S2. (In this system, an error of 180° is always regarded as an anticlockwise error.)

4.2.3 THE BIT LIMITER

If the telescope is more than one beamwidth away from the desired co-ordinates, the motors should drive at maximum speed. It was therefore decided to limit the error to six bits, since the telescope beamwidth is 20 R.U. and the

largest numbers representable by a signed six-bit binary number are +31 and -32. The MSB remains the sign bit and determines the direction. The bit a_4 is determined by the Boolean expression:

$$a_4 = (a_4 + a_5 + a_6 + a_7 + a_8 + a_9 + a_{10} + a_{11} + a_{12}) \cdot a_{13} + (a_4 \cdot a_5 \cdot a_6 \cdot a_7 \cdot a_8 \cdot a_9 \cdot a_{10} \cdot a_{11} \cdot a_{12}) \cdot a_{13} \quad \ldots 4.1$$

The bit limiter (circuit in Appendix 4.2) is made up the gates necessary to implement equation 4.1.

The output of the bit limiter (which will be referred to as the "error signal" from now on) goes in parallel to 2 six-bit latches, the altitude error latch and the azimuth error latch (Figure 4.4). The appropriate one of these two latches is loaded by the same pulse from the CTLM which is used to select the correct outputs of the two multiplexers, M1 and M2. The error signal for the altitude and the error signal for the azimuth therefore appear on the outputs of the altitude error latch and the azimuth error latch respectively as six-bit binary numbers. The error signal at this stage depends on the ERROR in the way shown in Figure 4.5. The cyclic variation in the error signal is due to the fact that the bit limiter only clamps the bit a_4.

4.2.4 FORMATTING THE ERROR SIGNAL

It was originally hoped to use the motors supplied with the antenna mount for driving the telescope. Figure 4.6,

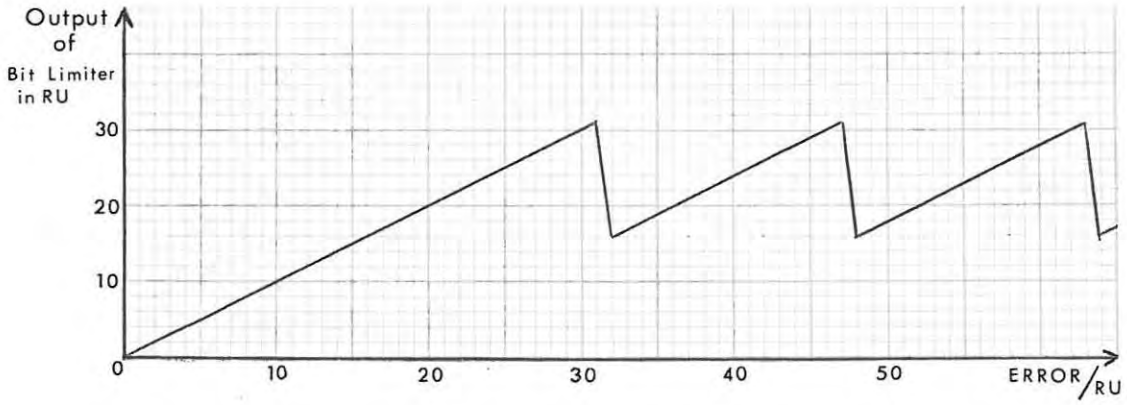

Figure 4.5 The output of the bit limiter versus ERROR

derived from a graph supplied by the technician who built the motor drive unit (section 4.3) for these motors, shows how the speed of a motor depends upon the d.c. voltage

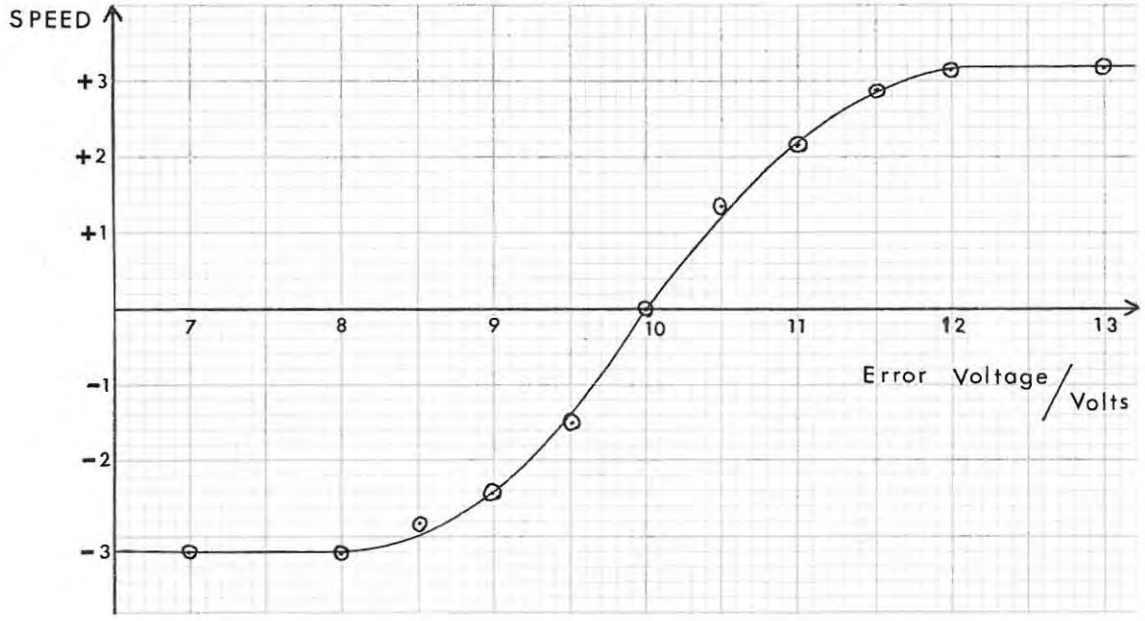

Figure 4.6 Error voltage required for motor drive unit

applied to the input of the motor drive unit. From Figure 4.6 it is clear that an error signal of +7 volts dc causes maximum speed of rotation one way, +10 volts dc causes no rotation at all, and +13 volts dc causes maximum

speed of rotation the other way. The error signal which appears at the output of the error latch must therefore be converted to a dc voltage level which varies between +7 and +13 volts dc depending upon the error. This is done by the last three stages of the digital junction, viz. the bit controllers, the digital-to-analogue converters and the off-setting amplifiers (Figure 4.4).

The six-bit error signal on the output of each latch goes to a set of logic gates, bit controller B1, which removes the cyclic variation in the error signal by making a_0 to a_3 equal to a_4 , if a_4 is not the same as a_5 . The error signal after this modification has been performed is shown

Error in R.U.	Modified error	Output of bit controllers
-30	1 0 0000	1 1 1111
-17	1 0 0000	1 1 1111
-16	1 1 0000	1 0 1111
-1	1 1 1111	1 0 0000
0	0 0 0000	0 1 1111
+1	0 0 0001	0 1 1110
+15	0 0 1111	0 1 0000
+16	0 1 1111	0 0 0000
+30	0 1 1111	0 0 0000

Table 4.3 The error signal after B1

in Table 4.3. B1 also inverts the bits a_0 to a_4.

From this point on in it is no longer convenient to regard the error signal as a signed number. This means that the maximum clockwise error signal is 0 and the maximum anticlockwise error signal is 63 at the output of B1 (Table 4.3). Figure 4.7 shows how the output of B1 depends

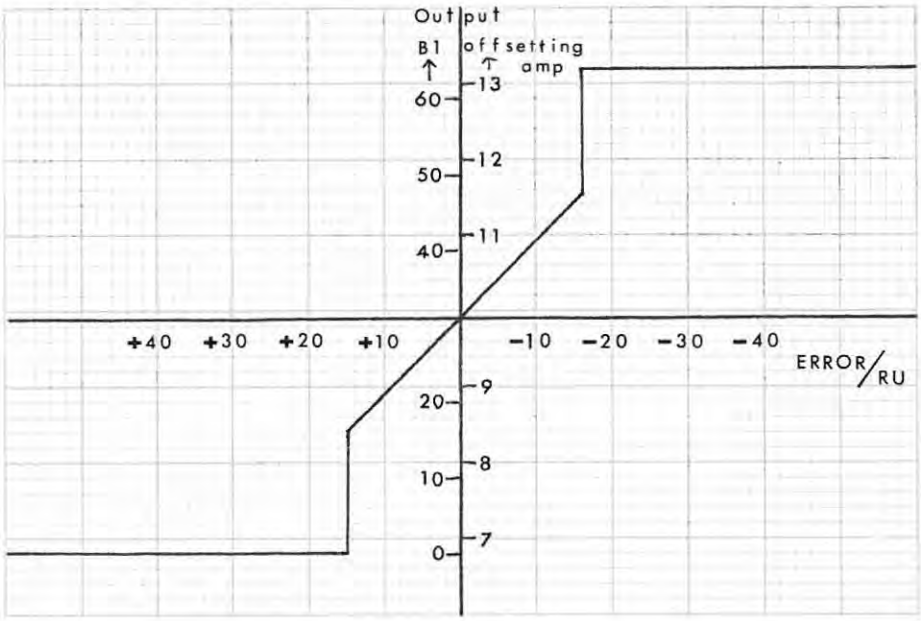

Figure 4.7 Output of B1 and off-setting amps versus ERROR

upon the ERROR.

The output of B1 goes via a second bit controller, B2, the function of which will be explained in section 4.2.5, to a six-bit digital-to-analogue converter (Figure 4.4). The circuit of the digital-to-analogue converter (Motorola 1973) may be found in Appendix 4.3. The output of the digital-to-analogue converter is designed to vary between 0 and +7 volts dc as the six-bit number on its input varies from 0 to 63.

Each digital-to-analogue converter is followed by an off-setting amplifier (National Semiconducters 1972a) (Circuit in Appendix 4.3) which is used to center the dc voltage on the output of the digital-to-analogue converter at +10 volts dc so that when the six-bit number on the input to the digital-to-analogue converter is 31, i.e. zero error, the output of the off-setting amplifier is +10 volts dc which is what is required by the motor drive unit for no movement of the telescope. The output of the off-setting amplifier, the error voltage, is therefore represented by the same graph which represents the output of the bit controller, B1 (Figure 4.7). The speed of the motors is thus a maximum until the telescope is 15 R.U. from the desired position.

There may be some uncertainty due to noise in the least significant bit of the ERROR and hence of the error signal, which will cause that bit to jump between "0" and "1". It was therefore decided to use only the five most significant bits of the error signal in the digital-to-analogue conversion with the least significant bit of the digital-to-analogue converter kept at "1". This means that the output of the off-setting amplifier (the error voltage) will be +10 volts when the telescope is at the desired position or when it is 1 R.U. anticlockwise of the desired position. The telescope should therefore be, on the average, 0,5 R.U. off position but the telescope will not be jerking back and forth between the two positions. (This

offset of 0,5 R.U. is not serious because it is about 1/40 of a beamwidth and allowance can in any case be made for it in the computer programs.)

The error voltage varies between +7 and +13 volts in 18 steps corresponding to 9 motor speeds each way. Furthermore, as can be seen from Figure 4.7, the error voltage does not vary linearly between +7 and +13 volts, but undergoes large stepwise increases when the error is +15 and -16 R.U.

4.2.5 THE OFF-POSITION DETECTORS AND AIDED START

The five MSB's of the output of B1 will represent the number 15 if the telescope is at the desired position or 1 R.U. anticlockwise of that position (Table 4.3). The five MSB's of the bit controller B1 therefore go to a set of gates, the off-position detectors, the output of which will be low if the number 15 appears on their inputs in binary. Because there is no front panel display of the desired co-ordinates of the telescope, they will not be known unless they have been entered via the thumbwheel switches on the front panel of the computer junction. The output of each off-position detector has therefore been wired to a light emitting diode on the front panel of the ALU (Figure 3.9), so that the operator can see whether the telescope is at the desired position or not.

The outputs of the two off-position detectors also go to an error flag flip-flop. As the system was originally envisaged, this flip-flop is set by a pulse from the computer junction each time a new position is transmitted from the computer. When the telescope has reached the desired co-ordinates, the flip-flop is cleared by a pulse produced as the off-position detector outputs go low. The output of this flip-flop should go to the telescope data capure unit (Nunn 1974) where its status would be logged along with the other telescope data to give a check as to whether the telescope was on position during the observations. Because the telescope executive and the data capture unit were removed before the completion of the tracking system, this flag has never been used. It has, however, been tested and is found to work as expected.

Each of the motors supplied with the telescope mount has a tachometer unit built into it (Singer 1961). The output of the tachometer is an ac voltage the amplitude of which is proportional to the speed of the motors. Each tachometer output is wired to a drive detector in the digital junction. The drive detector consists of an ordinary diode detector followed by a zero crossing detector. The output of the drive detector, which is connected to a light emitting diode on the front panel of the digital junction (Figure 4.8), will be high if the motor is turning fast enough to produce a tachometer signal which has an amplitude of more than 0,6 volts. (The slowest speed of the motors, corresponding

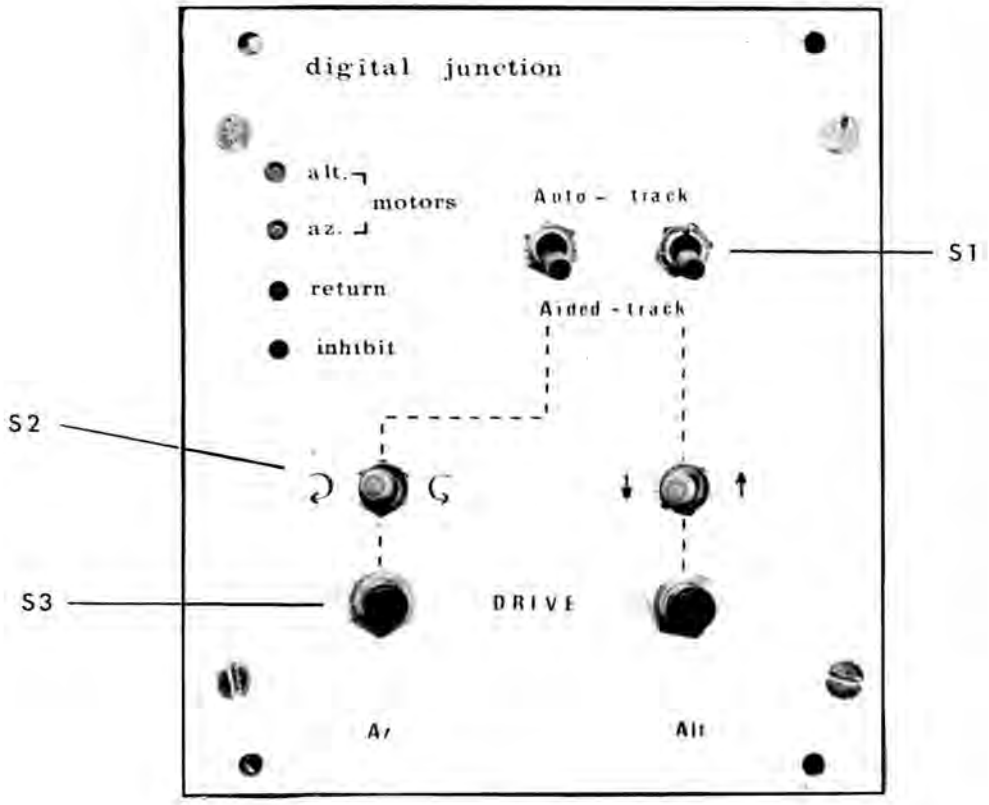

Figure 4.8 The digital junction front panel

to an error of 1 R.U., will produce a tachometer voltage which has an amplitude of more than 0,6 volts.)

The output of each drive detector and the corresponding off-position detector are used together with a second set of bit controllers, B2 in Figure 4.4, to provide an aided start system for the telescope drive unit. If the telescope is off-position, but the motors are not turning, which may happen if the error is small, the output of the off-position detector will be high and that of the drive detector low. These two outputs are applied via suitable gates to the bit controller B2 which inverts the bits a_3 and a_4 of the error

signal thereby increasing the error voltage, until the telescope is moving. (This system fell into disuse when the original motors were replaced with motors which have no tachometer output.)

4.2.6 THE SPECIAL FUNCTIONS

The "special functions" which are designed to simplify the operation of the tracking system, are produced in the digital junction by a system of logic gates and flip-flops which will be referred to hereafter as the "special function logic".

When the "run/hold" function is turned on either by transmitting the appropriate character ("K" for on, "L" for off) from the computer or by setting it from the front panel of the computer junction, the 14-bit two-to-one multiplexer in the computer junction (Figure 4.1) is cleared and pulses are produced which load both the altitude latch and the azimuth latch in the digital junction. At the same time, the bits a_{11} and a_{12} (in order to get the two's complement) of the altitude latch are inverted. This gives a desired altitude of 4096 R.U. and a desired azimuth of 0 R.U. The telescope will automatically track to these co-ordinates which are normally used as the "parked" position.

The "automatic return" function works in conjunction with

two switches which have yet to be installed on the azimuth axis of the telescope base, to prevent the cables leading up into the yolk of the telescope from becoming twisted up. The planned positions of the two switches are illustrated in

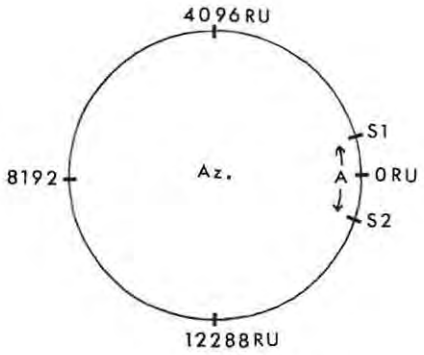

Figure 4.9 The positions of S1 and S2

Figure 4.9. The switches, S_1 and S_2, are connected to a system of flip-flops and gates. If either S_1 or S_2 is activated a number of times in succession, no effect is produced. If first S_1 and then S_2 is activated, the outputs of the special function logic clear the azimuth error latch and change the function of the azimuth bit controller, B1 , so that the bits a_0 to a_4 of the error signal are not inverted. The error signal at the output of B1 is then 0, the maximum clockwise error, and the telescope will retrace the path back towards S_1. As soon as S_1 has again been activated, the automatic return outputs again go low and the telescope will track to the co-ordinate stored in the azimuth latch. If S_2 is activated before S_1, the azimuth error latch is also cleared by the special function logic. In this case the bit controller, B1, is allowed to invert the bits a_0 to a_4 and also, although this is not

normally the case, the bit a_5, thereby producing the maximum anticlockwise error until the telescope has once again activated S_2. While the azimuth is rewinding, the altitude "lock" (see below) is on and the l.e.d. marked "return" on the front panel of the digital junction (Figure 4.8) is on.

Although the switches have not yet been mounted on the telescope, this function has been "bench tested" and is working as expected. It was decided to use push on/ push off switches for S_1 and S_2 and not microswitches which are perhaps the obvious choice for their light operation. The reason for this choice is that if there is a power failure while the telescope is outside the region marked "A" in Figure 4.9, information stored in a flip-flop by momentarily closing S_1 or S_2 would be lost.

The "automatic return" function is gated with the "automatic return inhibit" function in the special function logic. If the "automatic return inhibit" function is turned on ("M" for on, "N" for off), the "automatic return" signals will not reach the azimuth error latch or the azimuth bit controller and the l.e.d. marked "inhibit" lights up. This allows one to track past S_1 or S_2 if continuous observation is required at that time.

There is no difference between the "lock" and the "limits" functions. These two functions clear both the altitude and the azimuth error latches, but do not affect the bit

controllers so that zero error is produced at the output of B1 for both altitude and azimuth. When the power is turned on, the lock function is automatically turned on by the master reset in the computer junction so that there must be human intervention before the telescope will move. "Lock" may also be turned on and off from the computer by the transmission of the characters "C" and "D" respectively.

If more than one of the special functions are activated at the same time, the operation of the telescope is determined by the function with the highest priority. The order of priority (descending) is "lock" ("limits"), "automatic return" and then "run/hold".

4.2.7 MODIFICATIONS MADE TO ACCOMODATE THE NEW MOTOR DRIVE UNIT

The requirements of the second motor drive unit (section 4.3.2) are far simpler than those of the first. Three signals are required, a logic signal to set the direction ("0" for clockwise and "1" for anticlockwise), a dc voltage between zero and +5 volts to determine the speed of the motors, and a second logic signal to stop the motors when the telescope is at the desired position, i.e. an "on-position" signal. (The functions of these signals will be elaborated upon in section 4.3.2.)

The first of these signals was already present in the

digital junction as the bit a_5 of the error signal which is "0" for clockwise errors and "1" for anticlockwise errors. The other five bits of the error signal required some modification. The bit controller B2 was no longer required since the new motors have no tachometer output. It was therefore decided to use B2 to modify the error signal so that the output of the digital-to-analogue converter is a dc voltage between 0 and +7 volts proportional to the magnitude of the error. The bit controller B2 was therefore expanded to four bits and is used to invert bits a_0 to a_3 if bit a_5 is zero. The bit a_4 is not used after B1 in this system.

Error in R.U.	Input to B2	Output of B2
-30	1 1 1111	1111
-16	1 1 1111	1111
-15	1 0 1111	1111
-2	1 0 0001	0001
-1	1 0 0000	0000
0	0 1 1111	0000
+1	0 1 1110	0001
+2	0 1 1101	0010
+15	0 1 0000	1111
+16	0 0 0000	1111
+30	0 0 0000	1111

Table 4.4 The input and the output of the bit controller B2

Table 4.4 shows the input and the output of B2. The output of B2 is applied to the four most significant bits of the

digital-to-analogue converter so that the output of the converter varies between 0 and +7 volts in 16 steps. This gives 16 motor speeds in each direction, almost twice as many as before and in this case the output of the digital-to-analogue converter varies linearly between 0 and +7 volts as the error varies from 0 to -16 R.U. or 0 to +15 R.U. The off-setting amplifiers were modified to operate as adjustable gain dc amplifiers. The output of the off-setting amplifiers, the error voltage, thus varies between 0 and some maximum dc voltage determined by the gain of these amplifiers.

The bits a_0 to a_3 of the output of B2 go to the off-position detectors instead of bits a_1 to a_5 from B1. The off-position detectors were modified to give a low output if the number on their input is zero which means that the telescope is considered to be on-position if the error is zero or -1 R.U (see Table 4.4).

Fortunately no changes had to be made to the special function logic and the only circuitry which became redundant was that employed in the drive detectors.

The digital junction, in its present form, thus supplies to the motor drive unit an off-position signal, a direction signal and an error voltage, for each co-ordinate.

4.3 THE MOTOR DRIVE UNIT (MDU)

In this section, a brief description is given of the motor drive unit (MDU Mk1) which was designed and built by a technician in the Physics Department (Lichtenburg 1974). This is followed by a discussion of the problems encountered with the MDU Mk1 and the subsequent development by the author of a second motor drive unit (MDU Mk2).

4.3.1 THE MDU Mk1

The motors supplied with the telescope mount are two-phase low inertia ac motors (Singer 1961). Two-phase ac motors are often used in this type of application because they are small, rugged, reliable and comparatively cheap (Thaler and Brown 1960, Chapter 5). Another advantage of two-phase motors is that they provide a large torque, necessary for rapid acceleration, at zero speed (Ogata 1970, Chapter 4).

One phase of such a motor is continuously excited by a reference voltage (typically 115 V at 60, 400 or 1000 Hz) while the other phase has a control voltage of the same frequency applied to it. The torque produced by the motor and its angular speed depend on the amplitude of the control voltage and the phase difference between the reference and control voltages (op. cit.). The speed (torque) of the motor is a maximum in one direction when the phase difference between the reference voltage and the control

voltage is $+90^{o}$. When the phase difference between the two voltages is -90^{o}, maximum motor speed in the opposite direction is produced. If the two voltages are in phase, the motor is locked.

The MDU Mk1 was designed to produce reference and control voltages of constant amplitude (115 V at 400 Hz). The phase difference between these two voltages was continuously variable between -90^{o} and $+90^{o}$ and depended upon the error voltage from the digital junction. The dependence of the speed of the motors upon the error voltage has been discussed in section 4.2.4 (see Figure 4.6).

Figure 4.10 is a block diagram of the MDU Mk1. The reference oscillator provides a signal at a frequency of 4000 Hz. The frequency divider and phase shifter divides the 4 kHz signal down to produce two signals at 400 Hz, 90^{o} out of phase with each other. One of these (let its phase be 0^{o}) is amplified and used as the reference voltage to the motors. The second 400 Hz signal which has a phase shift of 90^{o} relative to the 400 Hz reference voltage is applied to the two variable phase shifters which adjust the phase of this signal in accordance with the error voltage from the digital junction. The phase of the 400 Hz signal at the output of the variable phase shifters relative to the 400 Hz reference voltage can vary from -90^{o} to $+90^{o}$ depending on the error voltage. When the error voltage from the digital junction is +10 volts dc the phase difference between the

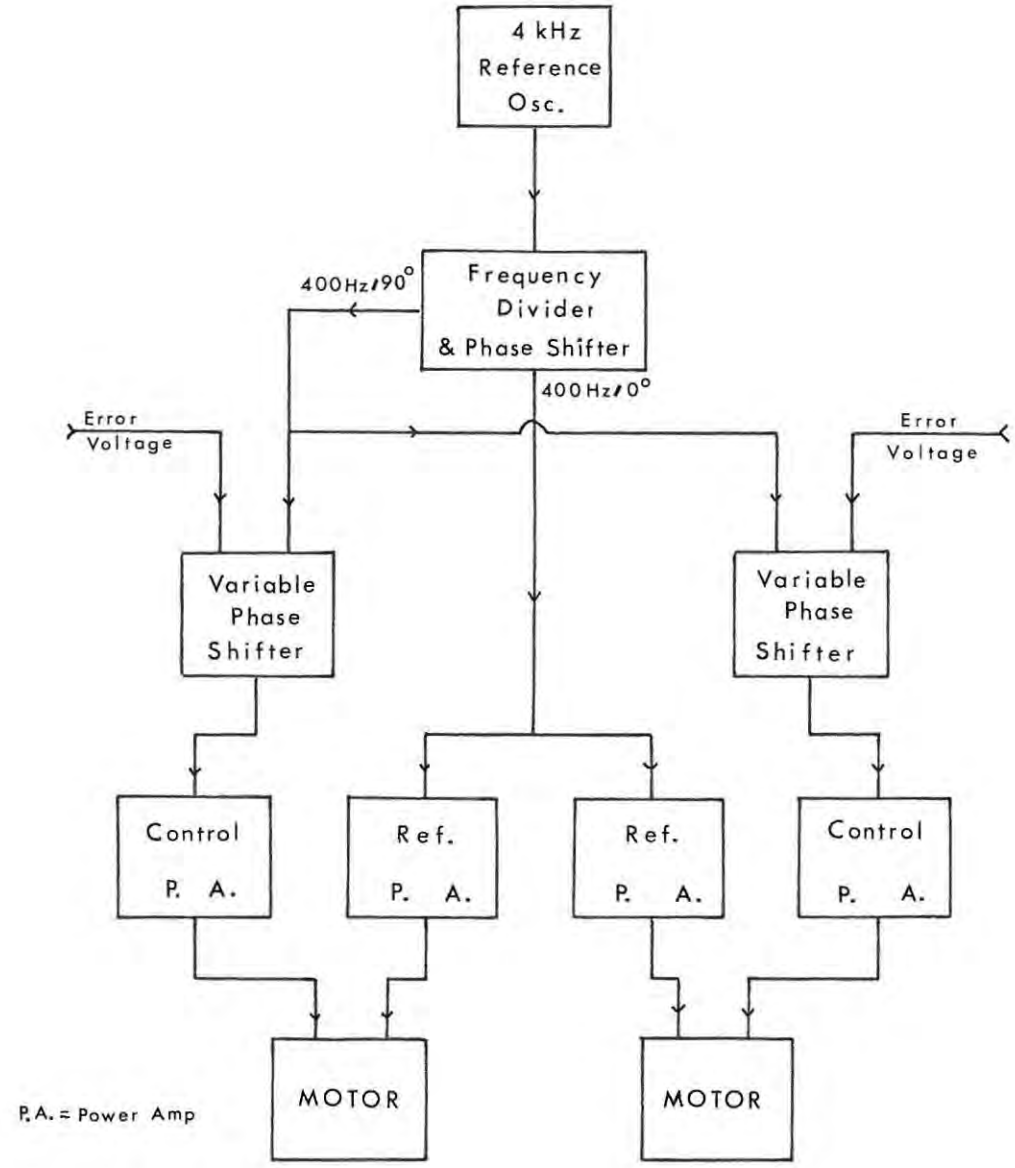

Figure 4.10 The MDU Mk1

two voltages is zero. The outputs from the variable phase shifters are amplified and applied to the control phases of the two motors. (The author wishes to point out that, had he designed or been involved in the design of the MDU Mk1, the above system would not necessarily have been employed.)

As soon as the MDU Mk1 was put into use with the rest of the tracking system, trouble was experienced with the power amplifiers. Figure 4.11 shows the circuit of one of the

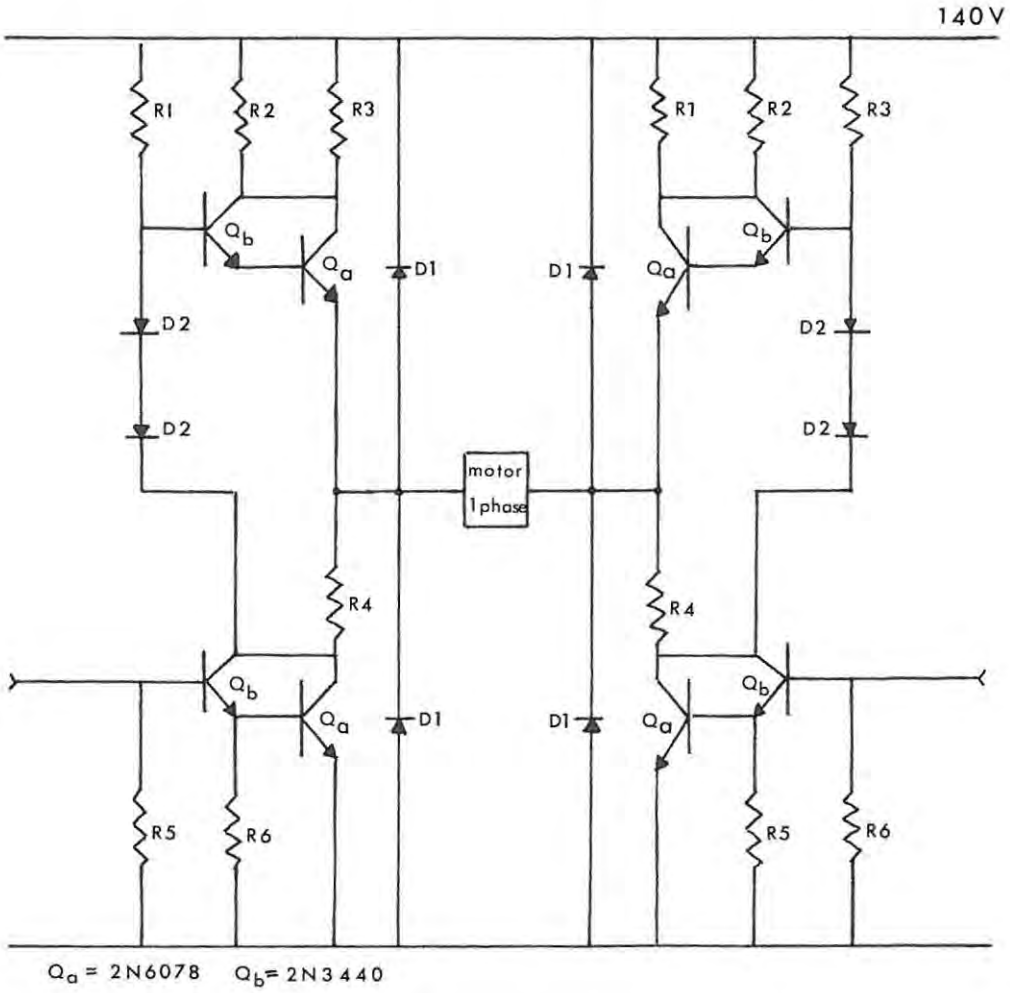

Figure 4.11 MDU Mk1 power amplifier circuit

power amplifiers. After the MDU had been on for a short while, one or more of the 2N6078 power transistors would be destroyed. In an attempt to solve the problem, the following points were considered:

i) In spite of the protective diodes (D1) across the motors, there may have been large spike voltages across the transistors which could destroy their junctions.

Protective diodes were tried across the emitter-collector, base-collector and emitter-base junctions of the transistors but no improvement was obtained.

ii) It was thought that perhaps transistors in opposing sides of the bridge were not being turned off at the same time. This could cause one of the transistors to run hotter than the others and eventual burnout could result. This was checked by careful measurement but no imbalance was found.

iii) All the power transistors were running very hot. Each power amplifier (8 transistors) had been built on a heatsink measuring 120mm x 90mm. The author rebuilt the power amplifier stages so that each pair of transistors (2N6078 and 2N3440) was located on a heat sink measuring 90mm x 90mm. This did not improve the reliability of the MDU Mk1.

iv) The 2N6078 transistor is capable of dissipating 45 W and has a maximum collector-to-base voltage, V_{CBO}, of 275 V almost twice the supply voltage (140 V). It was known that the transistors were operating rather close to their power limit and that spike voltages of twice the supply voltage could occur. The power amplifiers were therefore rebuilt a second time using 2N6307 transistors which are rated at 125 W and have a V_{CBO} of 600 V . The same effect was observed.

At this stage it was decided to abandon the MDU Mk1 and to

replace the two-phase ac motors with small 12 V dc motors for the following reasons:

i) Because of the system used in the MDU Mk1, i.e. variable phase shift, maximum power must be supplied to the motors at all times.

ii) The power-to-weight ratio and the efficiency of two-phase ac motors is low (Gille et. al. 1959, section 31.5).

iii) Dc motors had been used successfully on a similar antenna mount at Hartebeesthoek.

iv) A lot of time and money had been spent in the attempt to make the MDU Mk1 work reliably.

4.3.2 THE MDU Mk2

The two-phase ac motors were replaced with surplus dc windscreen wiper motors. The dc motor is much more efficient than the two-phase ac motor (Ogata 1970, section 4.5). It has separately excited fields and is either armature-controlled with a fixed field or field-controlled with a fixed armature current. Armature-control has certain advantages over field-control for dc motors. These include greater efficiency and the fact that it is easier to keep the field constant than it is to keep the armature current constant (op. cit.). Armature control has been used. The torque produced by an armature controlled motor is directly proportional to the armature current (op. cit.). It was therefore decided to use a

pulse-width modulated drive system to ensure a large torque even at low speeds. (In a pulse-width modulated system the instantaneous current and therefore the instantaneous torque is always at its maximum value during the on-time of the pulses.)

Figure 4.12 is a block diagram of one half of the MDU Mk2. If the triple pole single throw switch S1 on the front panel of the digital junction marked "autotrack" / "aided - track" (Figure 4.8) is in the "autotrack" position, "a" in Figure 4.12, the feedback loop is completed and the antenna will track automatically to the co-ordinates loaded from the computer or the thumbwheel switches on the front panel of the computer junction. In this case, the direction signal from the digital junction is connected to the field power supply unit, the "on-position" signal is applied to the drive inhibit gates and the manual drive push button switch (S3) is disabled.

The field power supply unit produces a dc potential of 12 volts, floating with respect to earth potential. This potential is applied to the field winding of the motor via a polarity-reversing relay in the field power supply unit. The polarity-reversing relay, which is activated by the direction signal from the digital junction, when S1 is in the "auto-track" position, is used to reverse the direction of rotation of the motor by reversing the sense of the applied field potential.

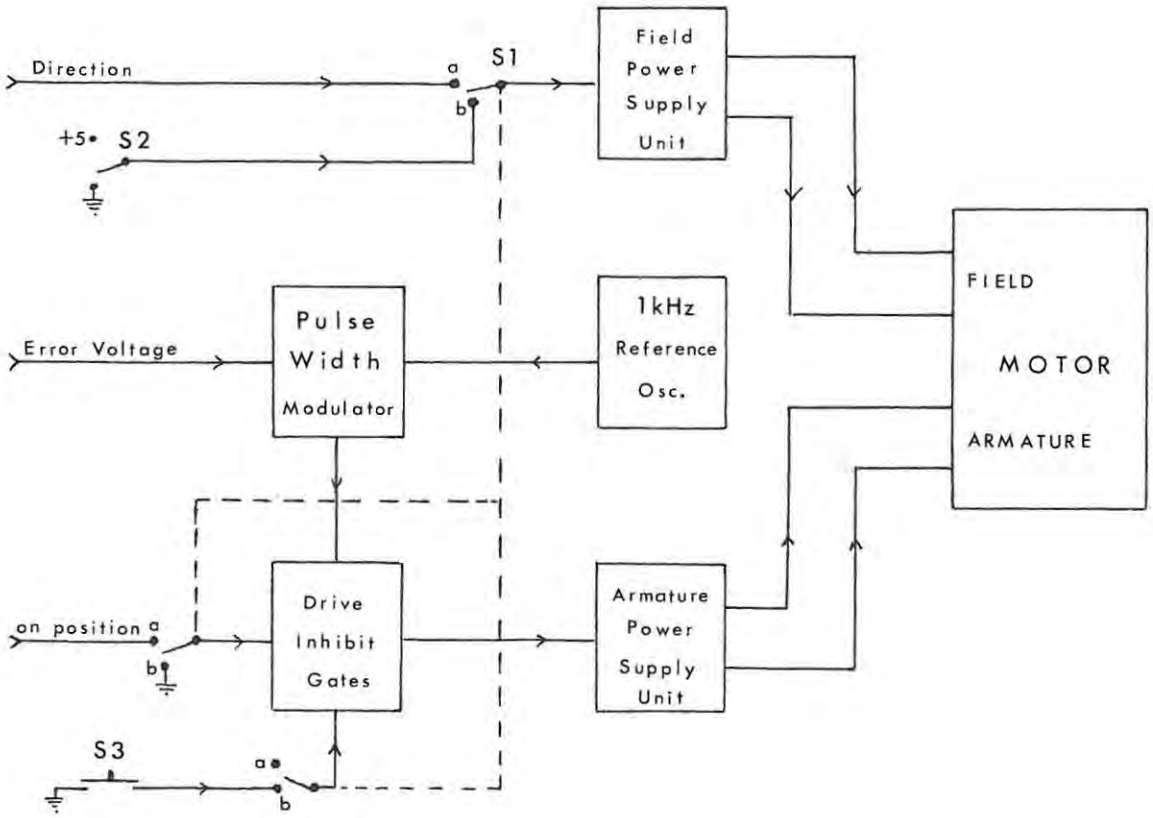

Figure 4.12 The MDU Mk2

The error voltage from the digital junction and the 4 kHz signal from the reference oscillator are applied to a pulse width modulator (Signetics 1973). (The circuit may be found in Appendix 4.4.) The width of the pulses appearing at the output of the pulse-width modulator is directly proportional to the error voltage from the digital junction. The minimum width of the pulses (slowest motor speed) can be varied by adjusting the modulator. The maximum width of the pulses is determined by the maximum error voltage applied to the modulator. These two adjustments allow optimization of the system response (section 5.3.2). The output of the pulse-width modulator is gated in the drive inhibit gates with the "on-position" signal from the digital junction.

Only if the telescope is "off-position" will the output of the pulse-width modulator reach the armature power supply unit. The armature power supply unit applies 12 volts dc across the armature winding of the motor via a power switching transistor. The output of the pulse-width modulator is used to turn the transistor on and off. The speed of the motors therefore depends on the width of the pulses, but an important feature of this system is that, for the duration of each pulse, the motor applies maximum torque to the load. Figure 4.13 shows how the speed of rotation of the output shaft of each of the two motors depends upon the error. In the case of the altitude, the two sets of points shown are for different maximum error voltage and minimum pulse width. (The speed was found to be independent of the direction of rotation.)

When the switch S1 (Figure 4.12) is in position "b" ("aided track"), it is possible to drive the telescope manually. In this case, the output of the pulse-width modulator does not reach the armature power supply unit, and the polarity-reversing relay cannot be activated by the direction signal from the the digital junction. The direction of rotation of the motor can then be set from the front panel of the digital junction by means of the switch S2. If the push button switch S3 is depressed, the power transistor in the armature power supply unit is turned on and the motor will drive the telescope.

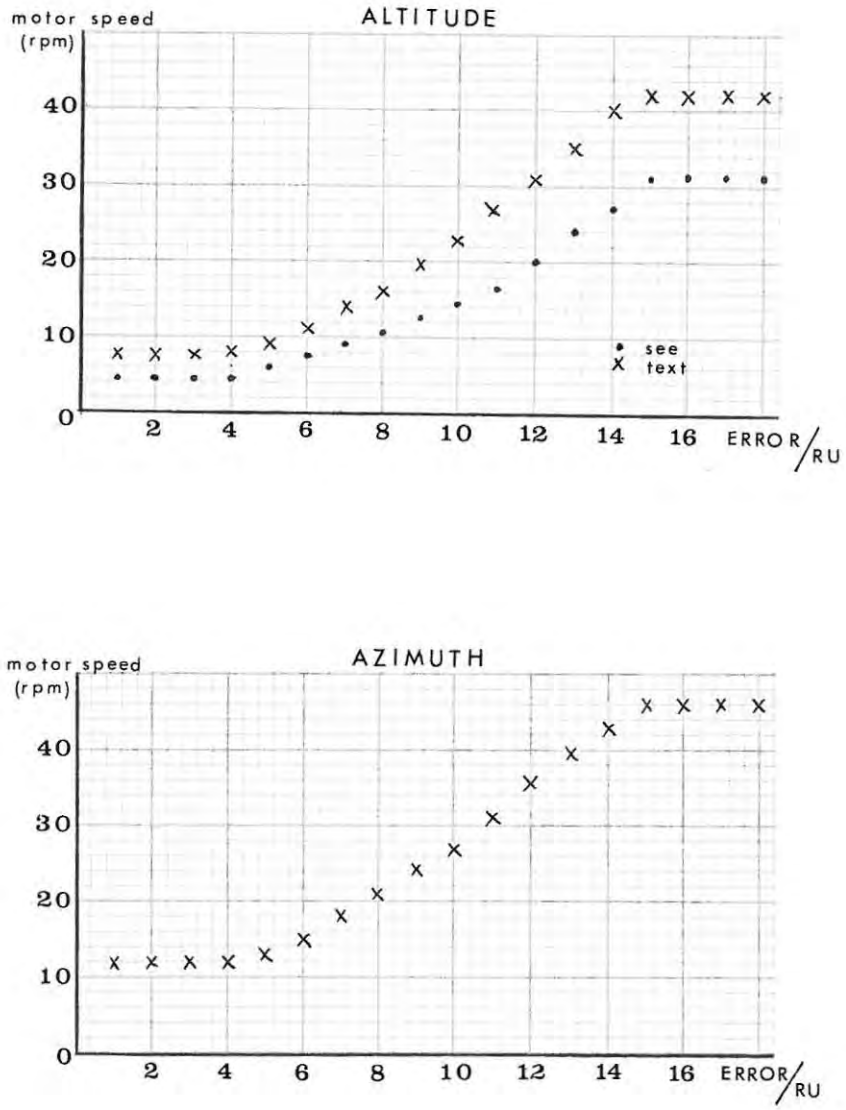

Figure 4.13 Altitude and Azimuth motor speed versus Error

The MDU Mk2 has been working reliably for 18 months. One improvement which could still be made is the replacement of the polarity-reversing relay in the field power supply unit with an electronic polarity-reversing bridge circuit.

CHAPTER FIVE

PERFORMANCE AND CALIBRATION

5.1 ALIGNMENT

The digital section of the tracking system, i.e. the ALU, the digital junction and the computer junction, required very little alignment, once the initial testing to check for wiring mistakes and correct circuit operation had been completed. The synchro-to-digital converter, however, required careful setting up according to a strict alignment procedure which is set out in block diagrammatic form in Figure 5.1.

After the initial circuit testing, the first step in the alignment of the converter was to set up the CTLM (Central Timing and Logic Module) for correct operation according to the scheme presented in section 2.2.7 (Figure 2.11). Particular care was taken to ensure that the pulse which loads the outputs of the zero-crossing detectors into a latch, occurs at exactly the middle of the first half cycle of the channel being measured. (This gives the zero-crossing detectors maximum sensitivity.)

The only other aspect of the CTLM operation which is critical to the operation of the converter as a whole is that the pulse which zeroes the peak detectors must extend a

Figure 5.1 Scheme for synchro-to-digital alignment

little way into the next channel. Once the CTLM was functioning correctly the analogue divider was adjusted for linear operation. This is particularly important because the calculations of θ_1 and $\theta_1/36$ (section 2.2.6) rely on the

fact that the input to the analogue-to-digital converter is proportional to the sine of the angle which the rotor of the synchro makes with the stator axis. The divider was set up according to the procedure recommended by the manufacturers (Motorola 1973).

The next step in the alignment of the converter was to set up the maximum voltage applied to the divider input. A switch has been provided on the channel select lines to the PRAM which precedes the divider and this can be used to select one peak detector output at a time. The gains of the peak detectors and the operational amplifiers which follow the PRAMs in the first section of the synchro-to-digital converter (Figure 2.7) were adjusted so that the voltage corresponding to the maximum stator voltage amplitude at the output of each peak detector is about eight volts. The analogue-to-digital converter was then adjusted to give its maximum output ($2^8 - 1$, since there are eight bits) when the voltage on the input to the divider is 8 volts. The input to the divider never actually reaches 8 volts under normal operation of the converter because the measurement switches to the next peak detector output when the stator voltage being measured reaches 0,866 of its maximum value. At that stage, if the system is operating linearly the number on the output of the analogue-to-digital converter will be 221.

From this point, it was possible to complete the alignment

of the synchro-to-digital converter without the use of sophisticated equipment. As the telescope is moved from 0 to 8192 R.U. (180^{o}), measurement takes place in three coarse segments. If the amplitude of the voltage in a coarse segment is too large or too small, the ALU will find that θ and θ_C differ by more than 5^{o} and will therefore add or subtract 455 R.U. as required. The ALU display was therefore watched as the telescope was moved from 0 to 8192 R.U. When a jump of 455 R.U. occurred, the amplitude of the stator voltage from the particular coarse synchro concerned was altered by altering the gain of the amplifier which follows the difference amplifier (Figure 2.7). Because the coarse angle θ_C is always taken to the nearest 10^{o} this adjustment is not critical. Since there are only three coarse stator voltages, if the alignment is correct in the first three coarse segments, it will also be correct in the other three.

The switch from the measurement of one fine synchro stator voltage to the next occurs at 0, 76, 152 R.U. etc. If the amplitude of the stator voltage being measured just before the switch to the next fine segment occurs, is too great or too small, there will either be repetition of numbers or numbers missing. This is illustrated in Figure 5.2. The telescope was driven to each of the positions 76, 152, and 228 R.U. and the amplitude of the fine synchro stator voltage concerned was adjusted to make the ALU readout continuous across the segment boundary.

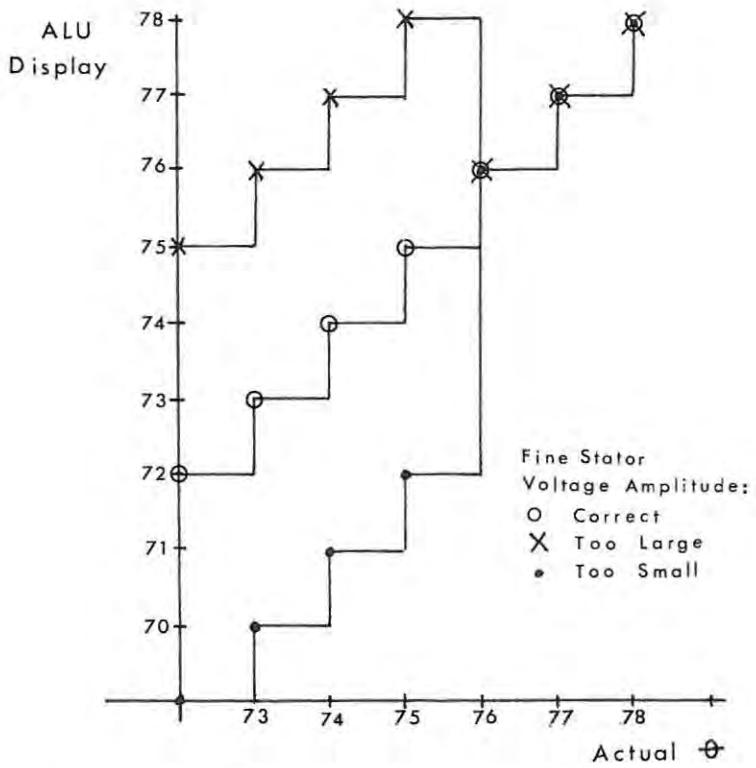

Figure 5.2 Possible fine stator voltage misalignment

Once the fine synchro stator voltages have been set up at these three points, the angular readout ought to be continuous over the full 360° of telescope movement.

5.2 LINEARITY CHECK

A vernier scale which can be read to the nearest 0,02° is mounted on each telescope axis. A comparison of readings taken from the vernier scale and the ALU was used to check the linearity of the system.

The telescope was moved 10° at a time according to the reading on the vernier scale. At each point the reading on the ALU was noted. The results obtained (Table 5.1)

suggested that the system was operating linearly. This was later proved not to be the case (section 7.2). (Nonlinearities within a fine segment are masked by the method used above because the measurement is always made at the same point in a fine segment.)

ALU Reading	Reading on Vernier Scale	Difference
397	80.00°	
		456
853	70.00°	
		454
1307	60.00°	
		456
1763	50.00°	
		456
2219	40.00°	
		454
2673	30.00°	
		456
3129	20.00°	
		455
3584	10.00°	
		456
4040	0.00°	

Table 5.1 Linearity check

5.3 CONTROL SYSTEM ANALYSIS

Four techniques are commonly used in the analysis of control systems (Pendrill 1978). They are

i) step response analysis

ii) impulse response analysis

iii) frequency response analysis (Nyquist or Bode diagram analysis)

and

iv) transfer function modelling.

Because of the nature of the system i.e. both the command co-ordinate and the telescope co-ordinate are 14-bit binary numbers, impulse response analysis and frequency response analysis were ruled out for practical reasons, because they both require the measurement of these co-ordinates as a function of time.

5.3.1 TRANSFER FUNCTION MODELLING

Mathematical modelling of the transfer function is complicated by the fact that the system under test is a sampled-data servomechanism. The frequency response of a sampled data servomechanism is derived either by means of an approximate transfer function (Thaler and Brown 1960, Chapter 11), or by Z-transformation techniques (Ogata 1970, Chapter 13). If the response time of the system (see Table 5.2 below) is very much greater than the sample period (80 ms), the system can be assumed to operate continuously as a first approximation. In order to derive a simple model for the tracking system, continuous operation was assumed. The schematic diagram and the simplified block diagram of the system are shown in Figure 5.3. An arbitrary input signal, r(t), is fed to the computer (via an analogue-to-digital converter if necessary). The position of the telescope at any time, t, is given by the function,

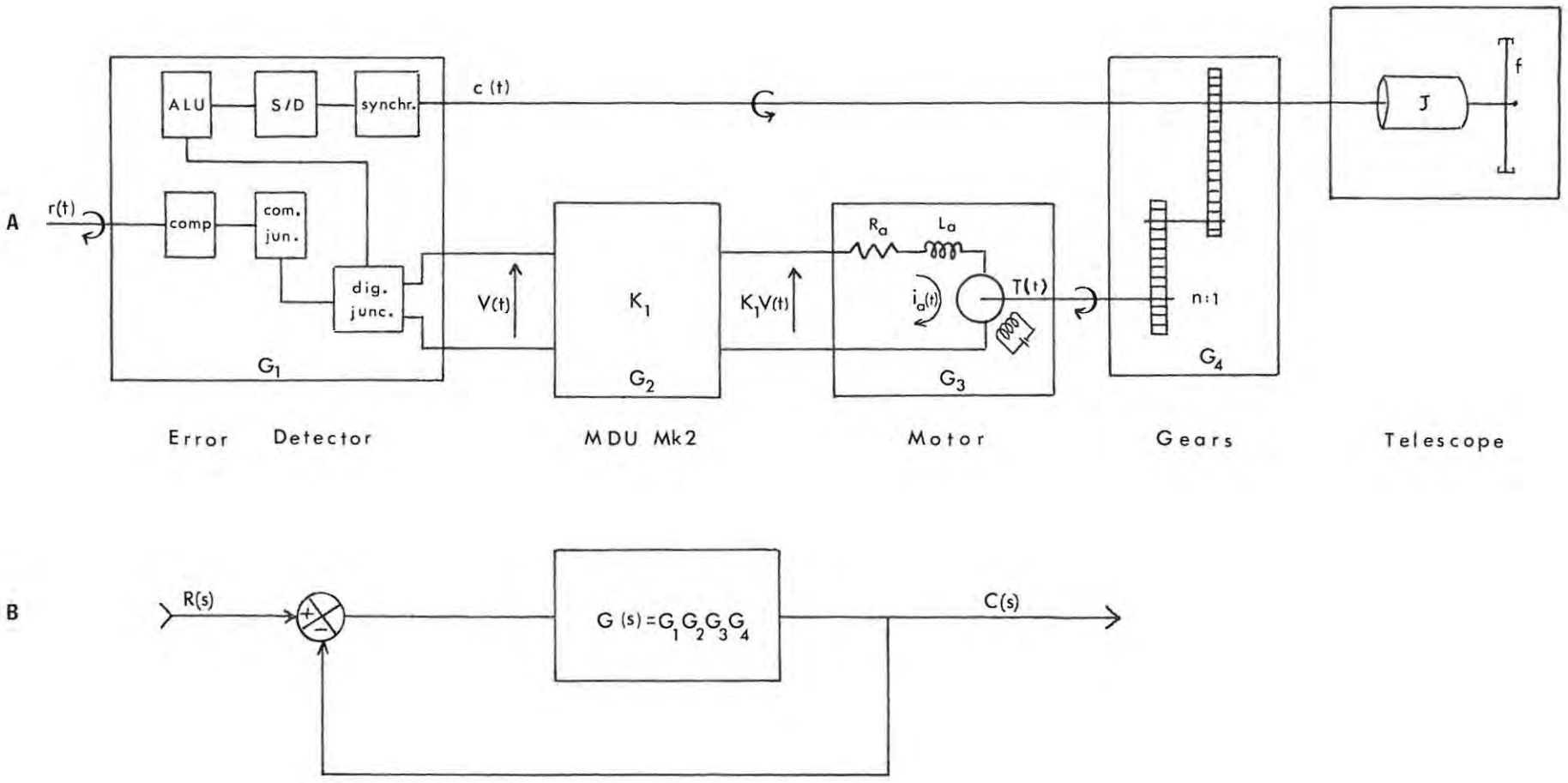

Figure 5.3 A: Schematic diagram of the system B: Simplified block diagram

c(t). The error voltage, V(t), applied to the pulse-width modulator in the motor drive unit is proportional to the difference between c(t) and r(t) i.e.

$$V(t) = K_o \cdot [r(t) - c(t)] \qquad 5.1$$

where K_o is the proportionality constant.

In Figure 5.3 A the armature controlled dc motor is represented by its equivalent circuit. R_a and L_a are the armature winding resistance and inductance respectively, $i_a(t)$ is the armature current and T(t) is the torque produced by the motor. In order to simplify the transfer function of the pulse-width modulated motor drive unit, one may assume that at any time, t, the motor applies an average torque, T(t), to the load when the motor drive unit supplies an average armature current $i_a(t)$. (This average would be taken over a time interval which is greater than the pulse repetition period (~1 ms) and would depend on the pulse width.) This is equivalent to the motor drive unit applying an effective voltage V'(t) to the armature winding. Because V'(t) would be proportional to V(t), one may write

$$V'(t) = K_1 \cdot V(t) \qquad 5.2$$

where K_1 is the proportionality constant. The torque produced by the motor is applied to the load, in this case the telescope, via a geartrain which has an n:1 gear ratio (the number of revolutions of the telescope to the number of revolutions of the motor output shaft). J (Figure 5.3)

represents the inertia of the motor, the geartrain and the telescope referred to the telescope axis of movement. The viscous friction coefficient of the system referred to the same axis is f.

Ogata (1970, pages 225 to 228) shows that the transfer function, G(s), for a system like this is given by the equation

$$G(s) = \frac{K}{(Js^2 + Fs)} \qquad 5.3$$

where $$F = f + \frac{K_2 K_3}{n^2 . R_a} \qquad 5.4$$

and $$K = \frac{K_o K_1 K_2}{n . R_a} \qquad 5.5$$

K_2 and K_3 are the motor torque and back emf constants respectively.

The closed-loop transfer function of this system is therefore

$$G'(s) = \frac{K}{(Js^2 + Fs + K)} \qquad 5.6$$

a typical second order closed-loop transfer function. For transient response analysis it is convenient to write

equation 5.6 in the form

$$G'(s) = \frac{\omega_n^2}{(\omega_n^2 + 2\omega_n\zeta s - s^2)} \qquad 5.7$$

where ω_n is the natural undamped oscillating frequency of the system and ζ is the damping ratio. Equation 5.6 is related to equation 5.7 by the following two equalities:

$$\omega_n^2 = K/J \qquad 5.8$$

$$\zeta = \frac{F}{2\sqrt{J.K}} \qquad 5.9$$

If the input command signal is sinusoidal, equation 5.7 may be written as

$$G'(j\omega) = \frac{\omega_n^2}{\omega_n^2 + j2\zeta\omega_n\omega - \omega^2} \qquad 5.10$$

The dynamic behaviour of the system is then characterised by the two parameters ζ and ω_n.

5.3.2 STEP RESPONSE ANALYSIS

If the command co-ordinate to the tracking system is altered by an ammount r_1 and then kept constant, i.e. if a step input, r_1, is applied, then the error voltage to the pulse-width modulator is

$$V(t) = K_o \cdot [r_1 - c(t)] \qquad 5.11$$

In the case of a unit step, equation 5.11 reduces to

$$V(t) = K_o \cdot [1 - c(t)] \qquad 5.12$$

This means that the step response of the system can be obtained from a graph of the error voltage versus time, after a step input has been applied.

The step response of the system depends on the damping ratio, ζ, and can be optimized to achieve minimum settling time, t_s, by adjusting the "gain" (K_1 in Figure 5.3 A) of the pulse-width modulator, since the damping ratio is related to the gain of the system (equation 5.9). If $\zeta \ll 1$ ($\zeta \cong 0$), the system is said to be "undamped" and oscillation will occur (Case A). If $\zeta < 1$ the system is "underdamped" and one or more overshoots will occur (Case B). If $\zeta = 1$ the system is said to be "critically damped" (Case C) and if $\zeta \gg 1$ the system is overdamped and the response will be very slow (Case D).

In the remainder of this section only the step response of the azimuthal control loop is analysed. In the altitude control loop a rather large gear ratio at present keeps the gain low (see equation 5.5) and results in a heavily overdamped system. A step of 16 R.U. is regarded as a unit step.

By examining the error voltage from the digital junction displayed on the screen of a storage oscilloscope, it was

possible to study, for a step input of 16 R.U., all four of the cases mentioned above. The different types of response were obtained by changing the "gain" of the pulse-width modulator and the dc amplifier which precedes it (section 4.3.2). Figure 5.4 shows labelled photographs of the oscilloscope screen for three of the cases defined above. (Figures 5.4 to 5.7 appear at the end of the present chapter). In the oscillating case (Figure 5.4 A), the direction signal has also been displayed since the error voltage is proportional to the magnitude of the error.

Making use of equation 5.12, the step response of the system was obtained from oscillographs for each of the four cases. The analysis of the oscillographs is somewhat simplified by the quantised nature of the error voltage and the regular sampling period (80 ms) of the synchro-to-digital converter. The four types of response are shown in Figures 5.5 A to 5.5 D. The error bars show the uncertainty due to the quantised sampling. Examination of Figures 5.5 A to 5.5 D reveals that the fastest response of the system (smallest settling time) occurs for case in which ζ is a little greater than 1, a slightly overdamped system. Because this is the response of the system when it is in normal operation, it was decided to analyse this particular case in more detail. Figure 5.5 C was therefore constructed from the data obtained from five independently obtained oscillographs of the error voltage.

An attempt was made to obtain the closed-loop transfer function via the analysis of Figure 5.5 C. This is possible because the transfer function is the Fourier Transform of the unit impulse response and the unit impulse response is the derivative (with respect to time) of the unit step response (or normalised step response) (Falkner 1969, sections 2.2 and 2.4). Using 47 normalised points on the step response curve, the derivative of the step response was calculated. The derivative points obtained are displayed in Figure 5.6A. Because of the noise on this data, a running mean (five points wide) was taken. Figure 5.6 B shows the resulting smoothed derivative curve, the impulse response of the system.

In order to obtain the closed-loop system transfer function, $G'(j\omega)$, the Fourier Transform of the smoothed impulse response was calculated. (A listing of the program used, written by the author, may be found in Appendix 5.1.) The effect of smoothing on the Fourier transform will be considered later. Figures 5.7 A and B show plots of $20 \log|G'(j\omega)|$ and phase of $G'(j\omega)$ respectively.

The amplitude plot (Figure 5.7 A) shows a number of interesting features. There appears to be a first order break point in the region of 0,5 Hz. The phase curve (Figure 5.7 B), however, does not substantiate this very well as the phase has decreased to -70° by the time the amplitude is 3 dB down. The rather rapid changes in both

amplitude and phase in the region from 1 to 2 Hz suggest a third order lag-lead network. This does seem rather unlikely in view of the small frequency interval over which the effect is operative. Hamming (1973, section 35.5) discusses the effect of smoothing on the Fourier Transform and it was wondered whether this effect had been produced by taking the running mean. In order to test this the Fourier Transform of the unsmoothed derivative data was calculated and it was found that the shape of the Bode plot was unchanged. If the dip is real, it could indicate that the smooth curve drawn through the data points in Figure 5.5 C is not a valid representation of the system response. Although this effect might be real further investigation of it has not been possible as yet.

Another noteworthy feature of the Bode plot is that although the phase of $G'(j\omega)$ decreases rather rapidly above 1,6 Hz, the slope of the amplitude of $G'(j\omega)$ does seem to exhibit another first order break point in the region of 3 Hz. Above 6 Hz the transform becomes very noisy but at this frequency the response is already attenuated by almost 40 dB and the noise is probably due to inherent randomization in the process of differentiation.

In order to obtain an equation to represent this observed closed-loop transfer function, the rapid changes between 1 and 2 Hz were ignored as a first approximation and it was assumed that $G'(j\omega)$ is represented by the dashed line in

that region as depicted in Figure 5.7 A. This leaves two first order break points, one at approximately 0,5 Hz and the other at aproximately 2,9 Hz. Such a transfer function may be represented by an equation of the form

$$G'(j\ ) = \frac{1}{(\ 1 + j\frac{\omega}{\omega_1})(\ 1 + j\frac{\omega}{\omega_2})} \qquad 5.13$$

where ω_1 and ω_2 are the two break frequencies. Using $\omega_1 = 3{,}40 s^{-1}$ (0,54 Hz) and $\omega_2 = 18{,}36 s^{-1}$ (2,9 Hz) in equation 5.13, the points marked with crosses in Figures 5.7 A and B were plotted. In the case of the amplitude curve the agreement with the experimental data is fairly good up to 5 Hz, but in the case of the phase curve the agreement is not as good. This is perhaps to be expected, as the determination of phase is inherently less stable.

It is interesting to note that equation 5.13 may be rewritten in the form

$$G'(j\omega) = \frac{\omega_1\omega_2}{\omega_1\omega_2 + j(\omega_1 + \omega_2)\omega - \omega^2} \qquad 5.14$$

which reduces to equation 5.10 if

$$\omega_n^2 = \omega_1\omega_2 \qquad 5.15$$

$$2\zeta\omega_n = \omega_1 + \omega_2 \qquad 5.16$$

The natural undamped oscillating frequency, ω_n of the system may be determined experimentally from Figure 5.5 A. The experimental value of ω_n is 7,73 s^{-1} whereas the square root of $\omega_1\omega_2$ is 7,90 s^{-1}. The agreement here is surprisingly good. The value of the damping constant obtained from equation 5.16 is 1,37 which is reasonable, because, although an attempt was made to adjust the system for critical damping, the response of the system is very sensitive to gain adjustments in this region.

It therefore seems that to a first approximation the system can be characterised by the simple model proposed in section 5.3.1 and that equation 5.10 can be used for the closed-loop system transfer function. Ogata (1970, section 9.7) considers the relationship between the transient resonse and the step resonse of a system having the closed loop transfer function of equation 5.10. He presents a graph which relates the phase margin of the open-loop frequency resonse to the damping ratio. If the damping ratio is 1,37, the phase margin of the system is 83^{o}, a very stable system. Table 5.2 summarises the azimuthal system performance in terms of the commonly quoted transient-reponse specifications. Wherever possible data has been included for the cases shown in Figure 5.5 A, B & D for comparison. The tracking system is normally operated with a gain which gives the response shown in Figure 5.5 C and the step response analysis has shown that this is the case which has the minimum settling time.

General:

Maximum speed = 22 R.U. per second

Unit step response: (unit step = 16 R.U.)

Natural oscillating frequency, ω_n = 7,73 s^{-1} (7,90 s^{-1})*

	Case C	Case A	Case B	Case D
Damping ratio, ζ =	1,37*	$\zeta \ll 1$	$\zeta < 1$	$\zeta \gg 1$
Delay time, t_d =	0,31s	0,28s	0,29s	0,34s
Peak time, t_p =	-	0,84s	1,03s	-
Rise time, t_r =	0,58s	0,47s	0,55s	0,96s
Settling time, t_s =	0,84s	∞	1,32s	1,34s

* indicates where an estimate has been made using data from the simple model.

Table 5.2 Summary of Azimuthal performance

5.4 CALIBRATION

The tracking system needs calibration in two respects. First, because the readings of altitude and azimuth on the front panel of the ALU are not absolute, it is necessary to determine the difference between the ALU co-ordinates and the true co-ordinates to which the telescope is pointing. Secondly, if the base of the telescope is not precisely horizontal the movement of the telescope will not be truly altitude/azimuth. This effect may be taken into account if necessary by a co-ordinate transformation in the tracking

program. It is likely to be a small effect and is therefore best studied by tracking a strong source for a long time and studying the variations in antenna temperature.

In order to determine the difference between the ALU co-ordinates and the true co-ordinates, the readings on the ALU were compared with computed solar altitude and azimuth at several times during the day. The results are tabulated below (Table 5.3).

Altitude offset = 587 ± 3 R.U.

Azimuth offset = 157 ± 3 R.U.

Table 5.3 Altitude and Azimuth constant offsets.

It was decided to assess the need for a co-ordinate transformation by tracking the sun for long periods at a time (Chapter 7).

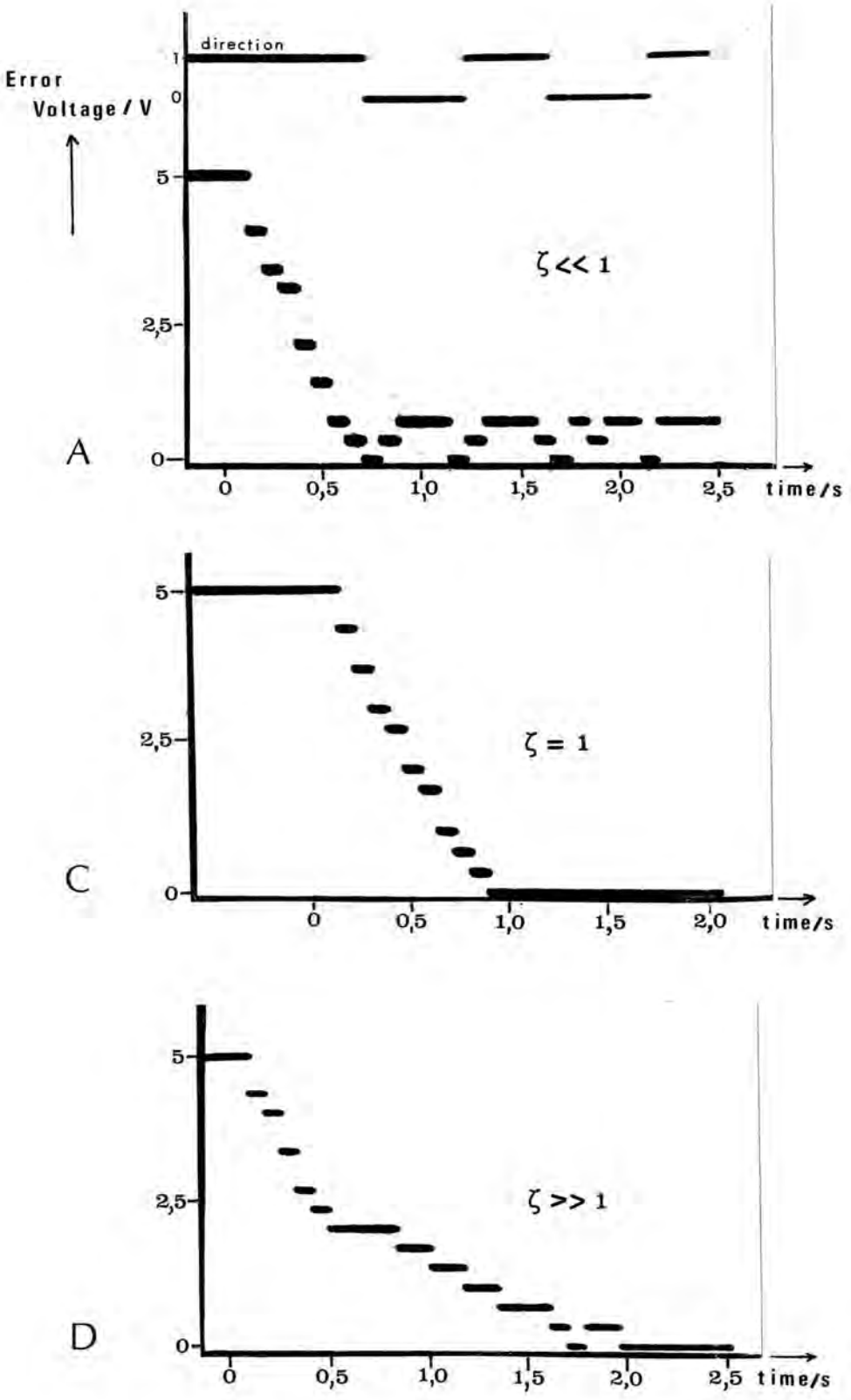

Figure 5.4 The error voltage for various system gain settings (damping ratios)

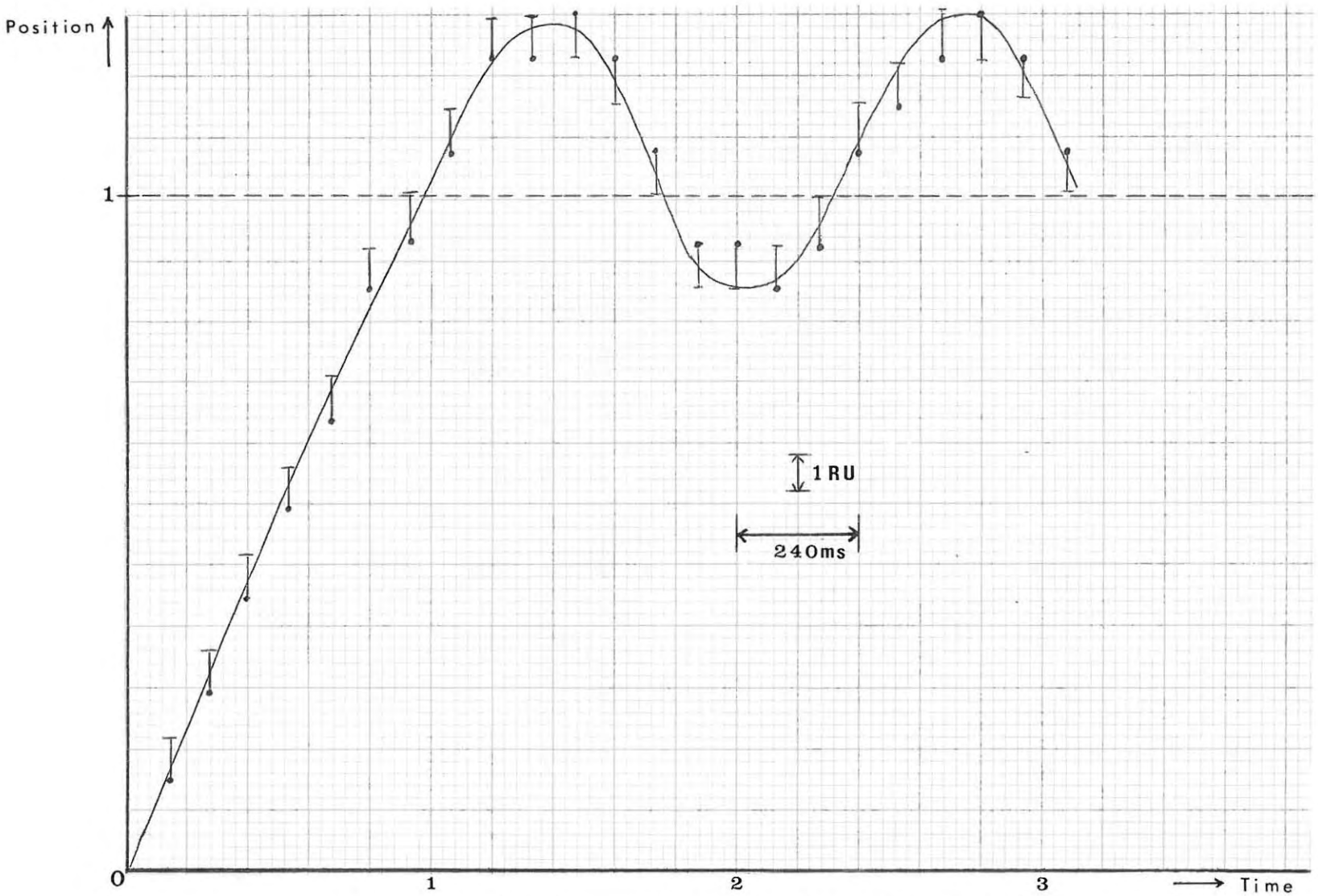

Figure 5.5A The response of the system - $\zeta \ll 1$

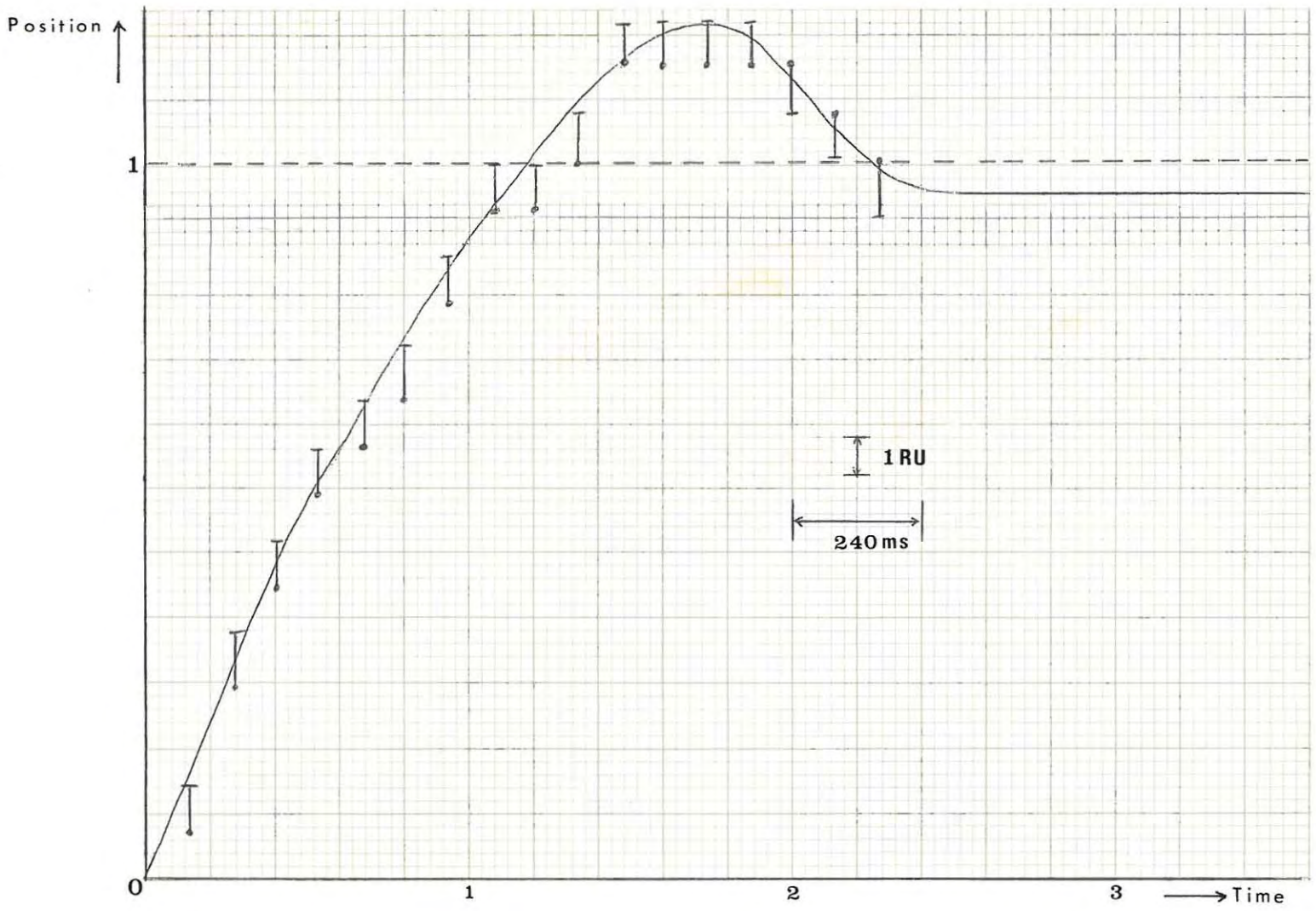

Figure 5.5B The response of the system - $\zeta < 1$

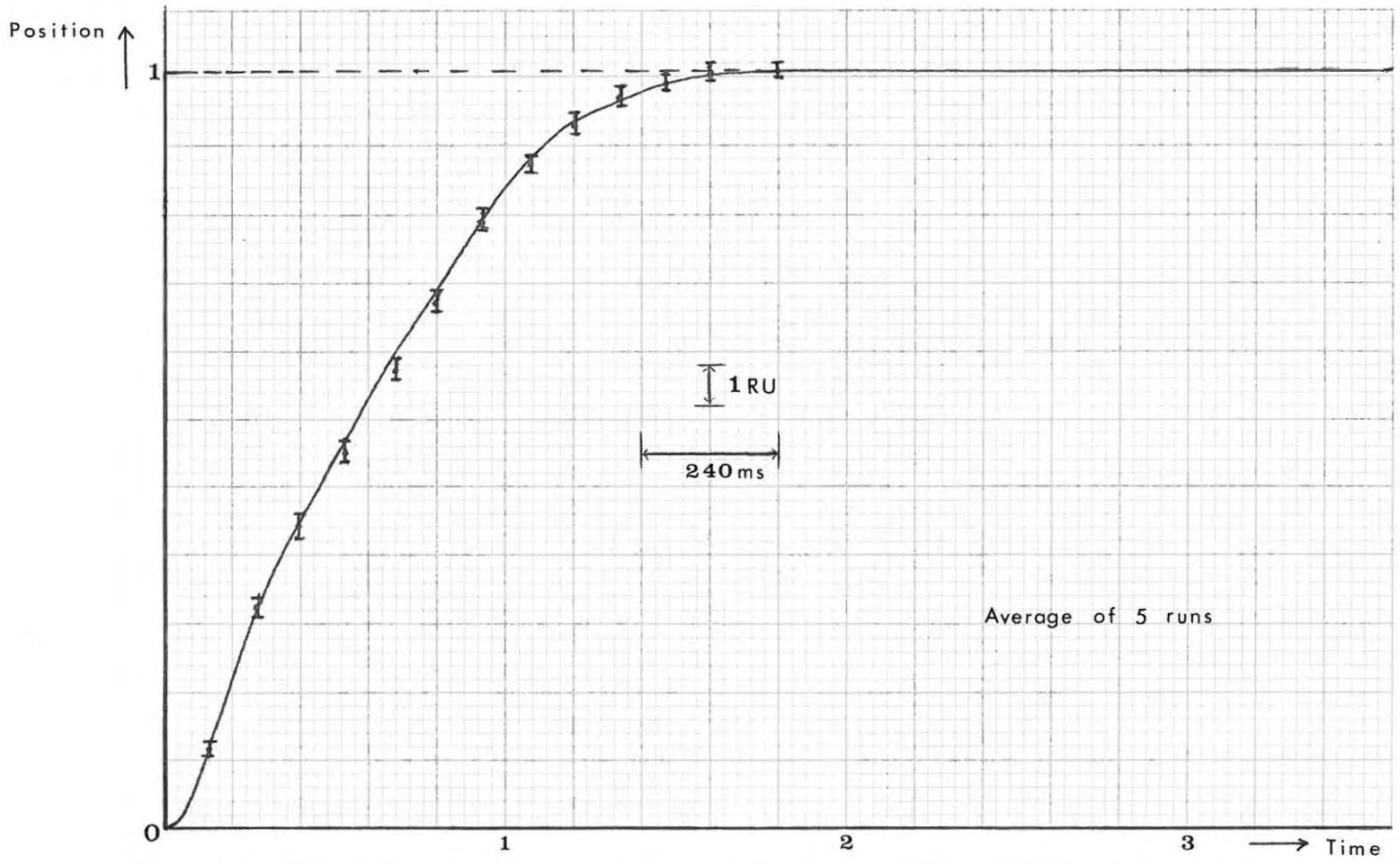

Figure 5.5C The response of the system - $\zeta \cong 1$

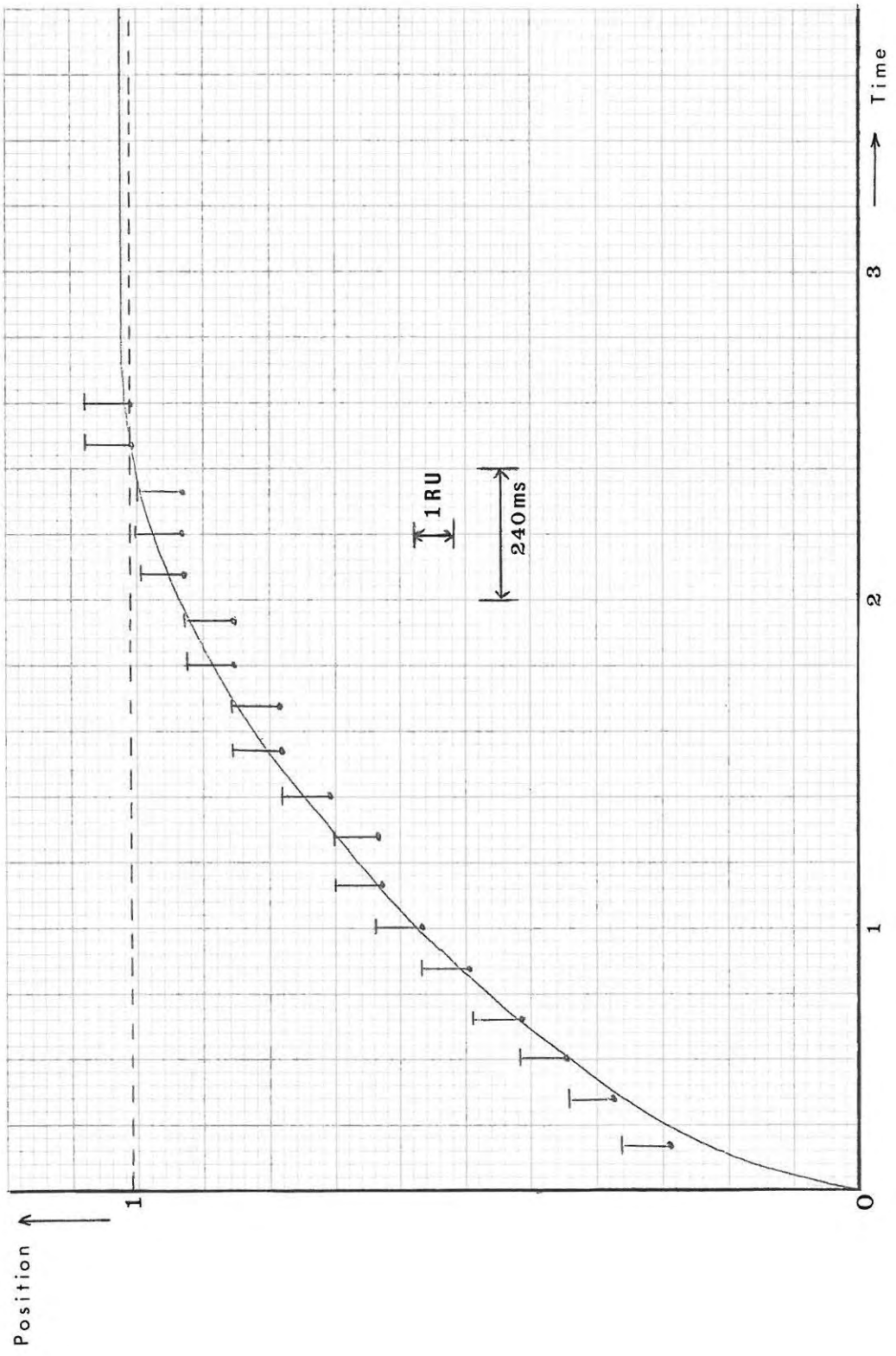

Figure 5.5D The response of the system - $\zeta >> 1$

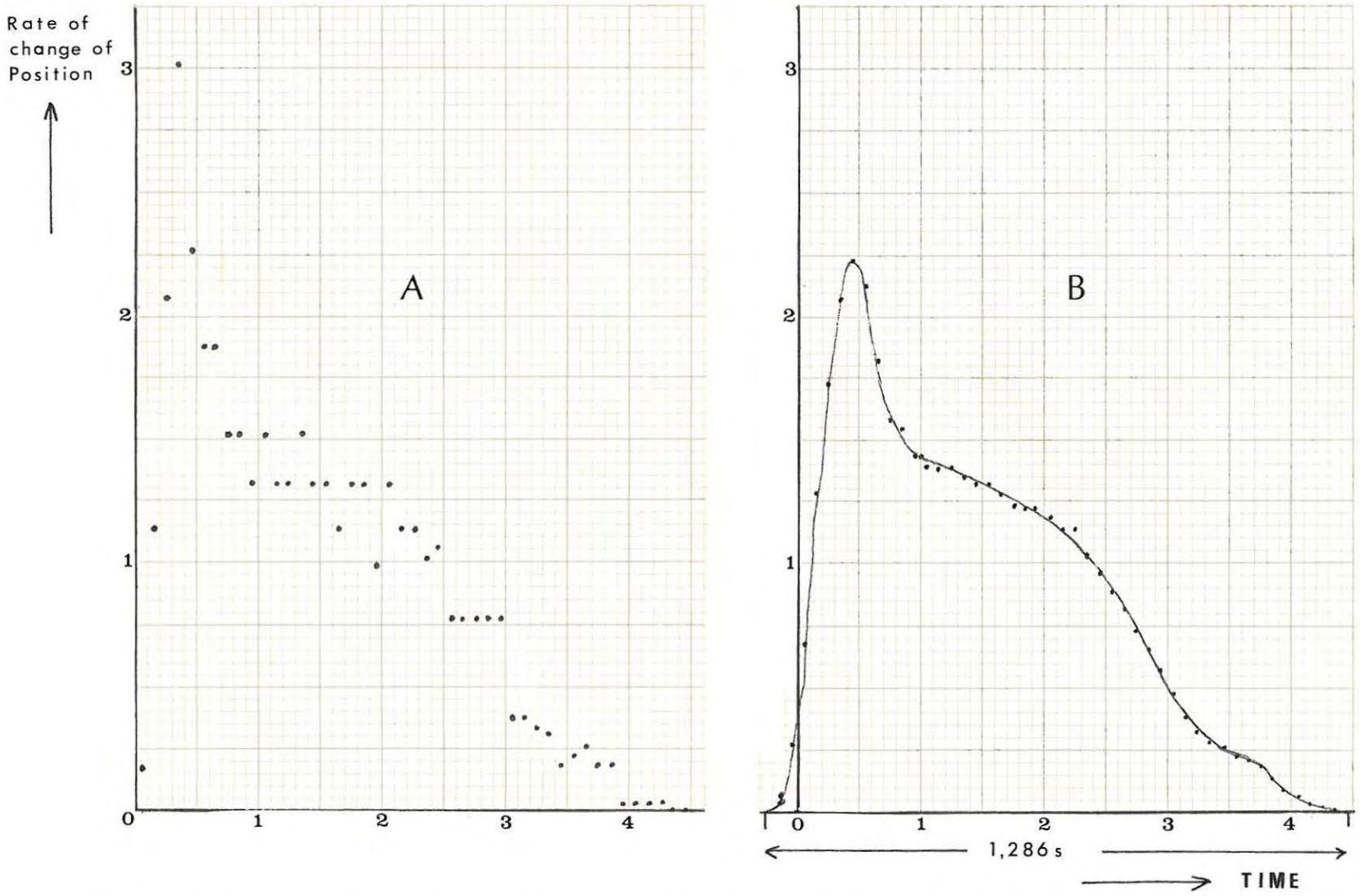

Figure 5.6 A: The derivative of the step response B: The smoothed derivative

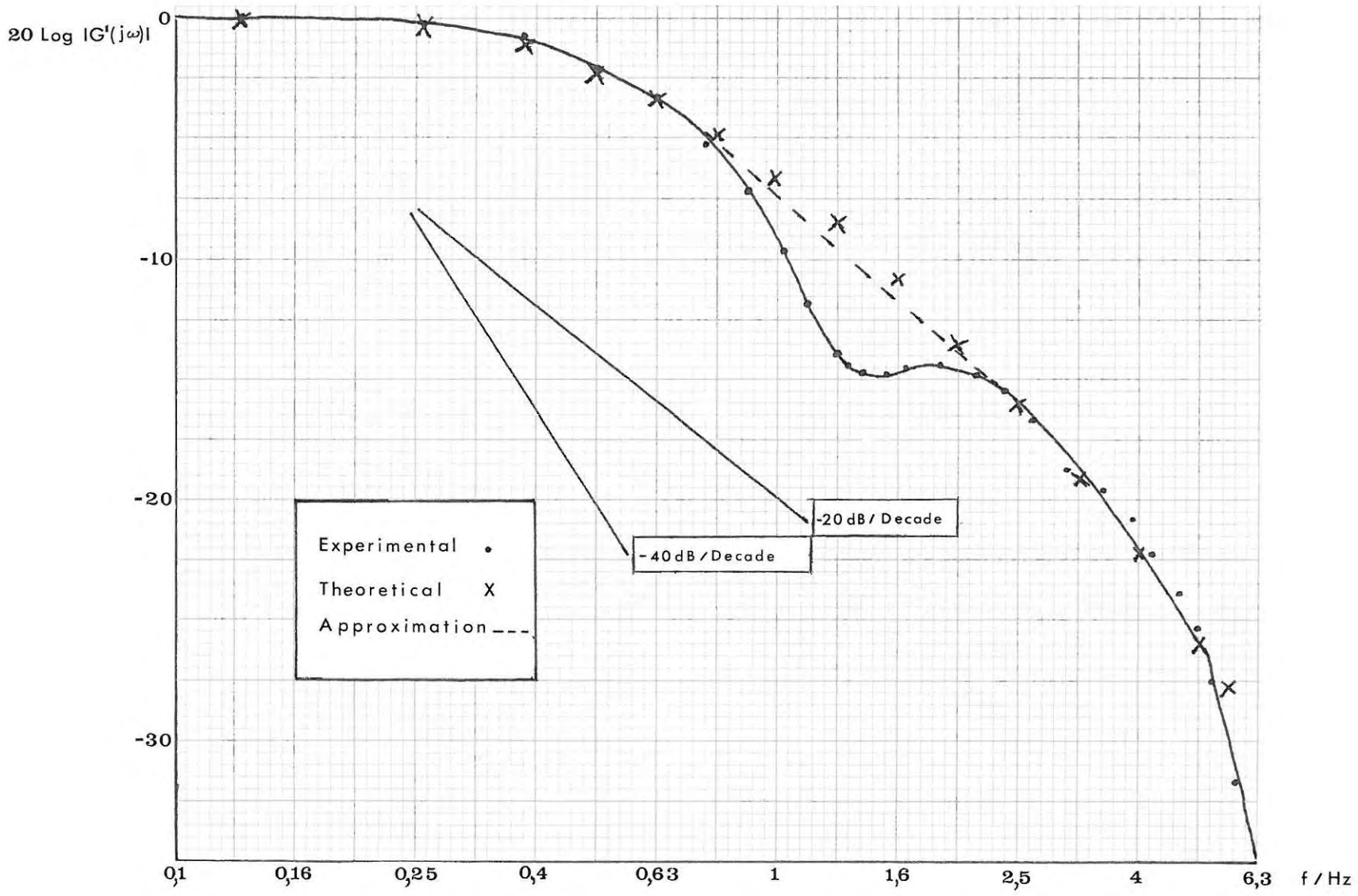

Figure 5.7A 20.Log |G'(jω)| versus frequency

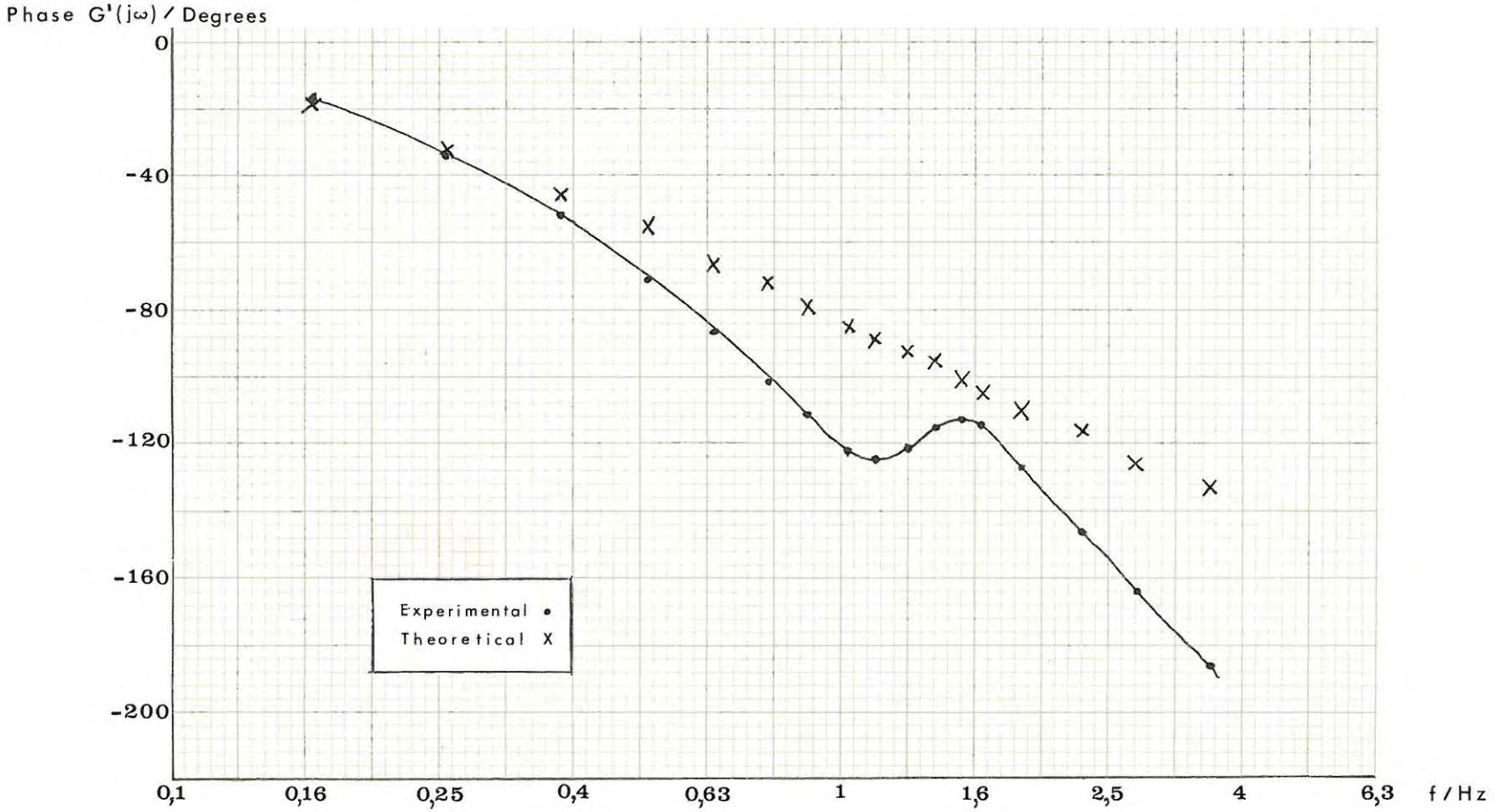

Figure 5.7B Phase of G'(jω) versus frequency

CHAPTER SIX

TRACKING PROGRAMS

6.1 MULTEXBASIC

As was mentioned in section 4.1.1, it was decided to use the language MULTEXBASIC (MULti-Task EXtended BASIC) on the Nova II computer in the Physics Department for the tracking programs because it would then not be necessary to dedicate the computer to the tracking system. Under MULTEXBASIC a number of tasks can be handled simultaneously by the computer (Perseus 1976, Chapter 7). Such a task exists as a separate BASIC program with its own program and data areas. The program and data area assigned to a particular task is referred to as the partition in which that task is executed.

Figure 6.1 shows how the computer is used to control the telescope under MULTEXBASIC. Each partition is assigned 6K of core (6 000 sixteen-bit words). 1K of core is also set aside for variables or arrays which may be declared as being in common with variables or arrays in programs running in other partitions. All programs are stored on floppy disk. The operator has direct access to partitions "1" and "-1" via the VDU terminal but not to partition "0". Partition "0" is connected directly to the tracking system which is treated as a separate terminal. It is possible to load and run programs in partition "0" from any of the other

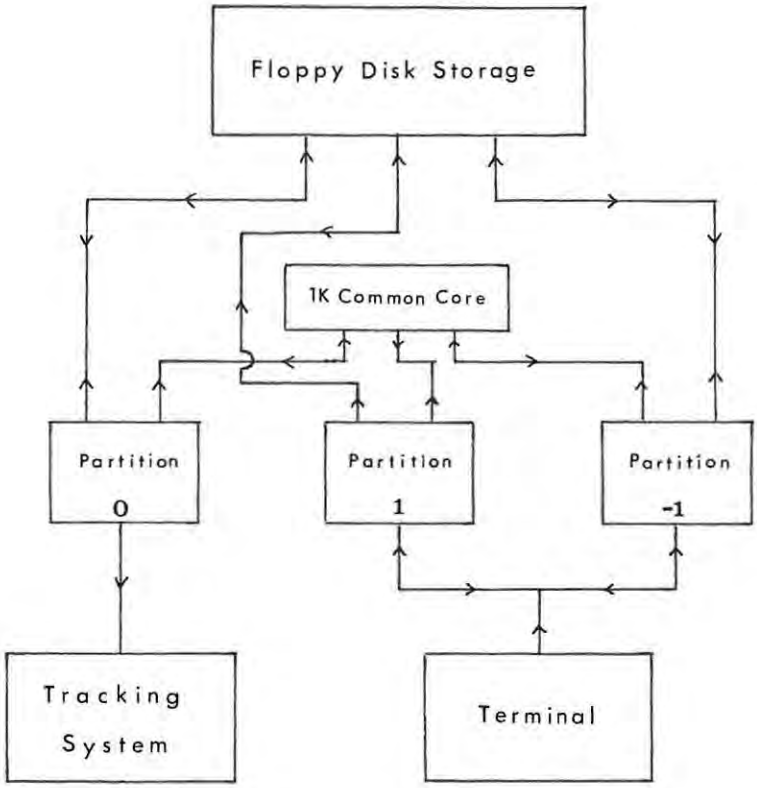

Figure 6.1 The use of the computer under MULTEXBASIC

partitions. A fourth partition, partition "2", is also available but has not been used.

Another important feature of MULTEXBASIC is the real time clock which can be set up when the language is loaded into core. This clock which has a resolution of one second, is used to control the transmission of data to the tracking system.

The tracking program runs in partition "0". The program in partition "-1" is used to load into the computer the relevant tracking data and also to monitor the real time

clock to indicate when the tracking program has ended. Partition "1" has been used for further program development while the tracking program is running. The original intention was to use only partition "0" for the telescope control and to leave the other three partitions free for other users of the computer. Although this is possible with the present system, the rather limited storage space in each partition has made it somewhat impractical.

6.2 GENERAL DESCRIPTION OF PROGRAMS

A number of programs have been written for use with the tracking system. The more important of these are as follows:

i) AUTOTRACK - tracks a source continuously

ii) NODDY - tracks alternately on and off the source

iii) NODDY2 - tracks alternately in each beam of the telescope to improve signal-to-noise ratio on weak signals

iv) MOON - for observations of the moon

v) DECSAN - maps a small area of sky

vi) DRIFT - permits a number of successive drift scans of the same source by asking for the "time of next drift scan"

vii) INTERTRACKER - used to load data for the other programs.

The specifications of the tracking programs i) to vi) are

all similar and therefore in the present section only NODDY, the most frequently used tracking program, and the interactive program, INTERTRACKER, will be considered. These programs are used only for tracking the sun.

6.2.1 CALCULATING THE SOLAR CO-ORDINATES

There are two ways of calculating the Right Ascension and Declination of the sun. The first is a direct calculation using the equations given in the Explanatory Supplement to the Astronomical Ephemeris (1961). The second is to do a linear interpolation using the known Right Ascension and Declination of the sun at 0:00 U.T. and 24:00 U.T. on the day of observation. Both of these methods were tried and it was found that, for the accuracy required by the telescope, the linear interpolation is adequate. It was therefore decided to calculate the R.A. and Declination of the sun by means of a linear interpolation.

The conversion from the R.A. and Declination co-ordinate system to the horizon system of co-ordinates is performed by means of the following equations (Explanatory Supplement to the Astronomical Ephemeris 1961, page 26):

$$\cos a \sin A = -\cos\delta \sin h \qquad 6.1$$

$$\cos a \cos A = \sin\delta \cos\phi - \cos\delta \cos h \sin\phi \qquad 6.2$$

$$\sin a = \sin\delta \sin\phi + \cos\delta \cos h \cos\phi \qquad 6.3$$

where h = hour angle = local sidereal time - R.A.

a = altitude

A = azimuth

ϕ = lattitude of observer

and δ = declination

The local apparent sidereal time may be calculated from the equation

L.S.T. = Greenwich apparent sidereal time at 0:00 U.T.
+ U.T. + sidereal correction + longitude of site 6.4

The resolution of the tracking system, 1 R.U., corresponds to approximately five seconds of time at the sidereal rate. The sun moves at an approximately sidereal rate and it was therefore decided to transmit a pair of co-ordinates to the tracking system every two seconds.

6.2.2 INTERTRACKER

Figure 6.2 is a flow chart of the program INTERTRACKER, so called because it allows the telescope operator to interact with the tracking program. INTERTRACKER initially sets the variable pointing offsets to zero and assigns variables in common storage for solar Right Ascension (R.A.) and Declination at 0:00 U.T. and 24:00 U.T., the local apparent Sidereal Time and the required start and end times of the run. The program then asks the operator to key in the known

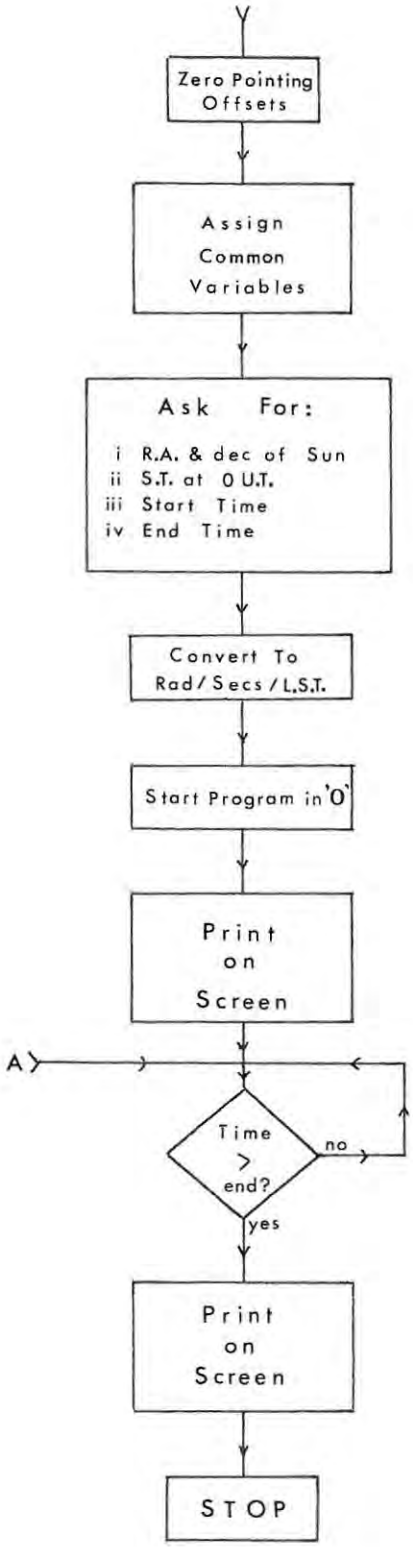

Figure 6.2 Flow chart of "INTERTRACKER"

solar Right Ascensions and Declinations, the Greenwich apparent sidereal time at 0:00 U.T. on the day of observation and the required start and end times of the run, also in U.T. After converting the co-ordinates to radians, calculating the local apparent sidereal time and converting all times to seconds, all of this data is stored in the common core space. INTERTRACKER then starts the program in partition "0" and a message appears on the screen of the VDU informing the operator that the tracking program is running. INTERTRACKER then monitors the real time clock until the time is greater than the required end time of the run at which stage a second message is printed on the VDU screen informing the operator that the run has ended. It is possible to stop this program at any time and change the pointing offsets (see below) while the other program is running in partition "0". The program may then be continued from the point "A" (Figure 6.2) and the program in partition "0" will make use of the new pointing offsets. Once the data has been keyed in, it is not essential to continue running INTERTRACKER.

6.2.3 NODDY

The most commonly used tracking program is NODDY, so called because the telescope nods on and off the source at regular intervals, usually 30 seconds on, 30 seconds off. The reason for the use of this observing technique is that by tracking off the sun every 30 seconds a base-line is

established. This was found to be essential because the base-line from the total power receiver exhibits a marked temperature drift (section 7.1).

When NODDY (See Figure 6.3) is started by INTERTRACKER, the same set of variables is assigned to common core. This gives NODDY access to the data necessary for the calculation of the solar altitude and azimuth. The start time is treated as the first co-ordinate transmission time and a linear interpolation is done to obtain the R.A. and Declination of the sun at that time. The sidereal time is then calculated, converted to radians and used to calculate the Hour Angle (H.A.) of the sun. The solar H.A. and Declination are converted to altitude and azimuth using equations 6.1 to 6.4 and pointing corrections are added to each of these co-ordinates. The pointing correction takes the form of two numbers, the constant offset (from Table 5.3) and a variable offset (G for altitude and K for azimuth) which can be controlled via the program INTERTRACKER. After the two co-ordinates have been converted to octal in the next stage of the program, the real time clock is examined. If the time is less than the desired start time, the telescope lock is turned on. The program then monitors the real time clock until the start time at which stage the telescope lock is turned off and the co-ordinate transmission time is incremented by two seconds. This time is then used to calculate a new set of co-ordinates for the telescope. As soon as the time

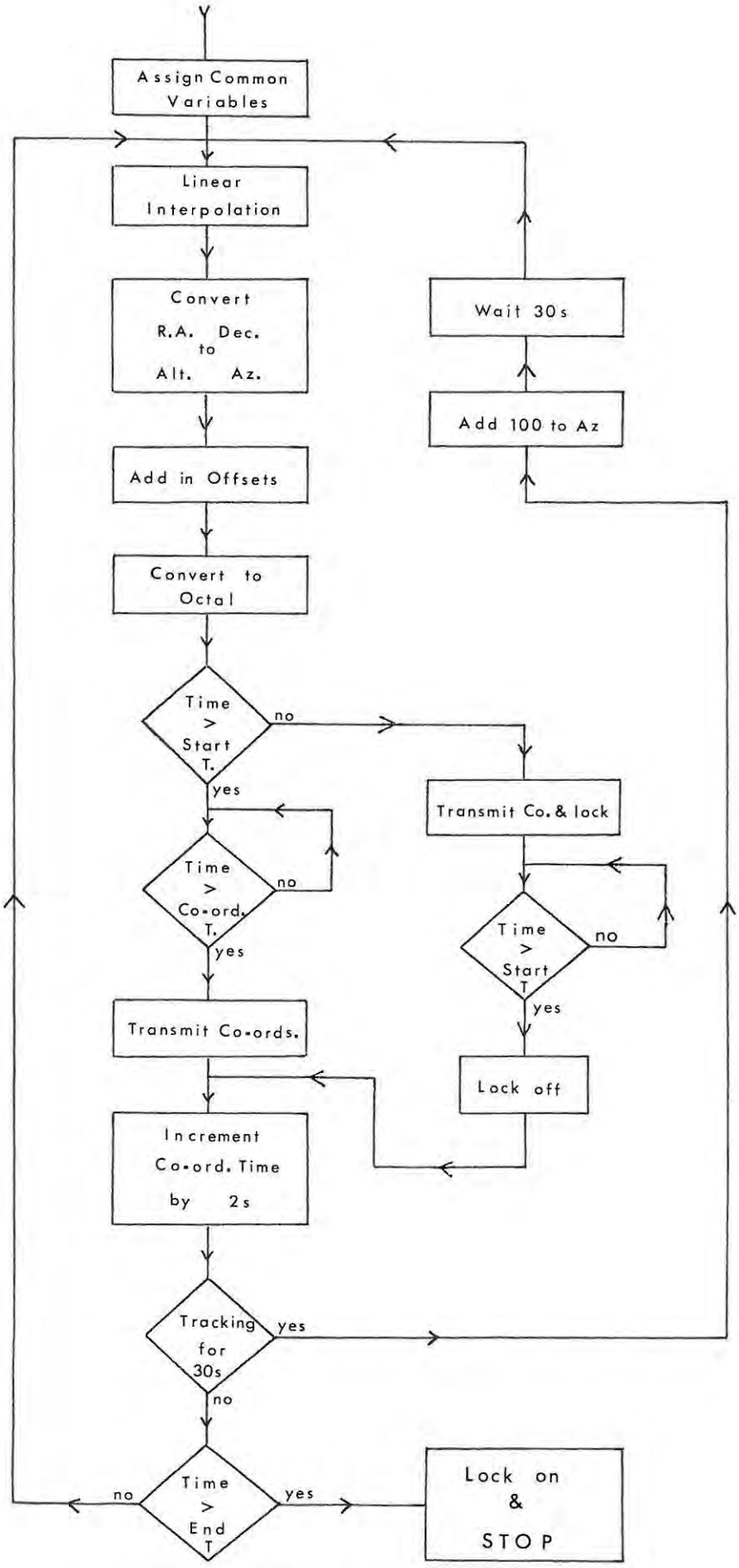

Figure 6.3 Flow chart of "NODDY"

indicated by the real time clock is greater than the new co-ordinate transmission time, the new pair of co-ordinates is transmitted to the tracking system. After 18 pairs of co-ordinates have been transmitted, in approximately 36 seconds, the telescope is driven 100 R.U. off source. Thirty seconds later, 30 seconds is added to the co-ordinate transmission time and the program continues. Results obtained with this program will be presented in the next chapter.

Because the telescope in its present form is not sensitive enough to observe objects outside of the solar system no programs have been developed for this purpose.

Listings of the programs "INTERTRACKER" and "NODDY" may be found in Appendices 6.1 and 6.2 respectively.

CHAPTER SEVEN

OBSERVATIONS

7.1 PRESENT STATE OF THE SYSTEM

The Rhodes 22 GHz radio telescope has been described in great detail by Nunn (1974), Mutch (1975) and Gaylard (1976). In this section, only the present state of the "front end" microwave section and the continuum receiver (Gaylard 1976, Chapters 3 & 4) will be evaluated.

7.1.1 REPAIRS CARRIED OUT

When the author began observations of the sun in April 1978, the telescope had not been used for 18 months. It was found that the telescope was extremely insensitive and that the output of the continuum receiver was very unstable particularly when a time constant of more than one second was used. Some idea of the poor signal-to-noise ratio of the system may be gained from Figure 7.1, a drift scan of the sun done with maximum receiver sensitivity. Figure 7.2, a drift scan through a section of cold sky with a ten second time constant, shows the instability in the continuum receiver output. These fluctuations do not appear to be due to thermal noise alone.

The continuum receiver and the chart recorder driver unit

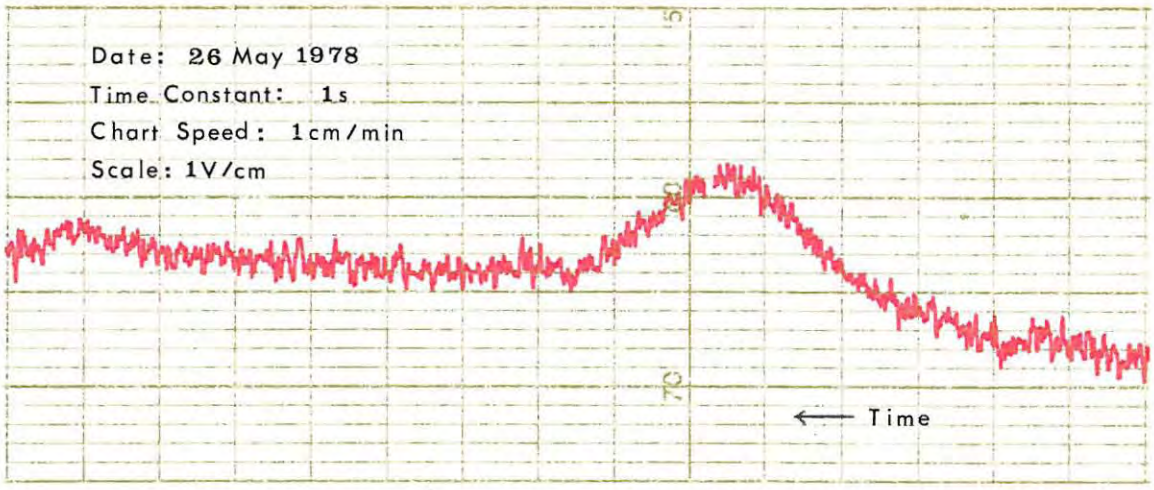

Figure 7.1 Drift scan of the sun with maximum sensitivity

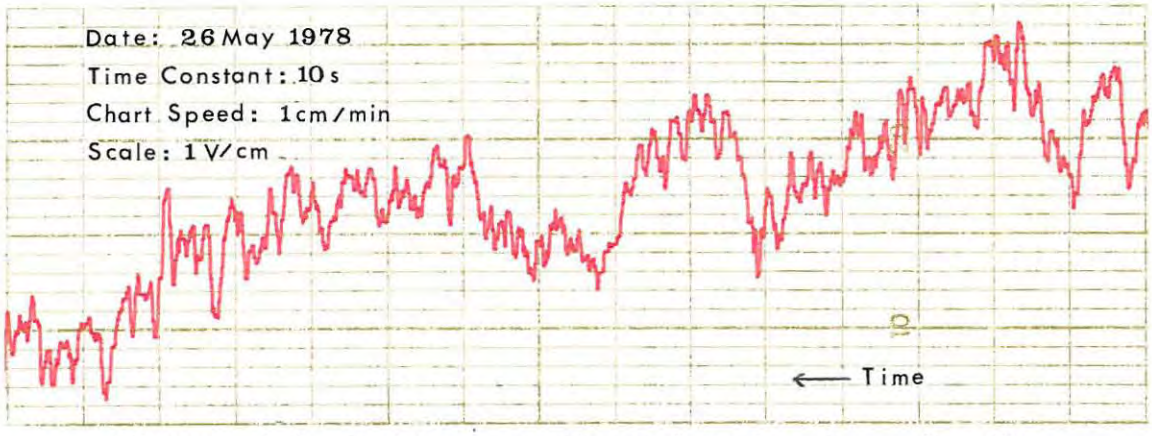

Figure 7.2 Drift scan through cold sky - τ = 10s

were checked for satisfactory operation and no faults could be found. Gaylard (1976, page 56) points out that the present system employed to obtain the various time constants (1, 3, 10 and 20 seconds) affects the gain of the integrating amplifier. This could be the explanation of the apparently large instability in the continuum receiver output when a large time constant is used.

In order to find the cause of the apparent receiver insensitivity, the microwave front end of the telescope was dismantled to check for satisfactory operation of the microwave components. Figure 7.3 is a block diagram of the

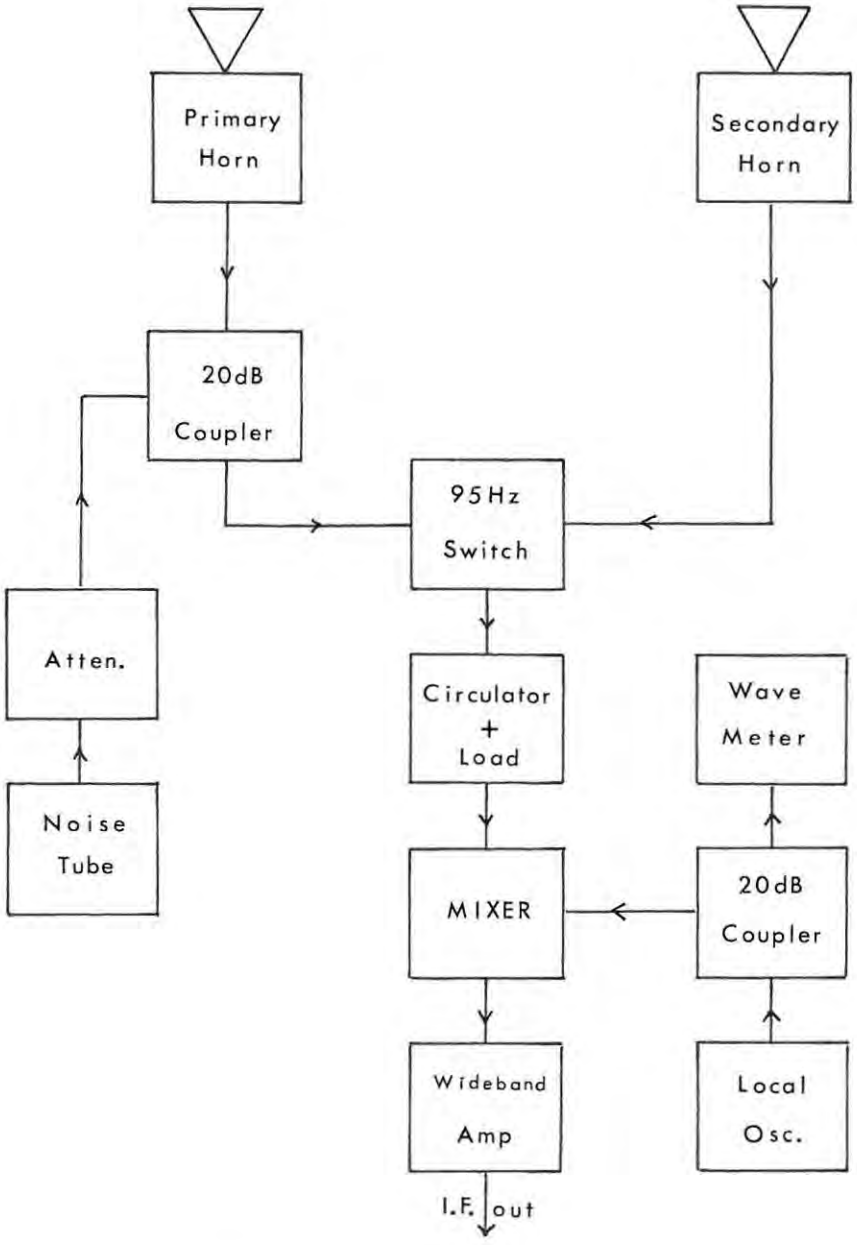

Figure 7.3 The microwave section of the telescope

microwave section of the telescope. On examination, it was

found that the waveguide had become filled with water at some stage owing to the weathering and the subsequent cracking of the mylar coverings which had been glued over the horns. It was found that the noise tube had been completely destroyed and that the barrel of the wavemeter had become rusted fast. Fortunately, calibration of the receiver was not necessary for the observations done to test the tracking system. The waveguide inside some of the components showed signs of corrosion and pitting. The switch and the circulator were rebuilt by the author and the mixer was stripped down and cleaned. Unfortunately, the diode encapsulations had been destroyed and the diodes had to be replaced with a spare pair, one of which was known to be faulty.

When the front end was put back into use, it was found that the sensitivity had been improved, but that it was still not very good. Figure 7.4, a drift scan of the sun done after the repairs had been completed, shows the improved sensitivity (cf. Figure 7.1).

7.1.2 ESTIMATION OF SYSTEM TEMPERATURE

Because the noise tube could not be replaced, an accurate determination of the system temperature was impossible. However, an estimate of the system temperature was obtained by observing first cold sky and then a tree which was located approximately 3 metres from the telescope. For

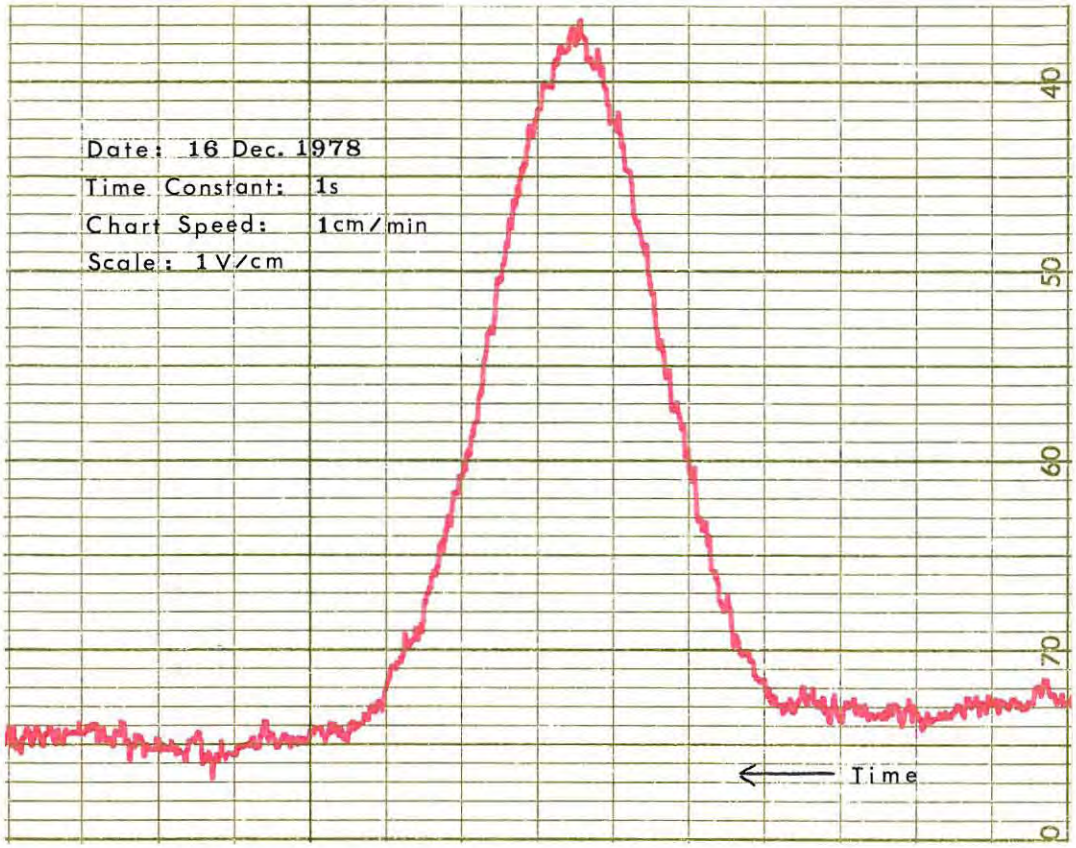

Figure 7.4 Drift scan of the sun after system repair

these observations, one of the horns was replaced by a matched load so that the telescope would be switching against a constant reference of 300 K. The antenna temperature, T_a, due to the atmospheric water vapour at a mean temperature T_{aw} is given by the equation (Fogarty 1975)

$$T_a = T_{aw} \cdot [\ 1 - 1/L_{at}\ ] \qquad 7.1$$

where L_{at} = atmospheric attenuation = exp [τ sec z]

and τ = optical depth; z = zenith angle

Fogarty gives the mean temperature of atmospheric water vapour as 280 K and Gaylard found that the clear sky zenith

attenuation varies between 0,5 dB and 0,9 dB. Using the values of 280 K for T_{aw} and 0,7 dB for the atmospheric attenuation, equation 7.1 gives an antenna temperature of 42 K. The tree observed at close quarters was assumed to be at a temperature of 300 K and was large enough to fill the telescope beam.

The change in antenna temperature between the observation of cold sky at the zenith and a tree at short range is therefore 258 K. Figure 7.5 shows the chart recorder output

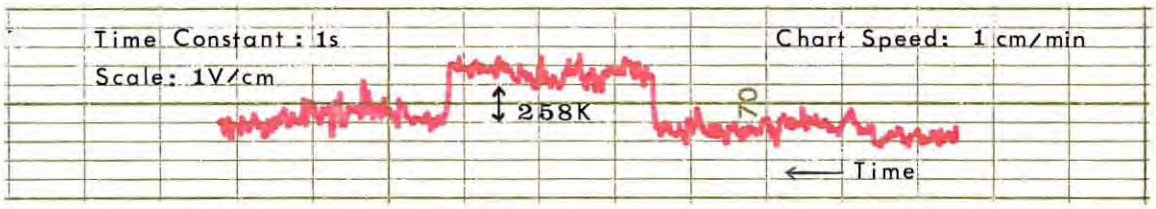

Figure 7.5 Estimation of system temperature

from the continuum receiver for these observations. Although the noise fluctuations in Figure 7.5 appear to be non thermal, a very rough estimate of the system temperature, T_{sys}, can be obtained from Figure 7.5 by estimating the minimum detectable temperature, ΔT_{min}. The system temperature, T_{sys}, is related to ΔT_{min} by the equation (Kraus 1966, page 102)

$$\Delta T_{min} = \frac{K_S \, T_{sys}}{\sqrt{B \, t \, n}} \qquad 7.2$$

where B = predetection bandwidth

t = postdetection integration time

n = number of records averaged

and K_S = receiver sensitivity constant

K_S for a beam switching receiver is 2 (op.cit., page 258), since the minimum detectable signal is double what it would be for continuous detection.

The minimum detectable temperature was taken to be one quarter of the peak to peak noise, taken over a time interval equal to ten times the post-detection integration time constant (Baart 1974). ΔT_{min} from Figure 7.5 is 44 ± 10 K. Using this value of ΔT_{min} in equation 7.2 yields a system temperature of 220 000 K ± 80 000 K. This indicates that the telescope is still not operating satisfactorily at the moment.

The value of 44 K for ΔT_{min} is less than the antenna temperature observed by Gaylard (1976, Figure 5.4) for the moon (50 K) and in fact all attempts at lunar observation by the author have been unsuccessful. Exclusive use has been made of solar observations for the testing of the tracking system described in the remainder of this chapter.

7.2 TRACKING THE SUN

Even before the microwave section of the telescope had been repaired, it was possible to show that the tracking system could make the telescope follow the sun for an entire day.

Figure 7.6 shows the result of six hours of solar observation. (All figures referred to in this section appear at the end of the present chapter.) The late sunrise and early sunset are due to the fact that the telescope is at present situated close to numerous trees and large buildings. The baseline slope in Figure 7.6 is due to the heating up of the telescope during the day. The effect is more pronounced on hot days than it is on cold days.

After the sensitivity of the telescope had been improved, it was possible to study better the performance of the tracking system. It was found that at times the antenna temperature remained constant for long periods of tracking which appeared to indicate that the tracking system was working satisfactorily. Figure 7.7 shows the result of 50 minutes of solar observation with the tracking system working well. At other times, however, a marked periodic variation in antenna temperature was observed. An example of this effect, which shall be referred to hereafter as "the ripple effect", is shown in Figure 7.8.

Analysis of Figure 7.8 revealed that the ripple period was equal to the period of time for which the solar azimuth co-ordinate was in each azimuth fine segment. It was first thought that the ripple effect was produced by misalignment of the fine synchro stator voltages as described in section 5.1 (Figure 5.2). If the effect was also present in altitude it would not be noticeable because at that time of

the year the solar altitude remained nearly constant and fell in the same fine segment for about two hours over the midday period.

On the 5th September the fine synchro stator voltages were set to the correct levels. Figure 7.9A shows the result of tracking the sun for a period of one hour, after the alignment had been carried out. The tracking system appeared to be working well. Figure 7.9B is the record obtained when the sun was observed at approximately the same Hour Angle the next day. The ripple effect had reappeared. The 6th September was a much colder day than the 5th (note the small baseline slope in Figure 7.9B) and it was found that the change of temperature had upset the alignment of the fine synchro stator voltages. The smaller antenna temperature recorded in Figure 7.9B does not have anything to do with the ripple effect. The maximum antenna temperature recorded in Figure 7.8 is the same as that of Figure 7.9A.

Although the misalignment of the fine synchro stator voltages due to changes in the ambient temperature appeared to be the cause of the ripple effect, it was later discovered that the ripple was not only due to fine synchro stator voltage misalignment. On more than one occasion it was found that immediately after the alignment had been performed a smaller ripple effect was still observed. This suggested a nonlinearity in either the gears, the synchros

or the synchro-to-digital converter. It was also realised that the linearity check carried out previously (section 5.2) would have masked such nonlinearities because the measurements were made at the same point in each fine segment. In order to check the linearity within each fine segment the telescope was moved 10 R.U. at a time according to the reading on the ALU and at each position the reading on the vernier scale on the telescope mount was recorded. These measurements were done in three consecutive fine segments for both altitude and azimuth. Figure 7.10 is a plot of the reading on the vernier scale against the ALU reading for one of the azimuth fine segments and one of the altitude fine segments. The solid line indicates where the points ought to lie. The error-bars represent a conservative estimate of the error in reading the vernier scale. They have been omitted in the case of the altitude for the sake of clarity.

From Figure 7.10 it can be seen that a nonlinearity exists between 30 and 70 R.U. and that the effect is almost identical for altitude and azimuth. The points in the other fine segments of both altitude and azimuth have the same distribution about the desired values. The fact that the nonlinearity is the same in all fine segments suggests that the fault almost certainly lies in the synchro-to-digital converter and not in the synchros themselves or the gears.

The first candidate for examination in the

synchro-to-digital converter was the divider (section 2.2.5). When the alignment of this device was checked, it appeared to be operating linearly. The divider was later removed from the circuit and replaced by an operational amplifier which was used to set the voltage on the output of the PRAM to the correct level for the analogue-to-digital converter. Although this opens the feedback loop which compensates for changes in the amplitude of the reference voltage, the system should remain stable for short periods of time. The points of Figure 7.10 were then rechecked and found to be unchanged.

If a nonlinearity is present in the synchro-to-digital converter, an explanation is needed for the fact that the ripple effect not noticable in Figure 7.8 and Figure 7.9A. From Figure 7.10 it can be seen that the departure from linearity is not more than 4 R.U. ($0{,}09^{o}$). If the telescope is moved 4 R.U. off-source, a change of about 10% in the antenna temperature should be observed (see Figure 1.1).

However, if the pointing offsets in the tracking program are such that the telescope is -2 R.U. off-source at the start and end of each segment, it would be +2 R.U. off-source in the middle of the segment, i.e. the telescope would never be more than 2 R.U. off-source. When the telescope is 2 R.U. off-source, a change of about three to four percent in the antenna temperature would be observed. This change

in antenna temperature would be hidden in the noise fluctuations in the output of the continuum receiver. The peak to peak noise is about 5% of the observed antenna temperature due to the sun when a one second time constant is used. The fact that it is possible for this effect to be hidden by changing the variable offsets in the tracking program accounts for the fact that it is not always observed.

The study of this nonlinearity has been hampered by the temperature instability associated with the fine synchro stator voltage alignment. If the base of the telescope mount were to be temperature-controlled, the frequent alignment of the tracking system would not be necessary and it would be easier to locate the cause of the nonlinearity observed in the fine segments. If all attempts to remove this nonlinearity fail, it could be removed in the tracking programs since it does not appear to be a random effect.

The cause of the ripple effect therefore appears to be two-fold. It occurs when the alignment of the fine synchro stator voltages is upset by changes in the ambient temperature. It is also due to a nonlinearity which seems to be present in the synchro-to-digital converter. This effect is the smaller of the two and is sometimes hidden in the flucuations in the continuum receiver output. Both of these effects can be eliminated.

Although the ripple effect has prevented the assessment of the need for a co-ordinate transformation as suggested in section 5.4, Figures 7.7 and 7.9A show that the tracking system meets up to the desired specifications when properly aligned.

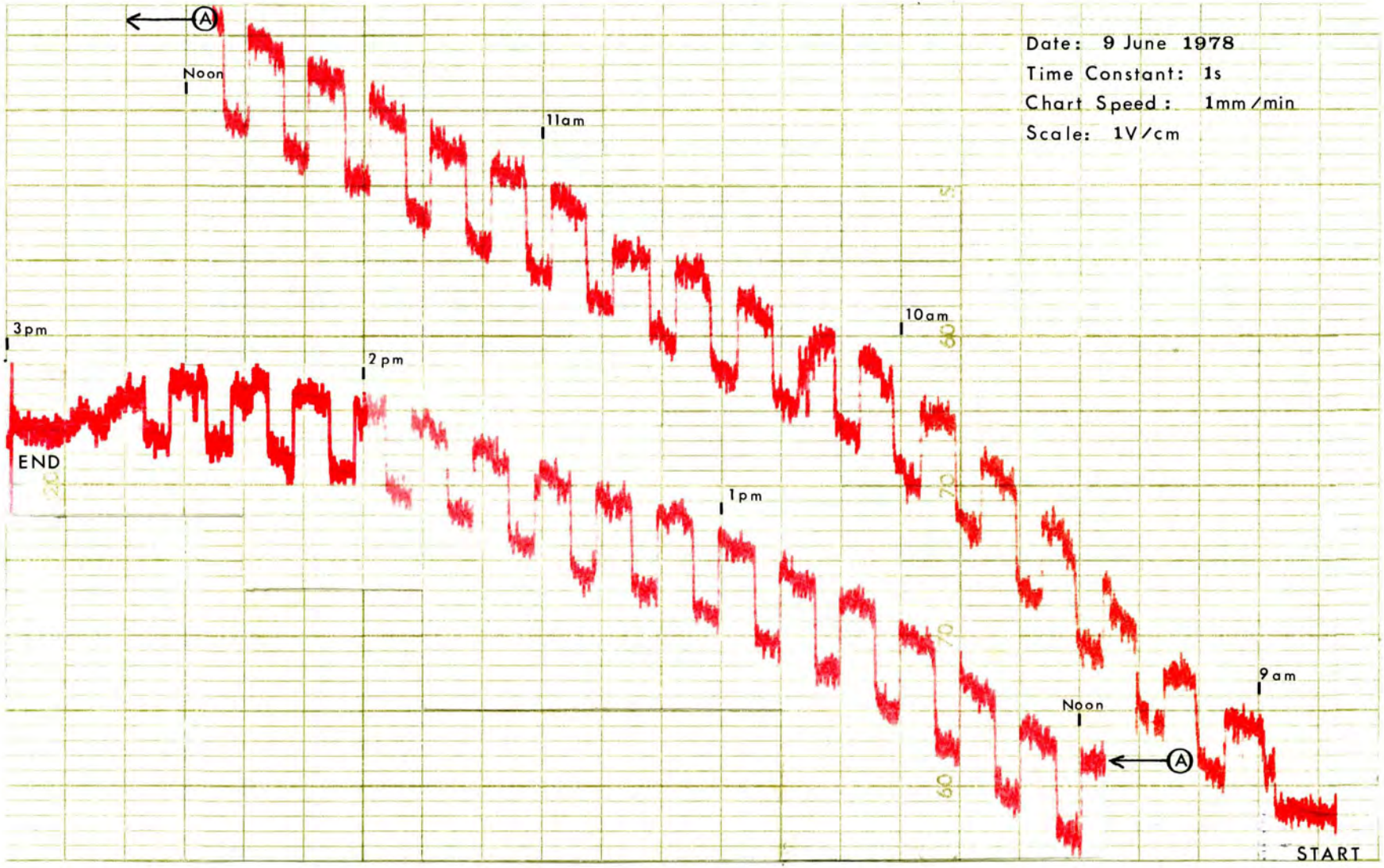

Figure 7.6 Six hours of Solar observation

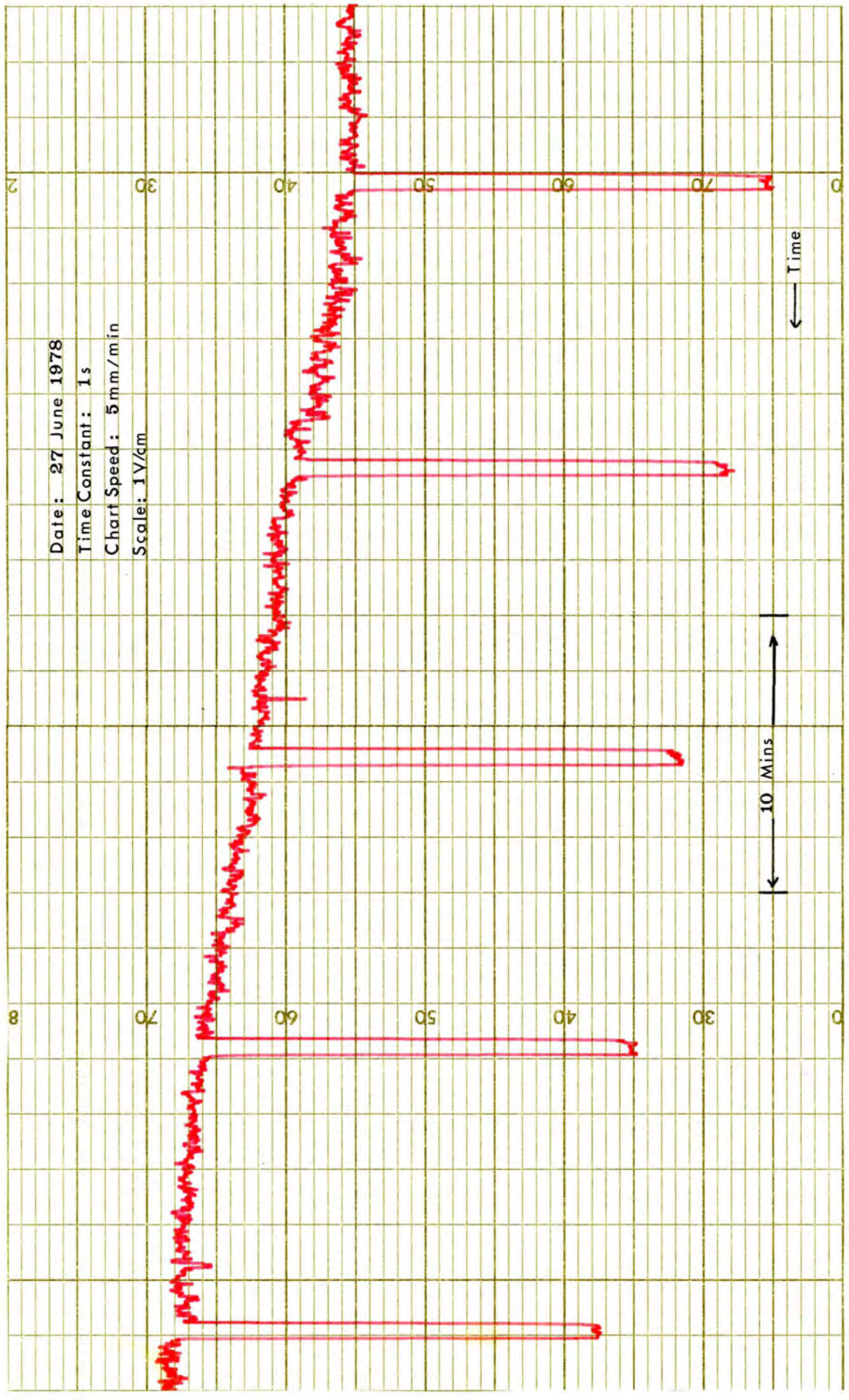

Figure 7.7 Solar observation after front end repair

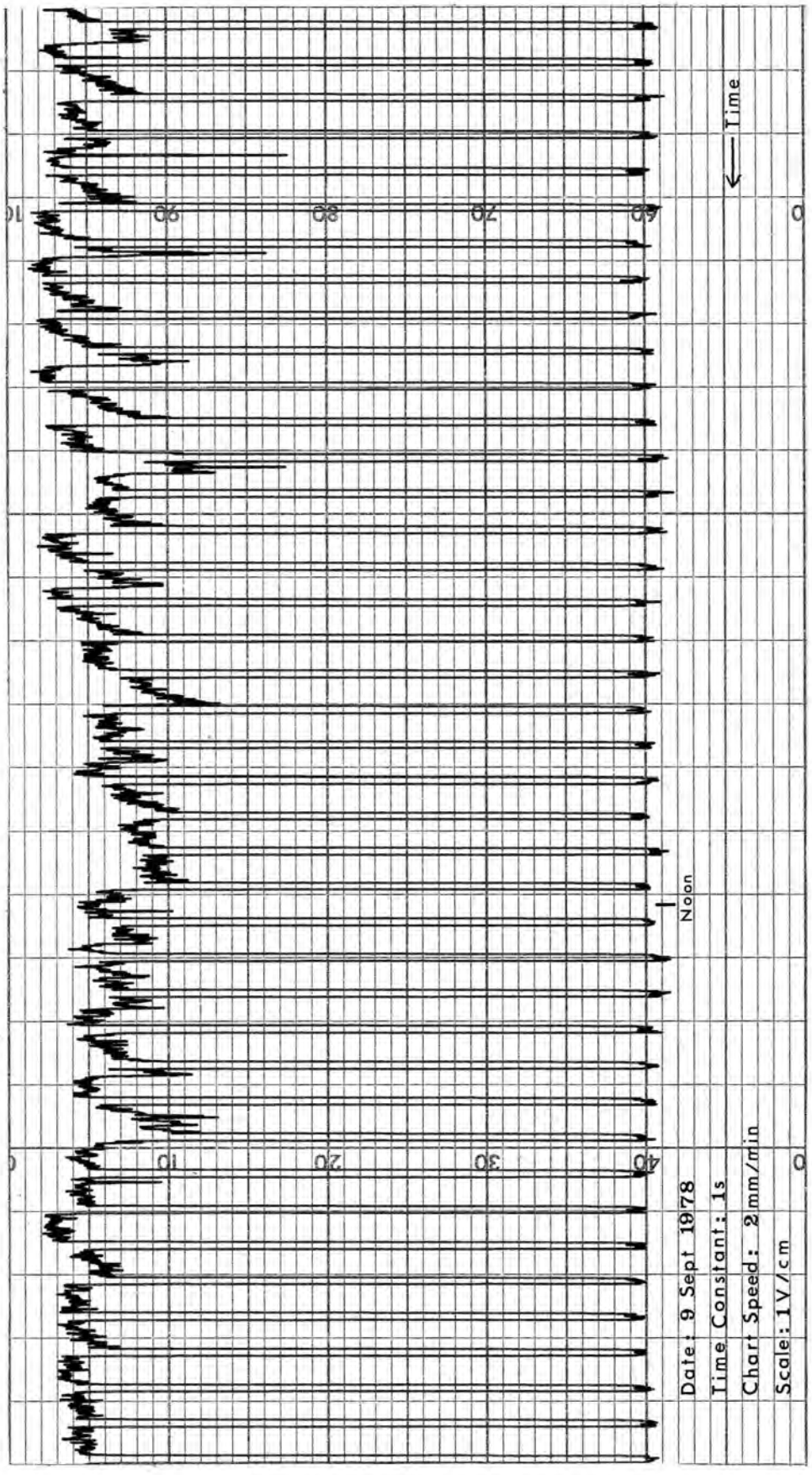

Figure 7.8 The ripple effect

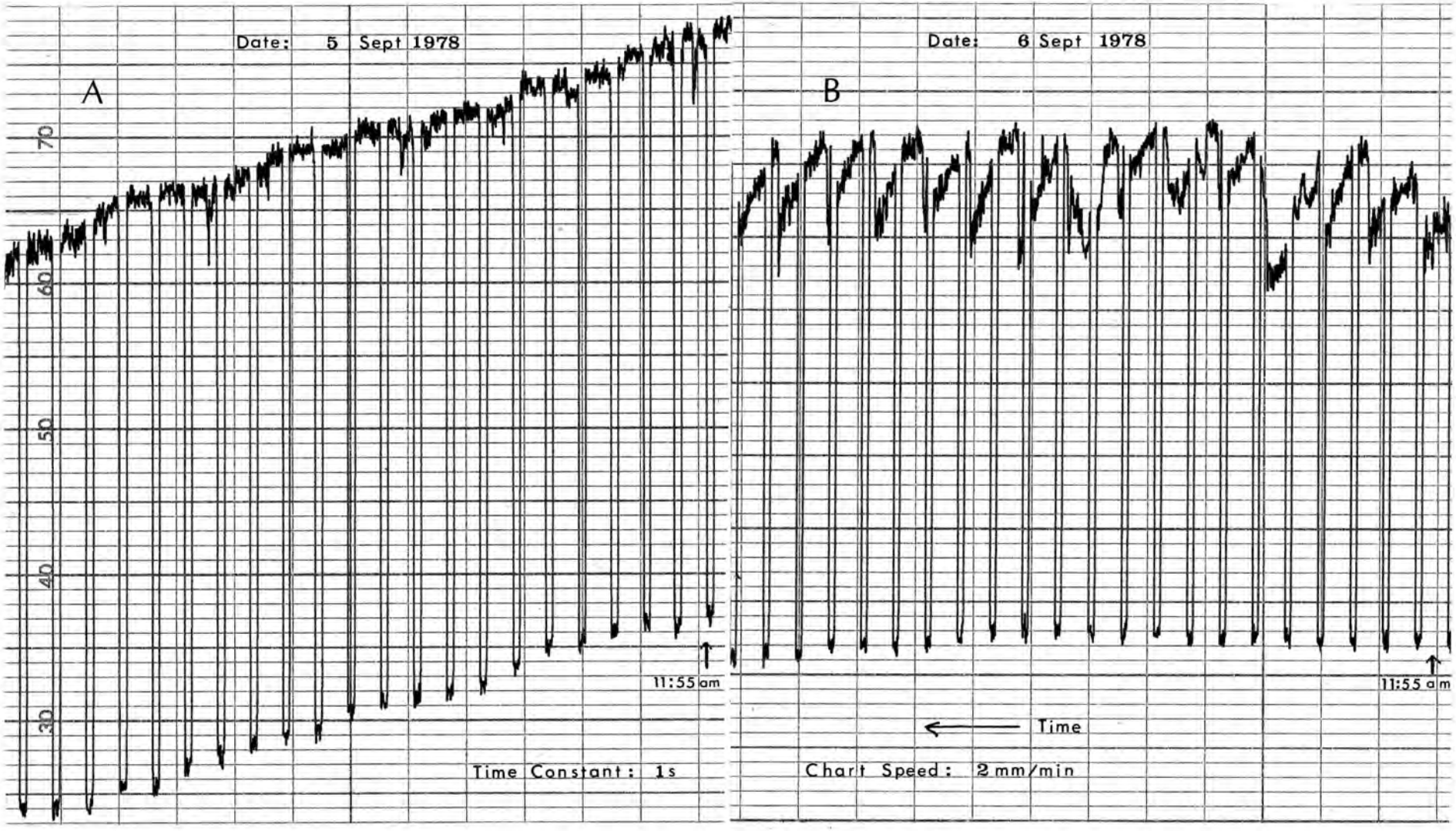

Figure 7.9 Solar observation on two consecutive days

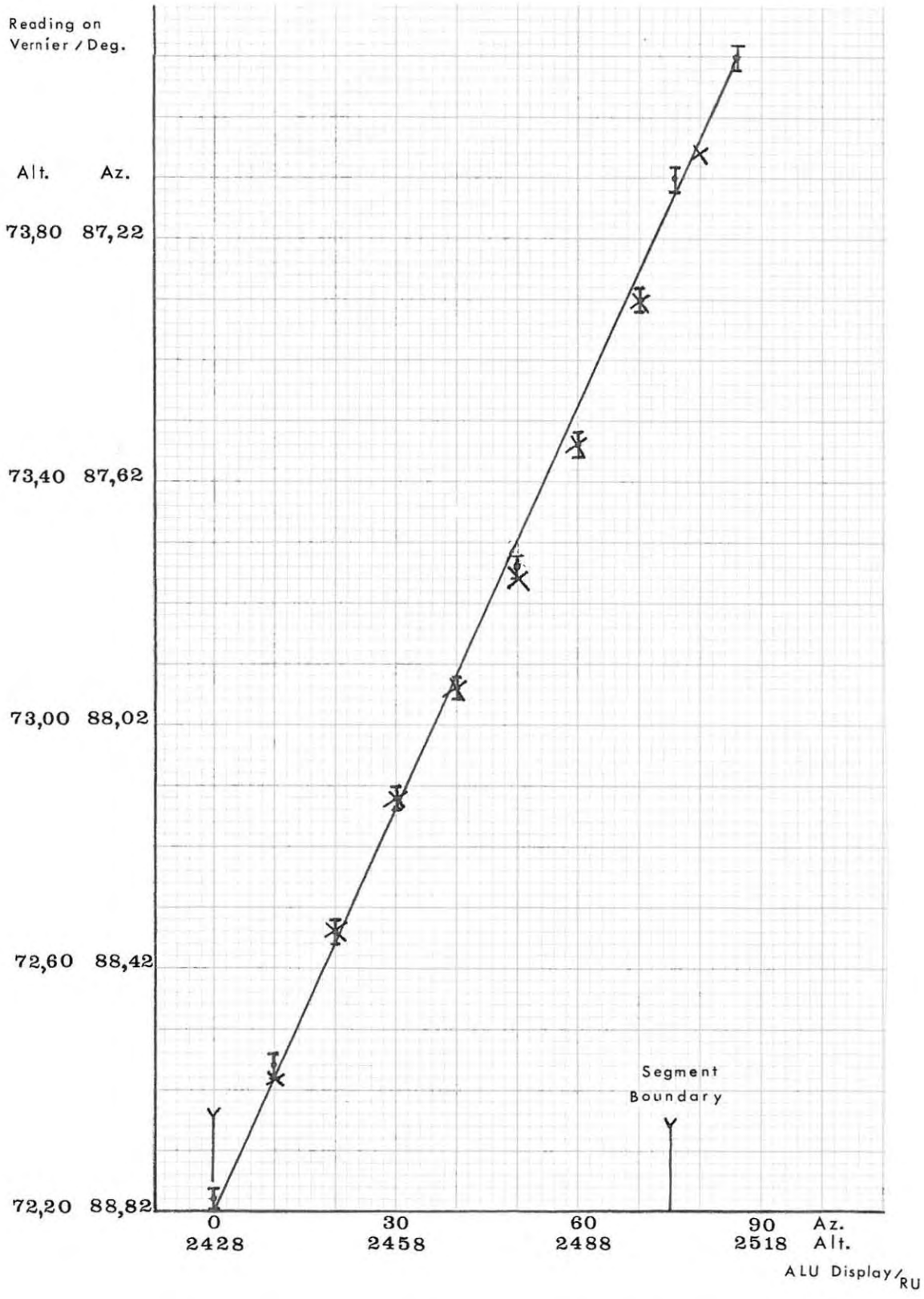

Figure 7.10 Fine segment linearity check

CHAPTER EIGHT

CONCLUSION

A computer-controlled tracking system with the accuracy envisaged in Chapter 1 has been designed, built and tested and the computer programs necessary for tracking the sun and the moon have been written. Although certain alignment problems still exist, it has been demonstrated by means of solar observations that the tracking system is capable of working satisfactorily.

Before the calibration of the tracking system can be completed, however, the ripple effect discussed in Chapter 7 will have to be removed. The first step in achieving the removal of this effect would be the installation of a temperature control unit for the equipment in the base of the antenna mount. After that it should be possible to locate and remove the nonlinearity which seems to be present in the synchro-to-digital converter. The calibration of the tracking system could then be completed and it would be ready for use.

However, before the telescope can be used for serious astronomy, the microwave section will need thorough servicing. In particular, a new noise tube and a new pair of mixer diodes will have to be installed. In addition, the continuum receiver will have to be improved before long

integration time constants can be used.

If the telescope is to be used for daily solar observation, it will have to be moved to a less obstructed site and, because of the limited size of the present computer, a dedicated computer for tracking and data logging will be required.

LITERATURE CITED

Baart, E.E. (1974). Private Communication.

Bendix Aviation Corporation (1962). Synchro, Autosyn (outline). Bendix Aviation Corporation, Montrose Division, U.S.A.

Datel (1973). Analogue-to-Digital Converter, Model ADC-E. Data sheet, Datel Systems Inc., U.S.A.

Explanatory Supplement to the Astronomical Ephemeris (1961). Her Majesty's Stationery Office, London.

Faulkner, E.A. (1969). Introduction to the theory of linear systems. Chapman and Hall Ltd., London.

Fogarty, W.G. (1975). "Total Atmospheric absorption at 22GHz." IEEE Trans. Antennas & Propagat. AP-23, 441-444.

Gaylard, M.J. (1976). The performance of a 22GHz. Radio Telescope. Msc. Thesis, Rhodes University.

Gille, J-C, Pelegrin, M.J. and Decauline, P. (1959). Feedback Control Systems. McGraw-Hill Book Co., New York.

Hamming, R.W. (1973). Numerical methods for Scientists and Engineers. McGraw-Hill Book Co., New York.

Harris Semiconductor (1973). Integrated Circuits. Harris Corporation, Belguim.

Hilburn, J.L. and Junlich, P.M. (1976). Microcomputers/ Microprocessors: Hardware, Software, and Applications. Prentice-Hall, Inc., New Jersey.

Hnatek, E.R. (1976). A User's Handbook of D/A and A/D Converters. John Wiley and Sons, New York.

Kline, R.M. (1977). Digital Computer Design. Prentice-Hall, Inc., New Jersey.

Kraus, J.D. (1966). Radio Astronomy. McGraw-Hill Book Co., New York.

Lichtenburg, J. (1975). Private communication.

Miller, R.W. (1977). Servomechanisms - Devices and Fundamentals. Reston Publishing Co., Virginia, U.S.A.

Motorola (1973). Linear Integrated Circuits Data Book. Motorola Inc., U.S.A.

Mutch, L.I. (1975). A 22GHz Radio Telescope. M.Sc. Thesis, Rhodes University.

National Semiconductors (Jan. 1972). Linear Applications. National Semiconductor Corporation, U.S.A.

National Semiconductors (Feb. 1972). MOS Integrated Circuits. National Semiconductor Corporation, U.S.A.

Nunn, B.J. (1974). A 22GHz. Water Maser Radiometer. M.Sc. Thesis, Rhodes University.

Ogata, K (1970). Modern Control Engineering. Prentice-Hall, Inc., New Jersey.

Pendrill, J. (1978). "Dynamic analysis of control systems." Electron. Engineering 50, 33-35.

Perseus (1976). Multexbasic Manual. Perseus Computing and automation (Pty.) Ltd., Pretoria.

Signetics (1973). 555 and 556 Timers. Signetics Corp., London.

Singer (1961). FPE 49 Low Inertia Motor W/ FDE 7 Tach Generator - Outline Drawing and Specifications. Singer MFG. Co., Somerville, U.S.A.

Texas Instruments (1973). Asynchronous Data Interface. Preliminary Data Sheet, Texas Instruments, Bedford, England.

Thaler, G.J. and Brown R.G. (1960). Analysis and Design of Feedback Control Systems. McGraw-hill Book Company, New York.

Upson, A.R. and Batchelor, J.H. (1966). Synchro Engineering Handbook. Hutchinson and Co., London.

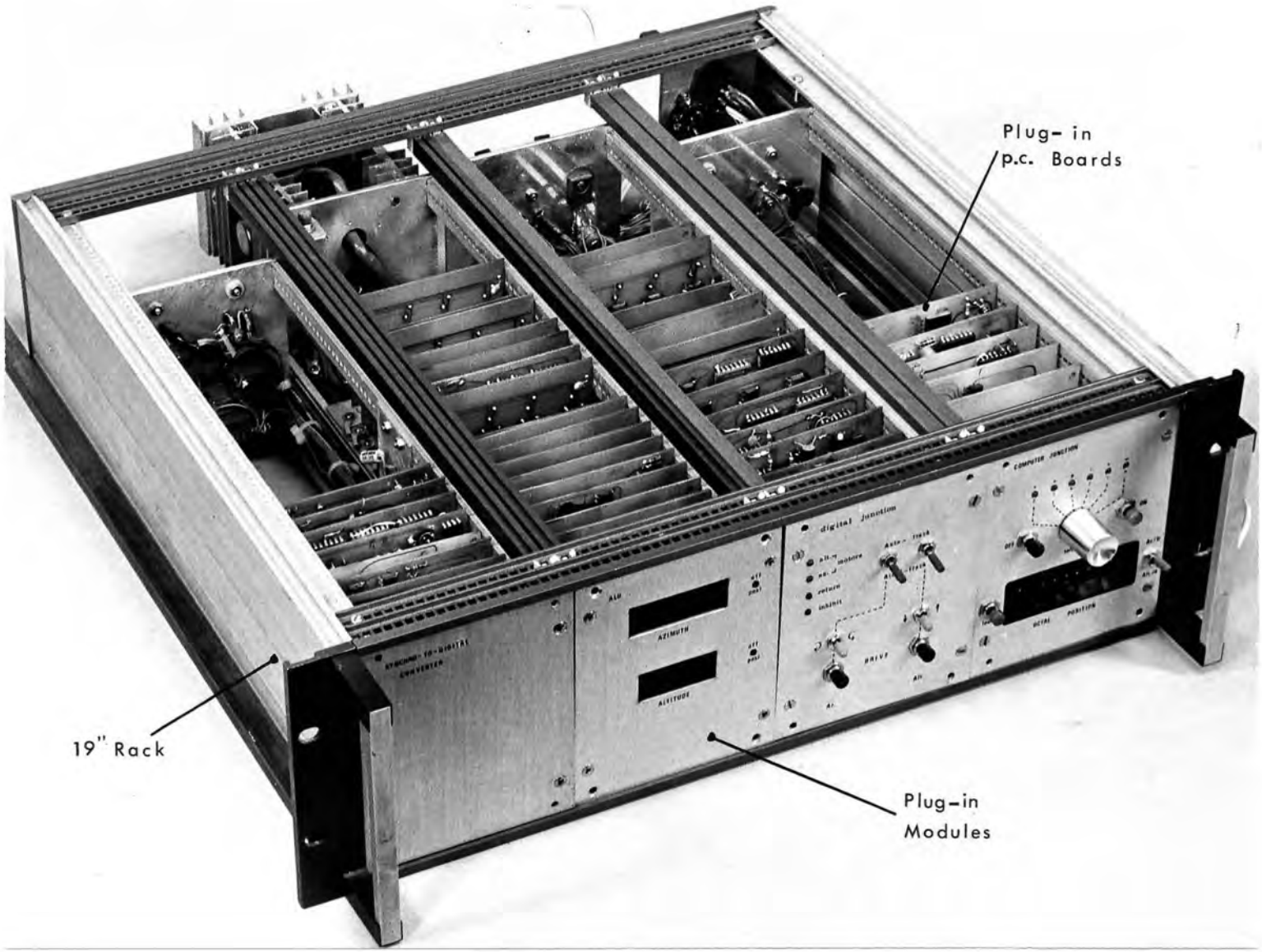

Appendix 1.1 Part of the tracking system

Appendix 2.1

The Difference Amplifier

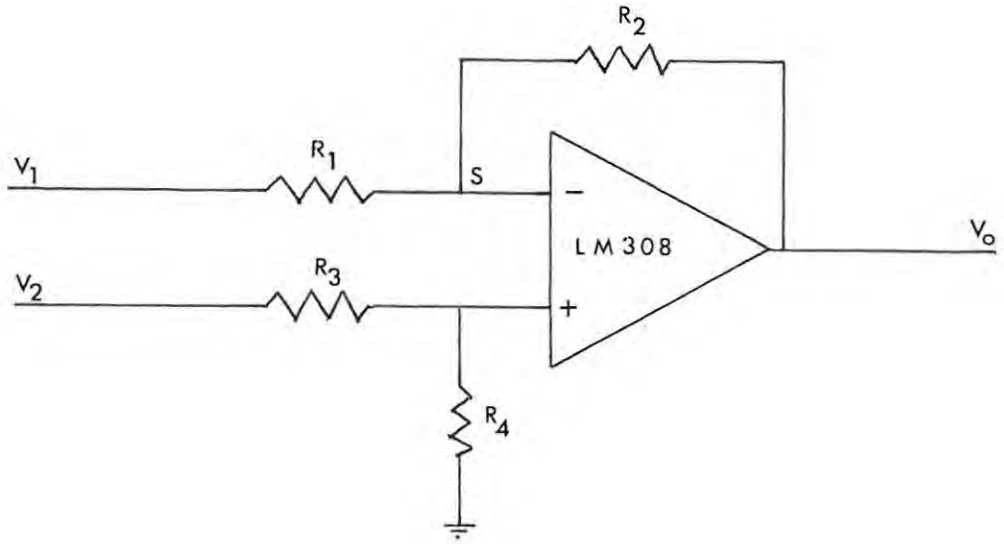

$$V_S = \frac{R_4}{R_3 + R_4} V_2$$

$$\text{and} \quad \frac{V_o - V_S}{R_2} = \frac{V_S - V_1}{R_1}$$

$$\therefore \quad \frac{R_1}{R_2} V_o - \frac{R_4 R_1}{R_2 (R_3 + R_4)} V_2 = \frac{R_4}{(R_3 + R_4)} V_2 - V_1$$

$$\text{Hence} \quad V_o = \frac{R_4 (R_1 + R_2)}{R_1 (R_3 + R_4)} V_2 - \frac{R_2}{R_1} V_1$$

$$\text{if} \quad R_1 = R_2 = R_3 = R_4, \quad \text{then } V_o = V_1 - V_2$$

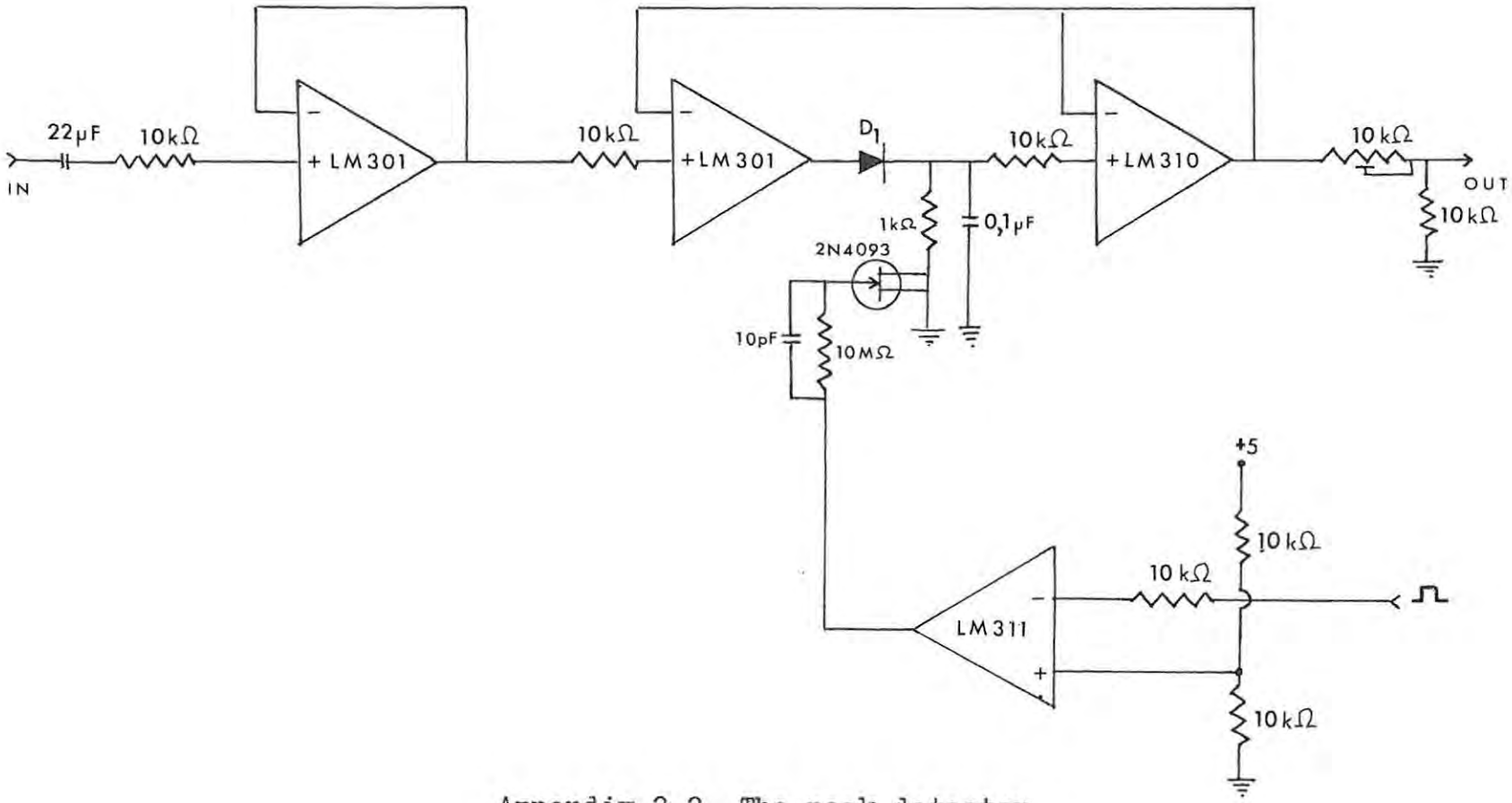

Appendix 2.2 The peak detector

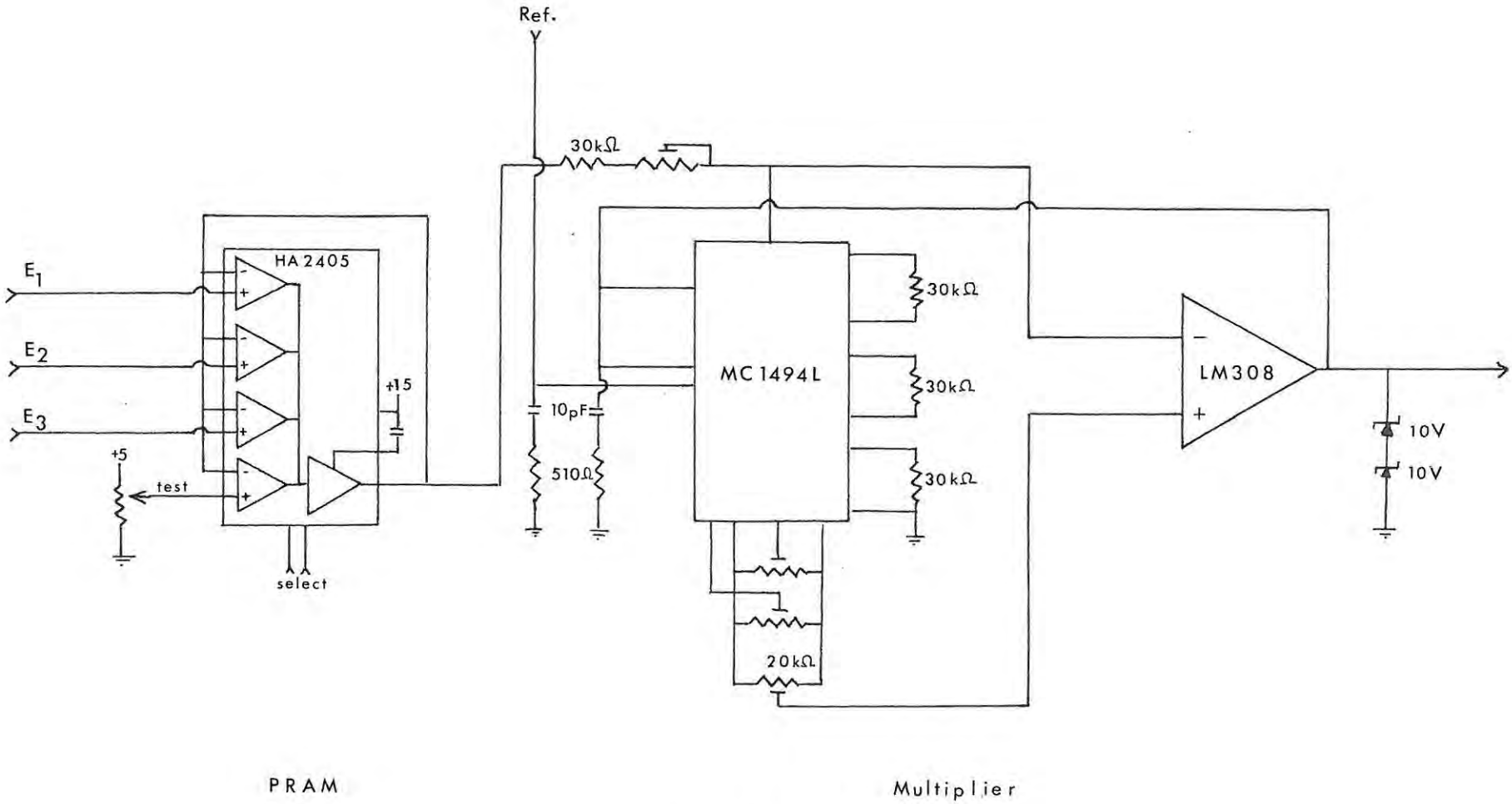

Appendix 2.3 The multiplier

Appendix 4.1

The ASCII Code

Character	Hexadecimal	Character	Hexadecimal
Space	20	@	40
!	21	A	41
"	22	B	42
#	23	C	43
$	24	D	44
%	25	E	45
&	26	F	46
'	27	G	47
(	28	H	48
)	29	I	49
*	2A	J	4A
+	2B	K	4B
,	2C	L	4C
-	2D	M	4D
.	2E	N	4E
/	2F	O	4F
0	30	P	50
1	31	Q	51
2	32	R	52
3	33	S	53
4	34	T	54
5	35	U	55
6	36	V	56
7	37	W	57
8	38	X	58
9	39	Y	59
:	3A	Z	5A
;	3B	[	5B
<	3C	\	5C
=	3D	]	5D
>	3E	↑	5E
?	3F	←	5F

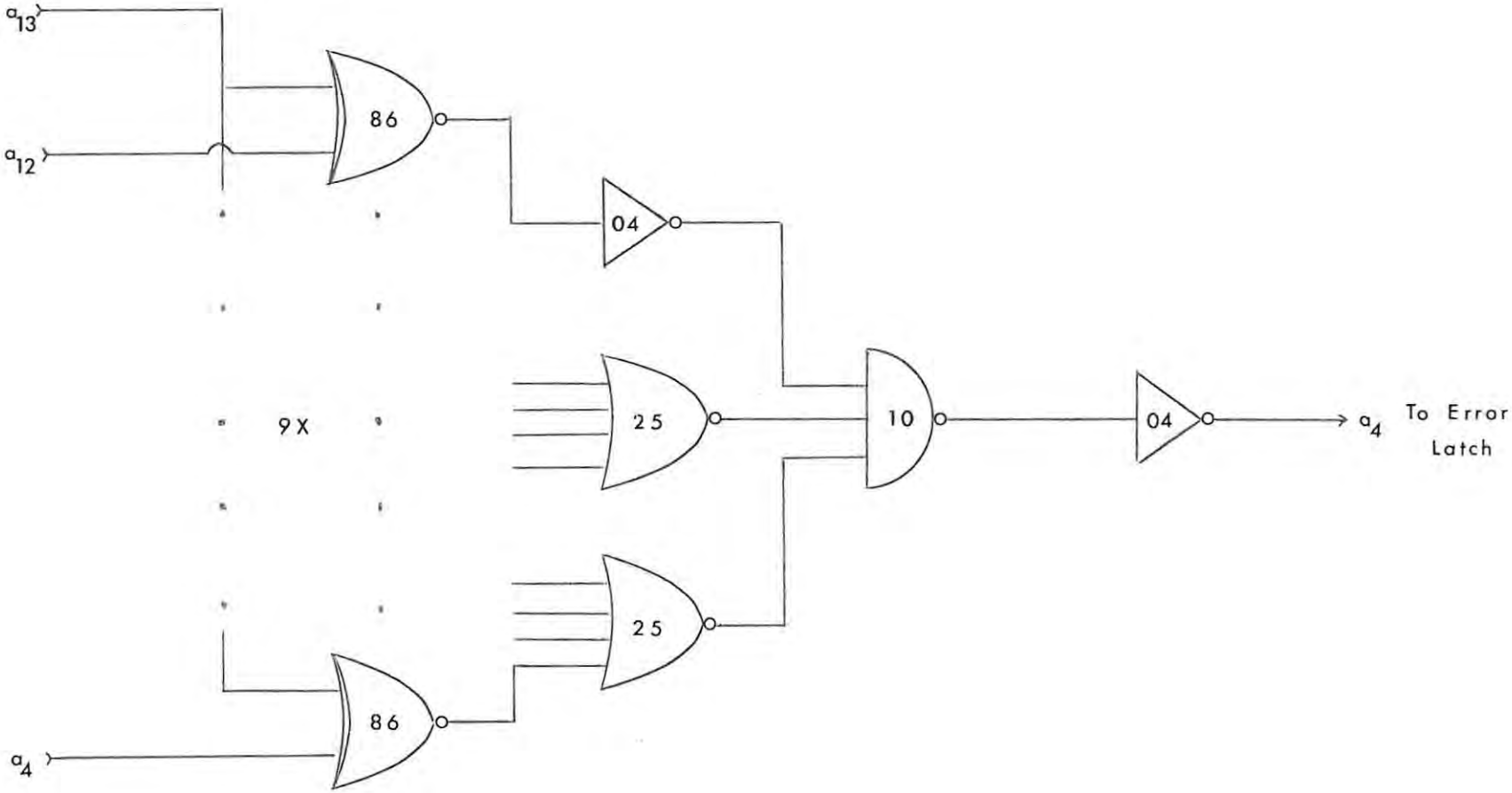

Appendix 4.2 The bit limiter

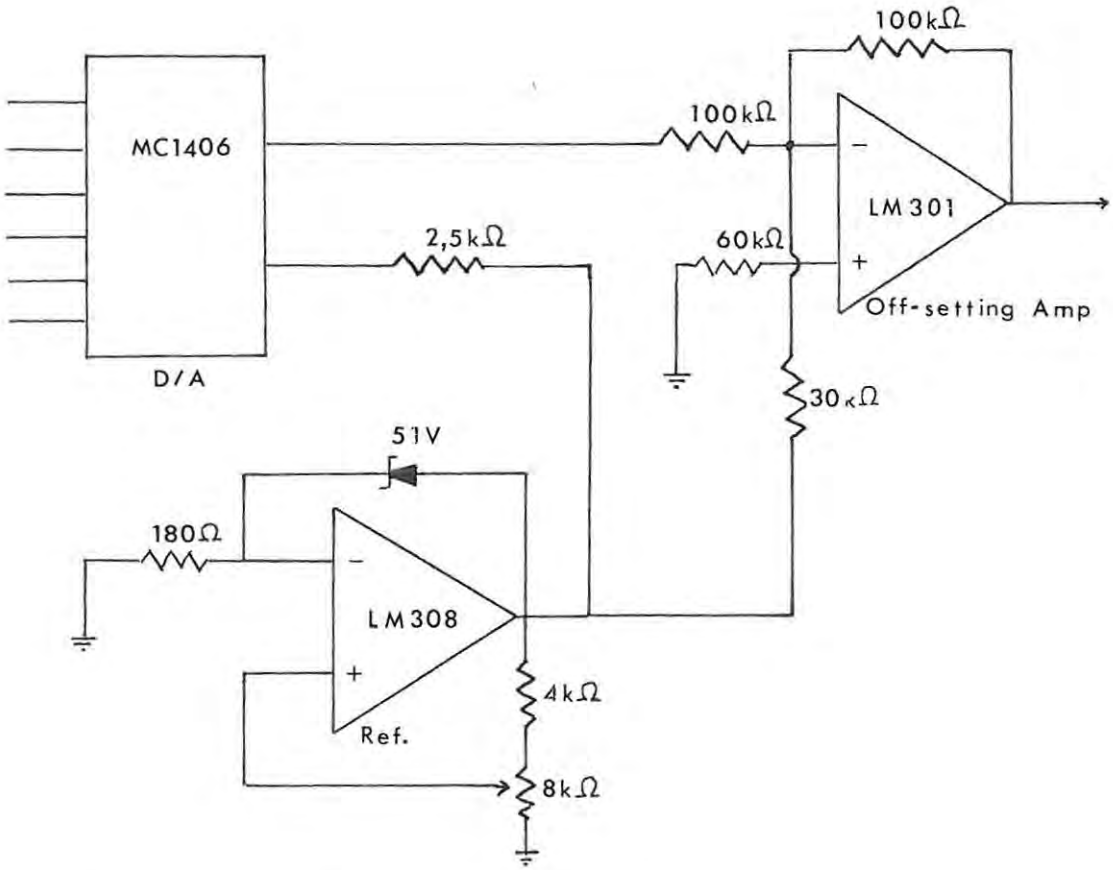

Appendix 4.3 The digital-to-analogue converter

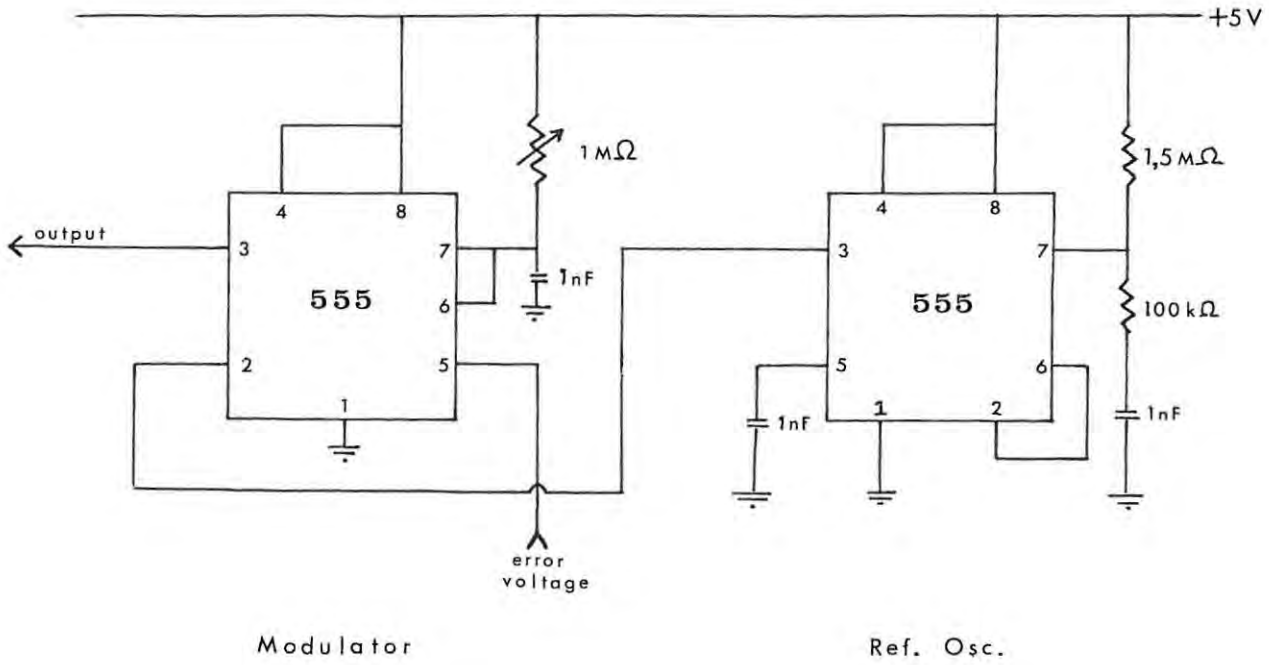

Appendix 4.4 The pulse-width modulator

```
 THE FOURIER TRANSFORM PROGRAM.
0100 LET V=0
0110 LET W=0
0120 DIM Y[330]
0130 DIM A[330]
0140 FOR I=0 TO 328
0150   READ A[I]
0160 NEXT I
0170 FOR N=1 TO 50
0180   FOR M=0 TO 328
0190     LET Y[M]=2*A[M]*COS(2*3.14159*N/1.128/7*M/47*1.128)/1.128
0200     LET V=V+Y[M]
0210   NEXT M
0220   FOR Q=0 TO 328
0230     LET Y[Q]=2*A[Q]*SIN(2*3.14159*N/1.128/7*Q/47*1.128)/1.128
0240     LET W=W+Y[Q]
0250   NEXT Q
0255   LET Z=(V*V+W*W)
0260   PRINT N/1.128/7,LOG(N/1.128/7)/2.303,Z,10*LOG(Z)/2.303,-1*ATN(W/V)*180/3.1416
0270   LET V=0
0280   LET W=0
0290 NEXT N
0300 STOP
0400 DATA 0,0,0,0,0,0.....ETC.
```

Appendix 5.1 The Fourier transform program

Appendix 6.1

```
INTERTRACKER
0100 REM THIS PROGRAM INTERACTS WITH THE TELESCOPE OPERATOR,
0110 REM INITIALLY DATA IS ASKED FOR, AFTER THAT THE OPERATOR
0120 REM MAY ENTER POINTING CORRECTIONS WHILE "NODDY" IS RUNNING,
0150 COM R1[10],R2[10],S1[10],D1[10],D2[10],U0[10],T0[10],G[10],K[10]
0160 LET G=0
0170 LET K=0
0180 DIM S$[10],N$[10],L$[10],Z$[10]
0190 LET P1=4*ATN(1)
0200 PRINT "R,A, @ 0 U,";
0210 GOSUB 0570
0220 LET R1=S0*P1/43200
0230 PRINT "R,A, @ 24 U,T,";
0240 GOSUB 0570
0250 LET R2=S0*P1/43200
0260 PRINT "DEC @ 0 U,T,";
0270 GOSUB 0630
0280 LET D1=S0*P1/180/3600
0290 PRINT "DEC @ 24 U,T,";
0300 GOSUB 0630
0310 LET D2=S0*P1/180/3600
0320 PRINT "S,T, @ 0 U,T, ";
0330 GOSUB 0570
0340 LET S1=S0+(26,5197*240)
0350 PRINT "START U,T,";
0360 GOSUB 0570
0370 LET T0=S0
0380 PRINT "END U,T ";
0390 GOSUB 0570
0400 LET U0=S0
0410 FOR N=1 TO 15
0420   PRINT
0430 NEXT N
0440 LET B=INT((U0/3600-INT(U0/3600))*60)
0450 EXECUTE,0,"RUN"
0460 PRINT "THERE IS A TRACKING PROGRAM RUNNING IN PARTITION '0',"
0470 PRINT "PLEASE DO NOT USE THE COMPUTER"
0480 PRINT "PROGRAM ENDS AT";INT(U0/3600);B;"G,M,T,"
0490 FOR N=1 TO 15
0500   PRINT
0510 NEXT N
0520 IF U0>SYS(0) THEN GOTO 0520
0530 PRINT "TRACKING PROGRAM HAS ENDED,"
0540 PRINT "TELESCOPE LOCK IS ON,"
0550 REM THIS SUBROUTINE ACCEPTS DATA AND CONVERTS TO SECONDS,
0560 STOP
0570 INPUT "HH,MM,SS",H0,M0,S0
0580 IF H0>24 THEN GOTO 0570
0590 IF M0>60 THEN GOTO 0570
0600 IF S0>60 THEN GOTO 0570
0610 LET S0=(H0*60+M0)*60+S0
0620 RETURN
0630 INPUT "DD,MM,SS",H0,M0,S0
0640 IF H0>360 THEN GOTO 0630
0650 GOTO 0590
```

Appendix 6.2

```
NODDY
0100 REM THIS PROGRAM CALCULATES THE CO-ORDINATES OF THE SUN
0110 REM AND TRANSMITS THEM TO THE TRACKING SYSTEM,
0120 COM R1[10],R2[10],S1[10],D1[10],D2[10],U0[10],T0[10],G[10],K[10]
0130 DIM S$[10],N$[10],L$[10],Z$[10]
0140 LET P1=4*ATN(1)
0150 LET A=1
0160 LET U=T0
0170 REM (180-200) LINEAR INTERPOLATION
0180 LET R=R1+(R2-R1)*U/86400
0190 LET D=D1+(D2-D1)*U/86400
0200 LET S=S1+U*1.00274
0210 REM (220) CALCULATE HOUR ANGLE
0220 LET H=S*P1/43200-R
0230 REM (240-300) CONVERT H,A. AND DEC, TO ALT,(L) AND AZ,(Z)
0240 LET L=-SIN(D)*.549213+COS(D)*COS(H)*.835682
0250 LET L=ATN(L/SQR(1-L*L))
0260 LET Z0=-COS(D)*SIN(H)
0270 LET Z1=SIN(D)*.835682+COS(D)*COS(H)*.549213
0280 LET Z=ATN(Z0/Z1)
0290 LET L=L/P1*8192
0300 LET Z=P1/2-Z
0310 REM CALCULATE U.T. OF OBS (V)
0320 LET V=U/3600
0330 LET M=(V-INT(V))*60
0340 LET S=(M-INT(M))*60
0350 LET V=INT(V)+INT(M)/100+INT(S)/10000
0360 LET Z=Z/P1*8192
0370 LET S8=L+587+G
0380 GOSUB 0630
0390 LET L$=S$,"A"
0400 LET S8=Z-157+K
0410 GOSUB 0630
0420 LET Z$=S$,"B"
0430 REM CHECK THE REAL TIME CLOCK
0440 IF T0>SYS(0) THEN GOTO 0540
0450 IF U>SYS(0) THEN GOTO 0450
0460 REM TRANSMIT CO-ORDINATES
0470 PRINT L$,,Z$
0480 LET U=U+2
0490 LET A=A+1
0500 IF U>U0 THEN GOTO 0600
0510 IF A=18 THEN GOSUB 0720
0520 GOTO 0180
0530 REM PRINT INITIAL CO-ORDINATES AND LOCK(C)
0540 PRINT L$,,Z$
0550 PRINT "C"
0560 IF T0>SYS(0) THEN GOTO 0560
0570 REM LOCK OFF(D) AND RUN
0580 PRINT "D"
0590 GOTO 0480
0600 PRINT "C"
0610 STOP
0620 REM (630-690) OCTAL CONVERSION
0630 LET S$="      "
0640 FOR J=5 TO 1 STEP -1
```

NODDY cont.

```
0650    ABBA,INT((S8/8-INT(S8/8))*8),N$
0660    LET N=LEN(N$)-1
0670    LET S$[J,J]=N$[2,2]
0680    LET S8=S8/8
0690 NEXT J
0700 RETURN
0710 REM (720-800) MOVE OFF SUN BY 100 R,U, AND WAIT 30 SECONDS
0720 LET S8=Z+100
0730 GOSUB 0630
0740 LET Z$=S$,"B"
0750 PRINT Z$
0760 DELAY;240
0770 LET A=0
0780 LET U=U+30
0790 REM START TRACKING AGAIN
0800 RETURN
```